universität wien

DIPLOMARBEIT / DIPLOMA THESIS

Titel der Diplomarbeit / Title of the Diploma Thesis

Large-scale isolation and characterization of prenylated flavonoids from the root bark of *Morus alba*

verfasst von / submitted by

Roland Rumpold

angestrebter akademischer Grad / in partial fulfilment of the requirements for the degree of

Magister der Pharmazie (Mag. pharm.)

Wien, 2020 / Vienna, 2020

Studienkennzahl lt. Studienblatt / degree programme code as it appears on the student record sheet:	UA 449
Studienrichtung lt. Studienblatt / degree programme as it appears on the student record sheet:	Diplomstudium Pharmazie
Betreut von / Supervisor:	Univ.-Prof. Mag. pharm. Dr. Judith Maria Rollinger
Mitbetreut von / Co-Supervisor:	Mag. pharm. Dr. Ulrike Grienke

ACKNOWLEDGMENT

First and foremost, I would like to thank Univ.-Prof. Mag. pharm. Dr. Judith Rollinger for giving me the opportunity to perform my diploma thesis in the Department of Pharmacognosy as well as to gain an insight into scientific working. Her calm, thoughtful and empathic way is inspiring, and I am very grateful for that.

I would also like to thank my co-supervisors Mag. pharm. Dr. Ulrike Grienke and Mag. pharm. Julia Langeder for their precise and understandable explanations about the devices and the phytochemical work in general. Whenever I ran into trouble or had questions, they were always ready to help and steer me in the right direction. Their supportive nature combined with their high interest in phytochemical work is very motivating.

Many thanks also to the whole team of the Pharmacognosy Department. Everyone was always very supportive whenever I needed help.

In general, I can safely say that the semester of my diploma thesis was an instructive, exciting and fun semester at the same time.

I am also very grateful for my long-time friends, Karina and Tom, who happened to work on their thesis at the same time at the same department. Thank you guys for making this time even more enjoyable.

During my studies I was always able to count on special people in my life. I want to say *Thank you* to my parents, Herbert and Johanna as well as to my brother Herwig, who always supported and motivated me. Special gratitude I owe my girlfriend, Maria, who accompanied me during almost the whole time of my studies and always had a shoulder ready to lean on. And last but not least, I would like to thank all the colleagues, who have become friends, that I met during my studies. Studying without you would definitely not have been this fun!

TABLE OF CONTENTS

ABSTRACT

Respiratory infections due to influenza viruses and/or pneumococci are causing approximately 2.2 million deaths annually worldwide. Consequently, finding a treatment against these pathogens remains an ongoing challenge.

In recent studies, prenylated flavonoids, constituents of the white mulberry root bark (*Morus alba* L.), showed an *in vitro* inhibitory effect against influenza A virus as well as *Streptococcus pneumoniae*. This renders the plant material a highly promising starting point for the development of a herbal remedy. However, in order to prove sufficient effectiveness and safety, to obtain knowledge about pharmacokinetics and pharmacodynamics, *in vivo* models are required.

Therefore, the aim of this thesis was to develop a method for the large scale isolation of prenylated compounds of the mulberry root bark and to make them available for *in vivo* studies in sufficient amounts. This work is based on enriched fractions produced during an earlier diploma thesis. By means of flash chromatography, mass spectrometry (MS) and nuclear magnetic resonance (NMR) spectroscopy, four pure compounds, namely sanggenon C, D, G and kuwanon L and one semi-pure compound, i.e. sanggenon O, have been successfully isolated in sufficient amounts and structurally identified.

ZUSAMMENFASSUNG

Mit weltweit ungefähr 650.000 Todesfällen durch Influenza und 1,6 Millionen Todesfällen durch Pneumokokken pro Jahr, stellt die Behandlung der respiratorischen Erkrankungen ausgelöst durch dieser beiden Erreger eine große Herausforderung dar (WHO, 2020a, 2020b).

In jüngsten Studien zeigten prenylierte Flavonoide aus der Maulbeerbaumwurzelrinde (*Morus alba* L.) eine hemmende Wirkung *in vitro* auf beide Krankheitserreger – Influenzavirus und Pneumokokken. Dies könnte in Zukunft eine wirksame Behandlungsstrategie darstellen. Um jedoch eine ausreichende Wirksamkeit und Sicherheit nachzuweisen, sowie Kenntnisse über Pharmakokinetik und Pharmakodynamik zu erhalten, sind *in vivo* Modelle erforderlich.

Ziel dieser Diplomarbeit war es daher, eine Methode zur Isolierung prenylierter Verbindungen aus der Maulbeerbaumwurzelrinde im Großmaßstab zu entwickeln, um die gewonnen Reinstoffe für *in vivo* Studien zur Verfügung zu stellen. Die Grundlage für diese Arbeit bildeten Fraktionen, die aus einer groben Auftrennung einer früheren Diplomarbeit bereits vorhanden waren. Unter Verwendung von Flash Chromatographie, Massenspektrometrie (MS) und nuklearen Magnetresonanz (NMR) Spektroskopie wurden vier Reinsubstanzen, namentlich Sanggenon C, D, G und Kuwanon L und eine semi-aufgereinigte Verbindung (Sanggenon O) in ausreichenden Mengen erfolgreich isoliert und strukturell identifiziert.

1 AIM OF WORK

Biological effects of flavonoids are well-known and supported by a variety of studies. Their effects range from antioxidative, hepatoprotective, anti-inflammatory, anticancer to antibacterial and antiviral activities (Kumar and Pandey, 2013).

Prenylated flavonoids, which are commonly produced in the *Moraceae* family, among others, have recently shown an inhibitory effect on the neuraminidase of influenza viruses and pneumococci (Grienke et al., 2016).

An extract from the white mulberry tree root bark was produced during a previous diploma thesis (Freisinger, 2020). Thereafter, a rough separation was performed using Flash Chromatography (FC) which resulted in eleven fractions (MAM01_01 – MAM01_11).

The aim of this diploma thesis was the further separation of the individual fractions in order to isolate compounds of high purity in a high yield and to confirm their identity using NMR spectroscopy.

Pure compounds in high yields are a prerequisite for assessing their potential toxicity and efficacy *in vivo*.

2 INTRODUCTION

2.1 *MORUS ALBA* L. – PLANT DESCRIPTION, CONSTITUENTS AND THEIR EFFECTS

The white mulberry tree (*Morus alba L.*) belongs to the family of Moraceae and has its origin in China. It is also largely cultivated in Korea as well as in Japan. The tree can rise up to 20 meters in height, its leaves are green and about 5.0–7.5 cm in length. The fruits are green and they turn into white when ripe (Chan et al., 2016).

Morus alba has a long history of a very diverse usage. It provides a delicious edible fruit and its leaves are used to breed silkworms.

It has also a very wide-ranging traditional medicinal use which includes antioxidant, antitumoral, neuroprotective, antiatherosclerosis and antihyperglycemic effects just to name a few examples (Yuan and Zhao, 2017).

2.1.1 MORI CORTEX RADICIS

The focus of this thesis lies on Mori cortex radicis (mulberry root bark), which is also called Sang-Bai-Pi (SBP). To obtain SBP, the roots of *Morus alba* are collected between late autumn and early spring. After removing the brown layer with a knife, the white root barks are dried with honey. SBP of good quality is white, thick and flexible (Wei et al., 2016).

In addition to being a dietary herb, SBP is also widely used in traditional Chinese medicine (TCM). It is used for the treatment of cough, bronchitis, xerophthalmia, pulmonary diseases, to name but a few (Wei et al., 2016). In Korea and Japan, patients with diabetes consume mulberry leaves as an antihyperglycemic supplement (Chan et al., 2016).

Figure 2 shows the mulberry root *in toto*, while Figure 1 shows commercially available SBP.

Figure 2. Morus alba root, https://tcmwiki.com/wiki/morus-alba-root, effective: November 2020

Figure 1. SBP without removal of brown layer (Wei et al., 2016, Figure 1)

2.1.2 CONSTITUENTS AND KNOWN ACTIVITIES

When exploring the chemistry of *M. alba*, a huge variety of different compounds is found. Its fruits are for example very high in protein compared to other berries, containing all nine essential amino acids required by humans. The berries also have a high proportion of polyphenolics, anthocyanins, flavonoids, phenolic acids, polysaccharides as well as melatonin, which makes the mulberry an excellent food (Yuan and Zhao, 2017). Its leaves contain flavonol glycosides as well as 2-arylbenzofuran derivates (Moracins). Compounds identified from the root and root bark include terpenoids, coumarins and flavonoids including Diels-Alder adducts such as sanggenons (Chan et al., 2016). The following chapters give an overview of the constituents and in which organ they can be found.

Flavonoids

Flavonoids are a group of naturally derived substances which are found in fruits, vegetables, grains, roots, barks and tea. They have a wide range of biological effects, including antitumor, antioxidant, wound-healing and antimicrobial activities (Escribano-Ferrer et al., 2019).

In the mulberry fruit, very well-known substances like quercetin (Figure 3), rutin or kaempferol can be found. The root bark contains a lot of flavanols and flavonols such as morusin, different kuwanons and sanggenons (Chan et al., 2016). Most of the flavonoids found in *M. alba* root bark are linked to prenyl- or geranyl groups.

The constituents that this thesis focuses on are the sanggenons. Sanggenons are Diels-Alder cycloadducts comprising a flavonoid diene and a 2'-hydroxy chalcone.

The reason for the high level of interest in these flavonoids lies in recent studies. Kuwanon L showed strong inhibition of the pneumococcal NA. Sanggenon D showed inhibition of pneumococcal NA and planktonic growth and biofilm formation of *S. pneumoniae*. Sanggenon G (Figure 4) and sanggenol A have not only shown an inhibitory effect on the bacterial NA of *S. pneumoniae* but also on the viral NA *in vitro* (Grienke et al., 2016). This could be revolutionary in the treatment of not only influenza or infections due to pneumococci, but also in the super-infection of those two pathogens.

Polyphenolics

In general, berries are a rich source of polyphenolics which also accounts for the white mulberry. Numerous studies of the biological activity of polyphenolics have been conducted so far (Yuan and Zhao, 2017).

Polyphenolics are associated with a reduced risk of cancer, cardiovascular diseases as well as neurodegeneration (Yuan and Zhao, 2017).

A subclass of polyphenolics are anthocyanins, which also have a wide range of biological effects such as antitumoral or antidiabetic activity. Cyanidin-3-glucoside makes up the largest part of anthocyanins in mulberry fruits, however, it is not contained in the root bark (Yuan and Zhao, 2017).

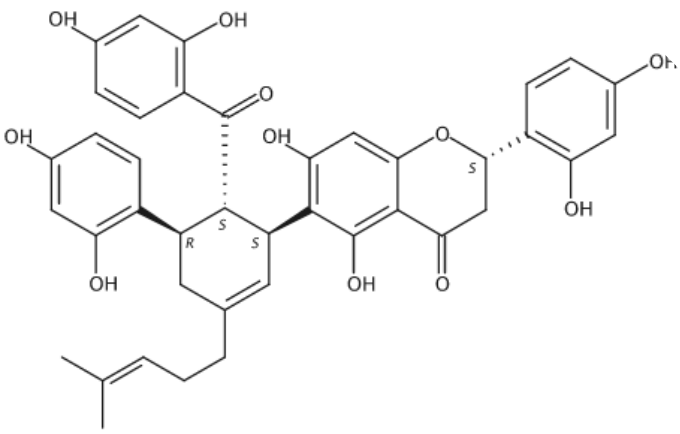

Figure 4. Sanggenon G.

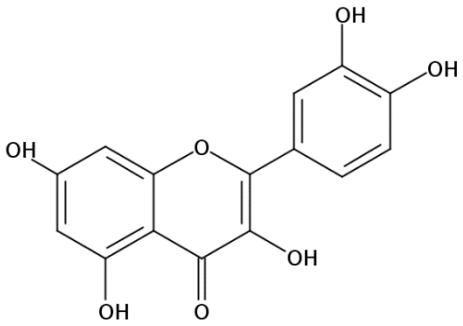

Figure 3. Quercetin.

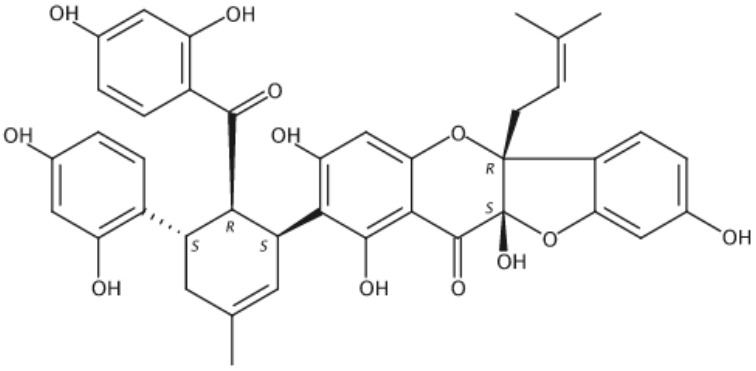

Figure 5. Sanggenon C.

Melatonin

Another substance, which can be found in mulberry fruits is melatonin. Melatonin is a neurohormone, which is naturally produced in the human body and its lack is associated with sleep disorders (Yuan and Zhao, 2017).

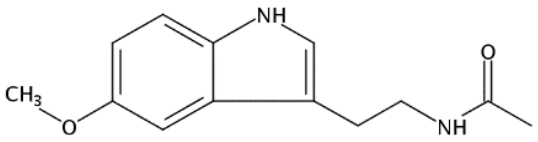

Figure 6. Melatonin.

2.2 INFLUENZA VIRUS

Influenza, more commonly known as 'flu' is a seasonal infection that is caused by influenza viruses. Generally, there are four types of seasonal influenza viruses - namely type A, B, C and D, whereof only type A and B cause seasonal epidemics. Type C only leads to mild illnesses and plays a tangential role in severe disease development. Type D influenza viruses are to date not known to affect humans (WHO, 2018).

The focus of this diploma thesis lies on type A influenza viruses, which can be further classified into subtypes depending on the combination of two proteins that occur on the surface of the virus: hemagglutinin (HA) and neuraminidase (NA). These two proteins, amongst others, are important targets to treat influenza (WHO, 2018).

Figure 7. Influenza A virus. https://www.impfen.de/impfwissen/was-ist-influenza-grippe/

The signs and symptoms of the seasonal influenza are fever, headache, muscle and joint pain, a sore throat and a usually dry cough. Most people recover from influenza infection in about one week without the need of medical treatment. However, influenza can also cause severe illness and death, especially for people with a weak immune system such as the elderly, children under 59 months, pregnant women or people with chronic medical conditions (for example chronic cardiac, pulmonary or renal diseases). For those people, an annual vaccination is strongly recommended. Annual vaccination is the most effective way to prevent an infection or at least a severe disease progression. The reason for annual booster vaccination is that the virus is constantly evolving, and virus strains of different pathogenicity can circulate every year (WHO, 2018).

Although most people recover from the illness without any medical treatment, people with a severe clinical disease with confirmed influenza should be treated with antiviral drugs as soon as possible. The drugs approved in Austria for treatment of influenza are Oseltamivir and Zanamivir, both are neuraminidase inhibitors (WHO, 2018).

2.3 PNEUMOCOCCI

The genus *Streptococcus* belongs to the kingdom of bacteria. *Streptococcus pneumoniae* bacteria, commonly known as "pneumococci", are responsible for a variety of human diseases such as lung infections, otitis media or meningitis. They are transmitted by speaking, coughing or sneezing and infest the nasopharynx (BMSGPK, 2020). About 1.6 million people die from pneumococcal infections annually, with the majority being children under the age of five (Sharma-Chawla et al., 2016).

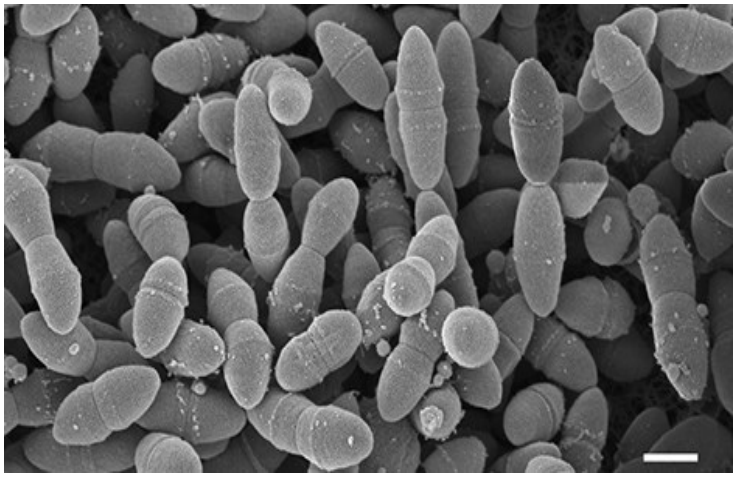

Figure 8. Pneumococci, https://www.rki.de/DE/Content/InfAZ/P/Pneumokokkeninfektionen/Pneumokokken_node.html, effective: November 2020

Comparable to influenza virus infections, people with a weak immune system are particularly vulnerable to pneumococci.

The most effective way of preventing an infection with pneumococci is vaccination, which is the reason why vaccination is highly recommended for children as well as people over the age of fifty (BMSGPK, 2020).

S. pneumoniae infection is treated with antibiotic therapy and supportive care including mechanical ventilation if necessary.

Beta-lactam antibiotics are the drugs of choice, followed by macrolides and fluoroquinolones if the pathogen appears to be beta-lactam resistant.

2.4 Co-Infection with Influenza and Pneumococci

Infection with secondary bacterial pathogens is attributed to be the major cause of excessive mortality during influenza A virus (IAV) outbreaks. This lethal synergism has been recognized as early as the beginning of the 20th century. The 1918-1919 IAV pandemic, the so-called *Spanish Flu*, resulted in an estimated global death toll of over 50 million people. Retrospective studies disclosed that 71% of the fatal cases during this pandemic were positive for *S. pneumoniae*, providing the first epidemiological evidence for viral-bacterial co-infections (Sharma-Chawla et al., 2016).

This lethal synergism poses a particular challenge in the treatment of both infections.

As mentioned in chapter 2.1.2., compounds like sanggenon G or sanggenol A, which have shown an effect on the NA of both pathogens, could be excellent drug candidates.

3 RESULTS

In a previous diploma thesis (Freisinger, 2020), an extract of Mori cortex radicis was generated using DCM in a defatting-step followed by MeOH as extraction agent. In this process 61.31 g of a crude extract were obtained out of 1,852.2 g plant material, which make up 3.31% of the plant material used. The crude extract was separated using flash-chromatography with DCM and MeOH as mobile phase on a normal phase silica column. In this process, eleven fractions were obtained, which formed the basis for further separations during this thesis (Table 1, Figure 9).

Table 1. MAM01_01 – MAM01_11

Fraction	Yield (g)
MAM01_01	2.51050
MAM01_02	6.55624
MAM01_03	1.45812
MAM01_04	1.24922
MAM01_05	2.79050
MAM01_06	3.77830
MAM01_07	1.64964
MAM01_08	1.27269
MAM01_09	3.16904
MAM01_10	8.39120
MAM01_11	13.70150

The first task was to get an idea of the composition of the compounds contained in the fractions. The technique used to accomplish this was an ultra high-performance liquid chromatography (UPLC) analysis with the conditions mentioned in chapter 4.2.2. The results are shown in Figure 10 and Figure 11 with MA5N as reference. MA5N is an enriched fraction, obtained in 2009, specifically containing the active sanggenons as described as MAF in Grienke et al., 2016.

The separation done by Freisinger (2020) already resulted in strongly enriched fractions. Some of the constituents were highly enriched. Based on previous experiments and by comparing retention times and UV spectra, it became clear that sanggenon C and sanggenon O were contained in fraction MAM01_05. As sanggenon C was one of the compounds of high interest (Grienke et al., 2016), the focus lied on the separation of MAM01_05.

Figure 9. MAM01_01 – MAM01_11

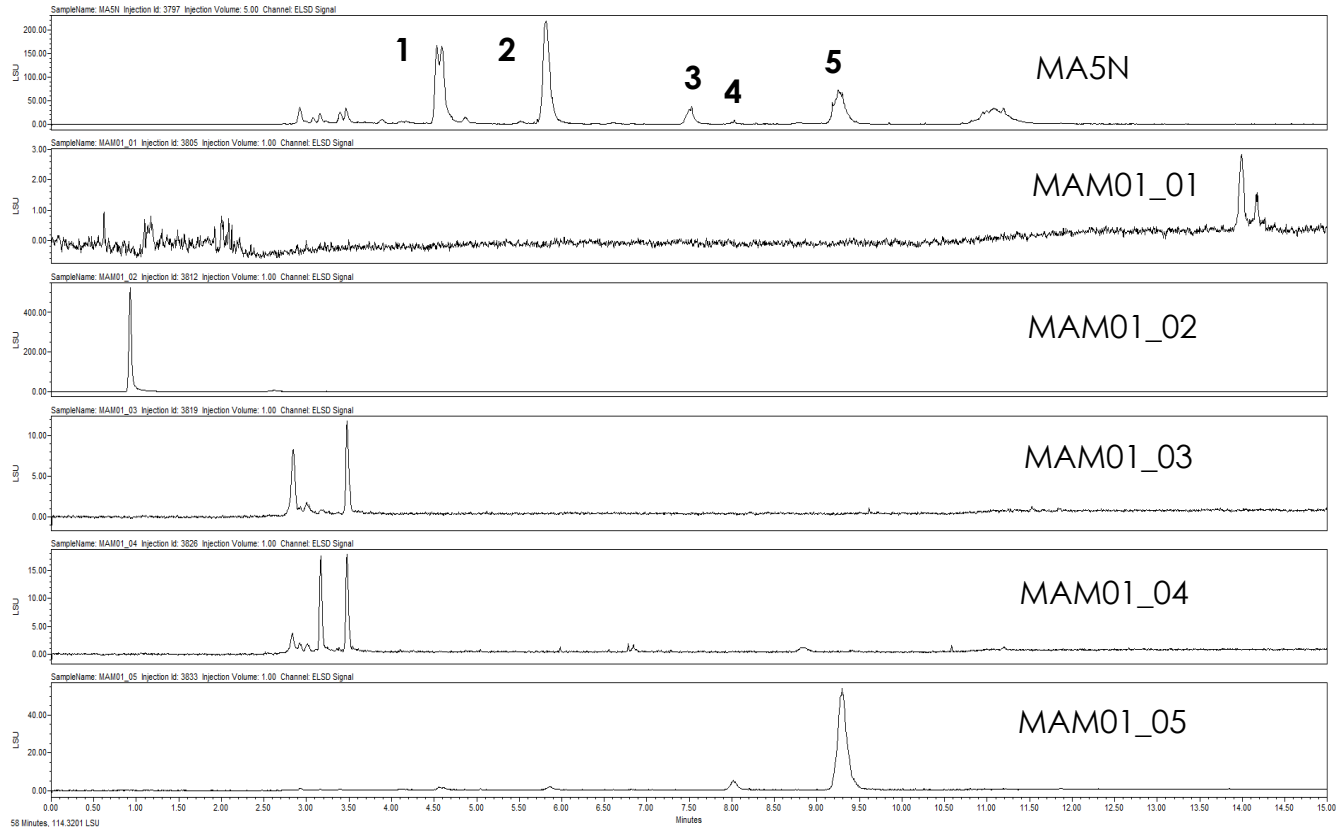

Figure 10. UPLC-ELSD chromatogram of fraction MA5N (top as reference) and MAM01_01 – MAM01_05
Method: MA_PDAELSD_col1_598_50iso_15m, see chapter 4.2.2

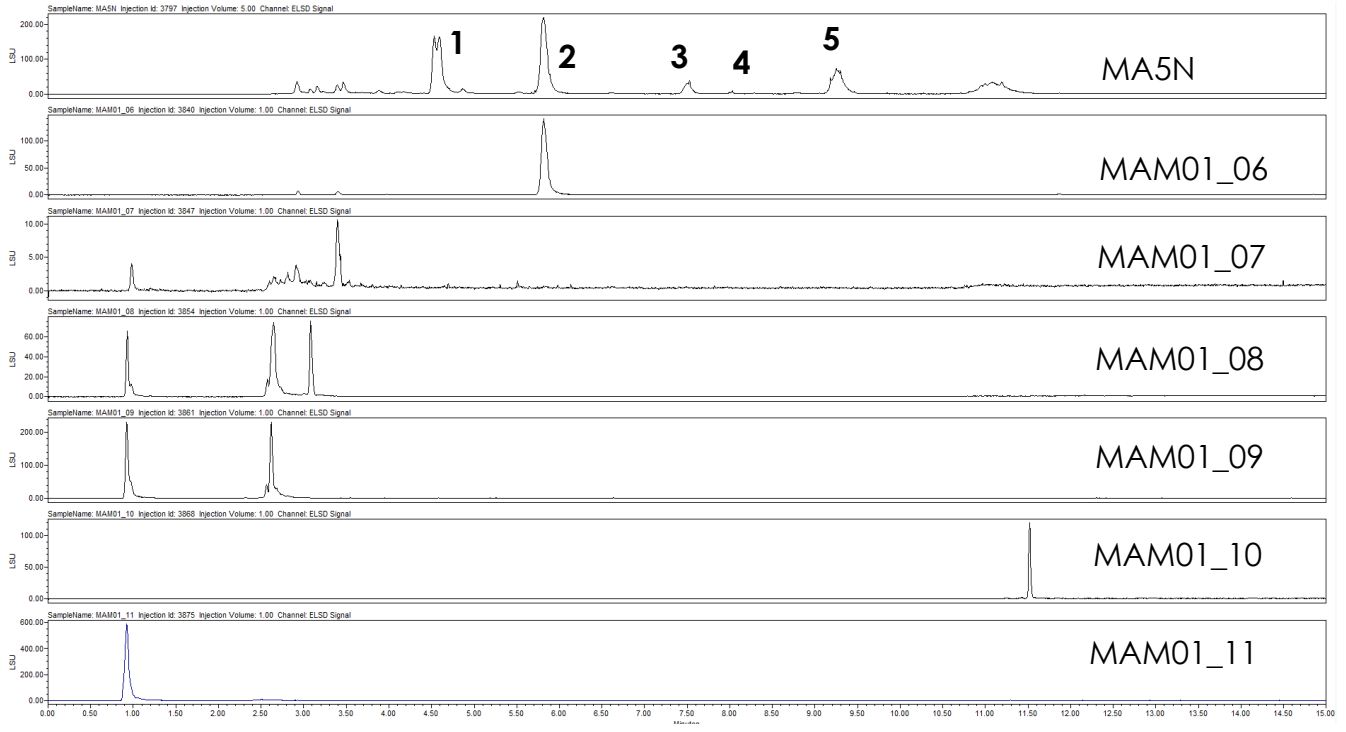

Figure 11. UPLC-ELSD chromatogram of fraction MA5N (top as reference) and MAM01_06 – MAM01_11
Method: MA_PDAELSD_col1_598_50iso_15m, see chapter 4.2.2.

Table 2 shows the peak numbers used in Figure 10 and Figure 11 with corresponding compound names.

Table 2. Compounds shown in Figure 10 and Figure 11 given as numbers.

Nr	Compound
1	Kuwanon L
2	Sanggenon D
3	Sanggenon G
4	Sanggenon O
5	Sanggenon C

3.1 PHYTOCHEMICAL INVESTIGATION OF MAM01_05

Fraction MAM01_05 was found to contain sanggenon O as well as sanggenon C (Figure 12). The aim was to efficiently isolate these two compounds.

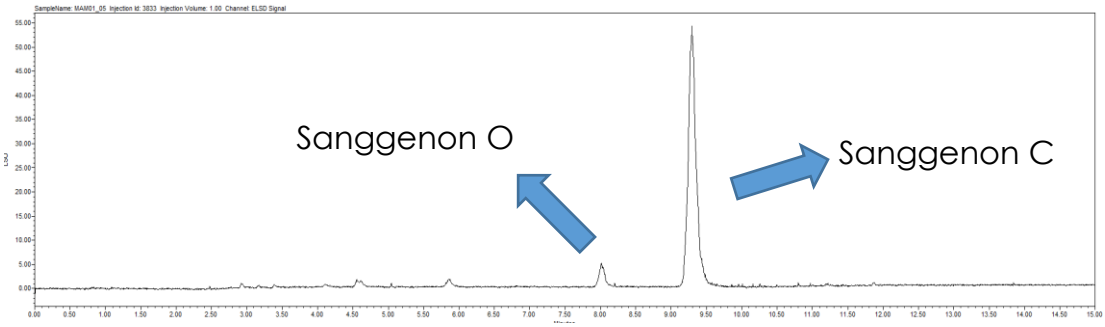

Figure 12. UPLC-ELSD analysis of MAM01_05.
Method: MA_PDAELSD_col1_598_50iso_15m, see chapter 4.2.2.

High-performance Countercurrent Chromatography (HPCCC) was chosen as a first separation technique, because of its advantage of no irreversible adsorption to stationary phase. Therefore, a selection of different solvent mixtures was made for preliminary experiments (Table 3). The individual solvent mixtures resulting in 2-phase solvent systems which are given as numbers in the following paragraphs. Five different HEMWat systems were tested alongside two solvent systems described in literature (no. 1 and 4). HEMWat stands for "Hexane – Ethyl acetate – Methanol – Water". These HEMWat systems are very common solvent mixtures in which the four solvents are mixed in different proportions reflecting different polarities.

The aim of the preliminary tests was to find a suitable solvent system in order to later efficiently separate the substances from one another using a preparative method.

Table 3. Solvent mixtures prepared for preliminary experiments

No.:	Solvent system	Ratio
1	$CHCl_3$ + MeOH + H_2O	4:4:3
2	HEMWat	4:6:4:4
3	HEMWat	10:11:11:8
4	Petroleum ether, ethyl acetate, ethanol, water	1:1,2:1,2:1
5	HEMWat 17	1:1:1:1
6	HEMWat 21	5:2:5:2
7	HEMWat 15	2:3:2:3

The process of preparing those solvent mixtures is described in chapter 4.2.3.

The individual mixtures resulted in two phases (an aqueous and an organic phase) in which a small amount of the sample MAM01_05 was dissolved so that the compounds could be distributed between the respective phases. Then an aliquot of each phase was evaporated.

This was a quantitative analysis, which means that the resulting dried samples of the lower as well as the upper phase were dissolved in an equal amount of MeOH and analyzed by UPLC-ELSD (conditions see Chapter 4.2.2). The following list contains the results of the UPLC-ELSD analysis of the individual solvent mixtures (referred to as numbers). The upper chromatogram always shows the upper phase of the mixture, while the lower chromatogram shows the lower phase.

Solvent system No. 1

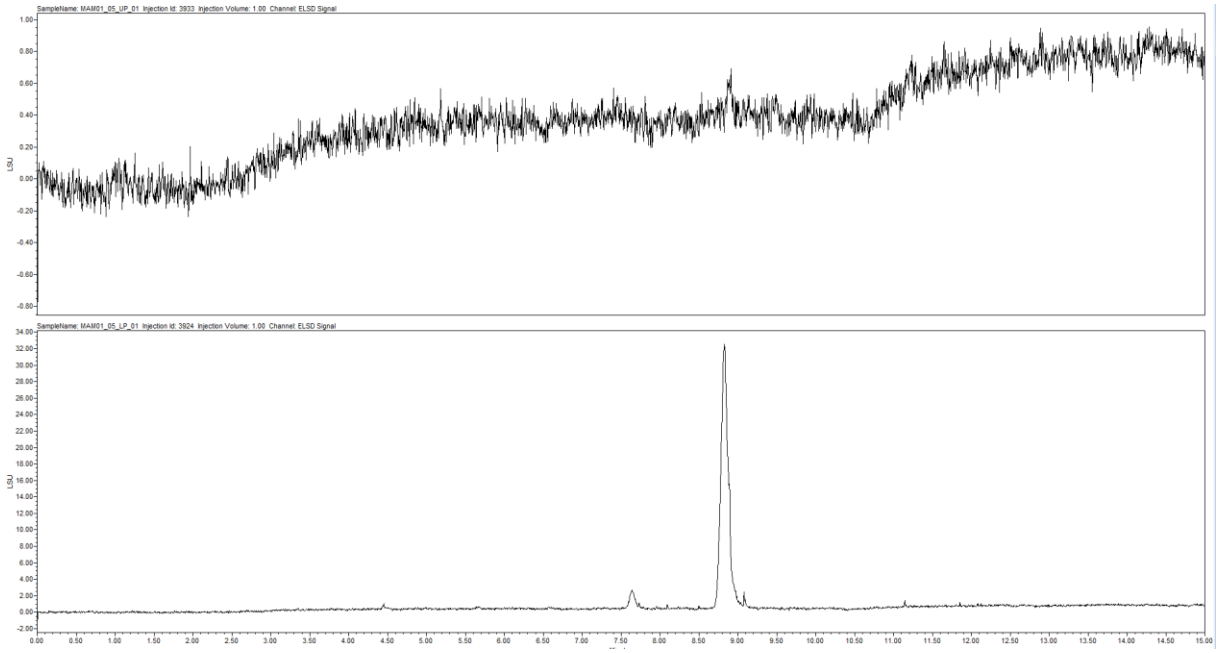

Figure 13. UPLC-ELSD analysis of solvent system No. Method: MA_PDAELSD_col1_598_50iso_15m, see chapter 4.2.2.

Solvent system No. 2

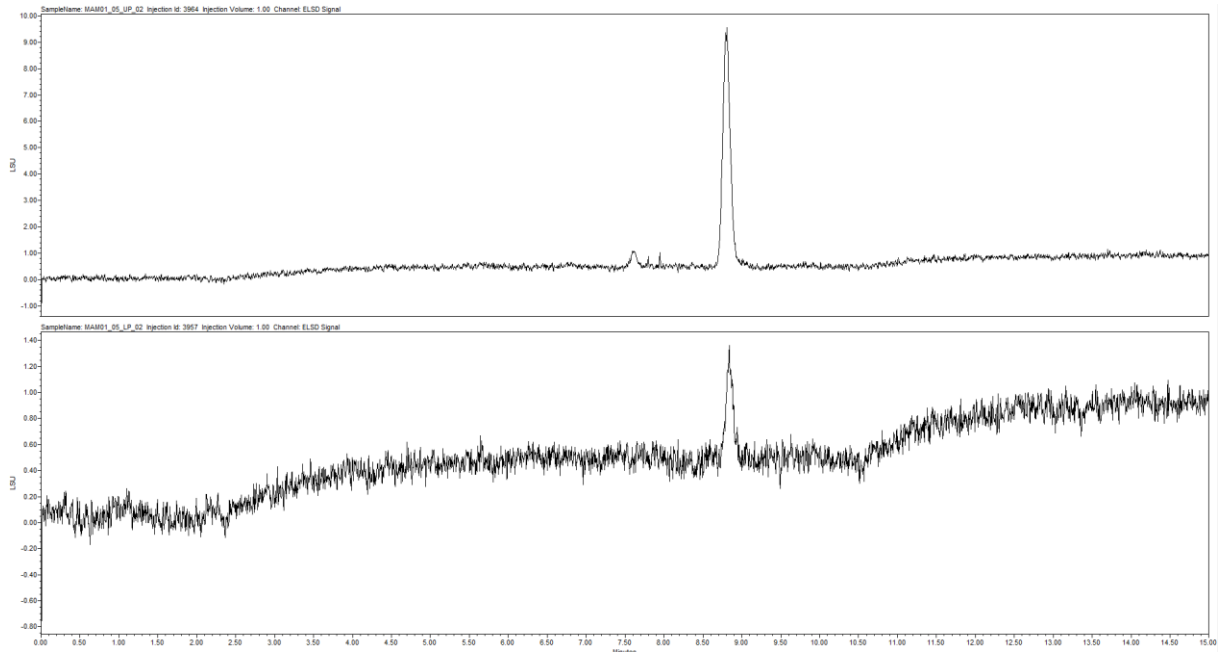

Figure 14. UPLC-ELSD analysis of solvent system No. 2. Method: MA_PDAELSD_col1_598_50iso_15m, see chapter 4.2.2.

Solvent system No. 3

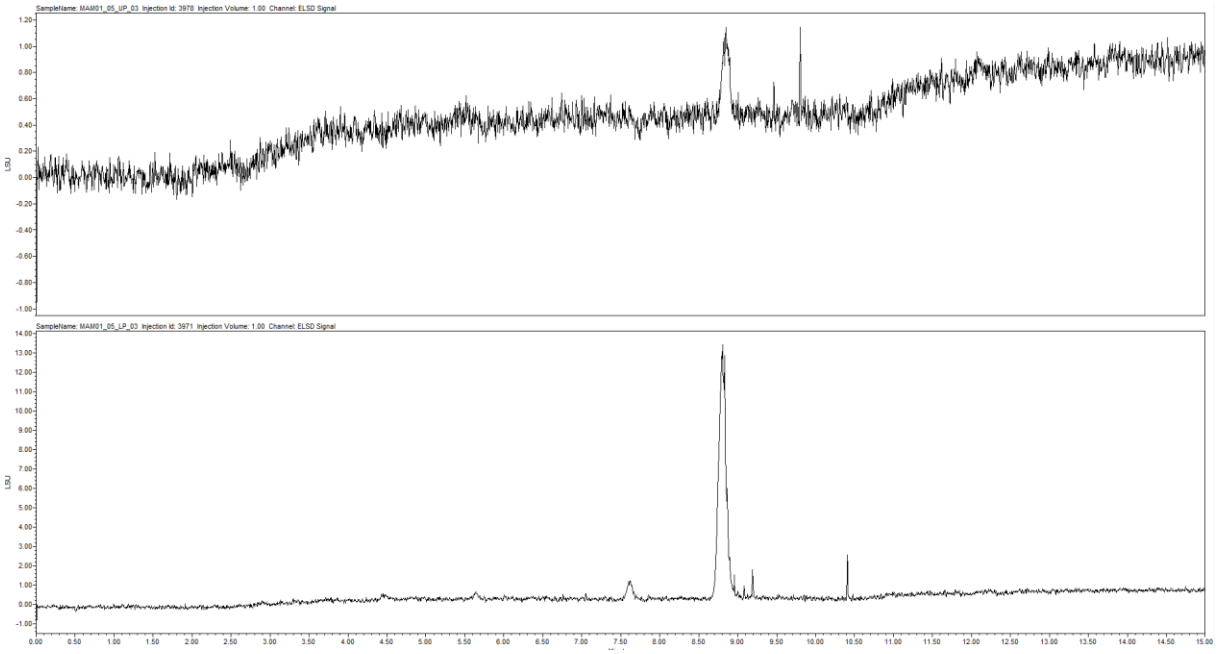

Figure 15. UPLC-ELSD analysis of solvent system No. 3. Method: MA_PDAELSD_col1_598_50iso_15m, see chapter 4.2.2.

Solvent system No. 4

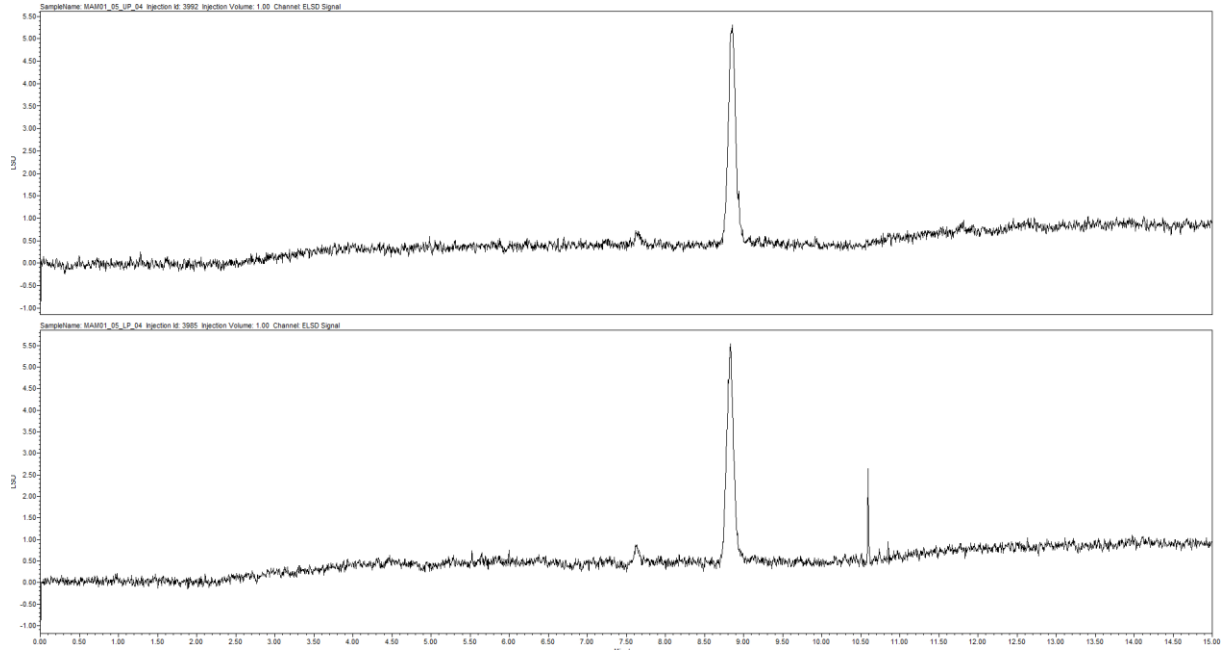

Figure 16. UPLC-ELSD analysis of solvent system No. 4. Method: MA_PDAELSD_col1_598_50iso_15m, see chapter 4.2.2.

Solvent mixture No. 5

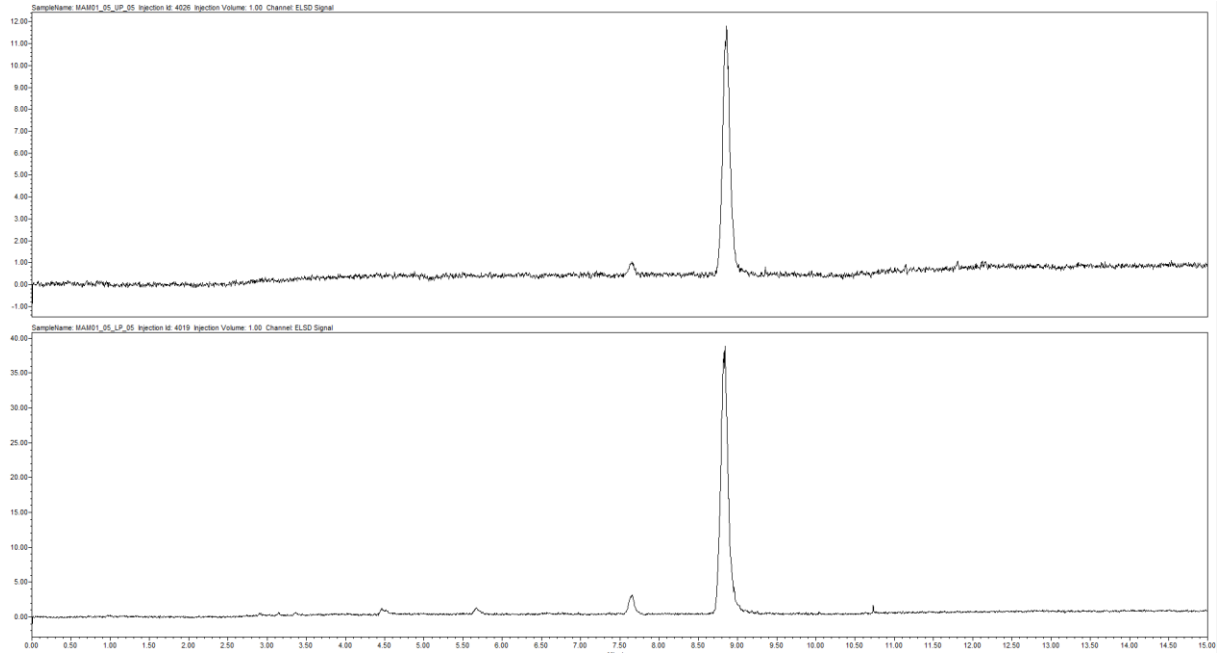

Figure 17. UPLC-ELSD analysis of solvent system No. 5. Method: MA_PDAELSD_col1_598_50iso_15m, see chapter 4.2.2.

Solvent mixture No. 6

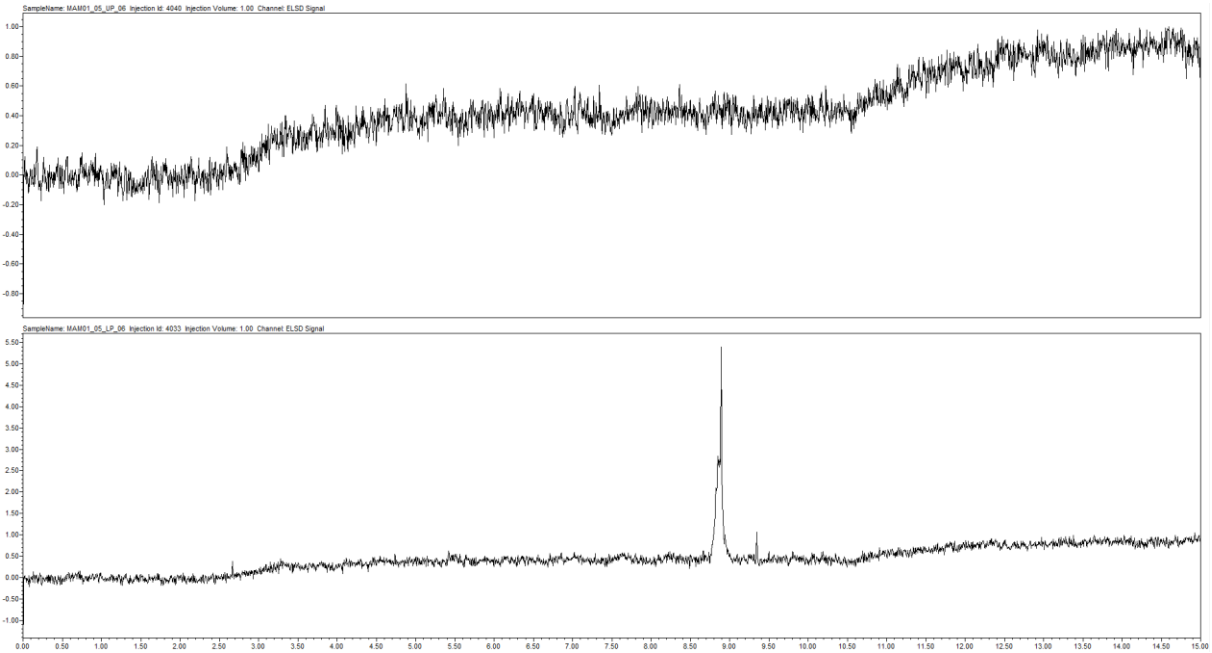

Figure 18. UPLC-ELSD analysis of solvent system No. 6. Method: MA_PDAELSD_col1_598_50iso_15m, see chapter 4.2.2.

Solvent mixture No. 7

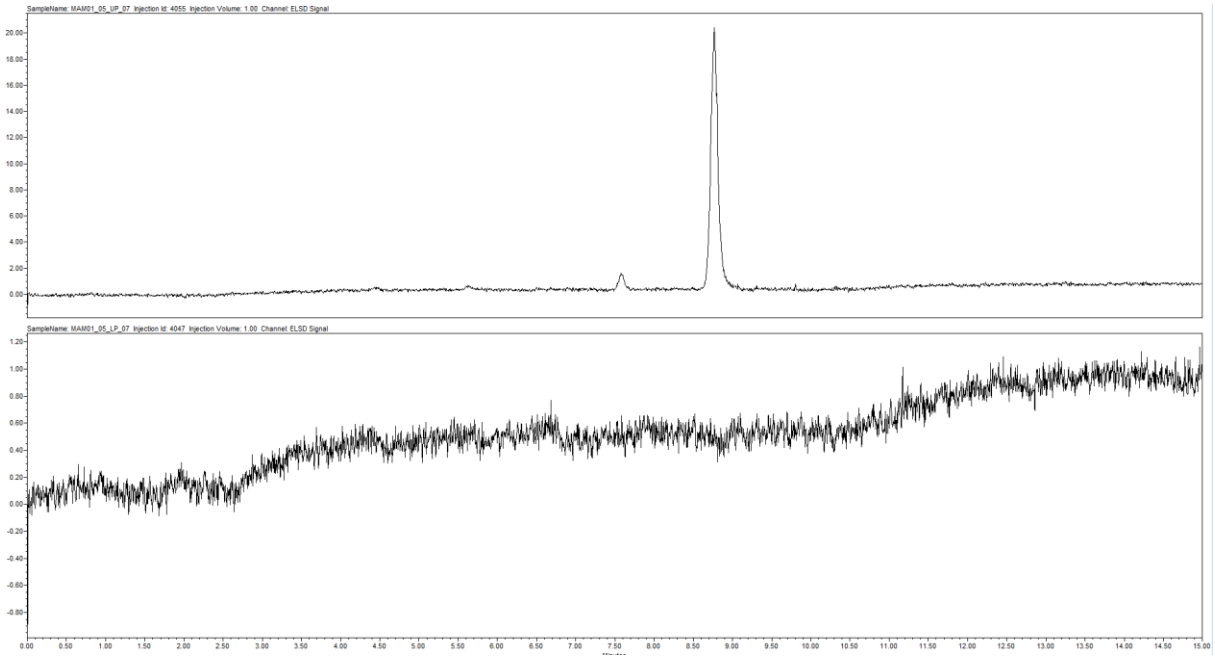

Figure 19. UPLC-ELSD analysis of solvent system No. 7. Method: MA_PDAELSD_col1_598_50iso_15m, see chapter 4.2.2.

The next step was to calculate the *K* values for the compounds of each solvent system. *K* values are expressed as the ratio of the concentration of an analyte in the stationary phase to its concentration in the mobile phase. A solvent system is considered suitable when *K* values of the compounds to be isolated range in the area of 0.5 – 2.0 (Ito, 2005). For the calculation, the peaks of the upper and lower phases of a compound must be integrated. Then the integrated areas are divided. In a reversed phase system, the upper phase is divided by the lower phase. In a normal phase system, it is exactly opposite.

The corresponding K values for reversed phase (RP) and for normal phase (NP) are shown in tables 4 and 5, respectively.

Table 4. Calculated RP K values for each compound in each solvent system.

Reversed Phase			
Solvent system No.	Solvent system ratio	Compound No.	
		Sanggenon O	Sanggenon C
1	4:4:3	0.00	0.00
2	4:6:4:4	0	9.10
3	10:11:11:8	0.00	0.08
4	1:1.2:1.2:1	0.66	0.10
5	1:1:1:1	0.18	0.28
6	5:2:5:2	0.00	0.00
7	2:3:2:3	0.00	0.00

Table 5. Calculated NP K values for each compound in each solvent system.

Normal Phase			
Solvent system No.	Solvent system ratio	Compound No.	
		Sanggenon O	Sanggenon C
1	4:4:3	0.00	0.00
2	4:6:4:4	0.00	0.11
3	10:11:11:8	0.00	13.23
4	1:1.2:1.2:1	0.6	1.00
5	1:1:1:1	0.18	0.28
6	5:2:5:2	0.00	0.00
7	2:3:2:3	0.00	0.00

It was decided to use the solvent system No. 4 to try a separation test. The reason for choosing solvent system No. 4 lies in the good partition coefficients, which are in the range between 0.5 and 2.0 (Ito, 2005).

The HPCCC instrument was hyphenated to the Interchim PuriFlash Chromatograph (HPCCC-Flash) as mentioned in chapter 4.2.3. In this

combination the Interchim instrument provides the detectors and serves as the pump, whereas the HPCCC device serves as the "column".

3.2 Separation of MAM01_05 by analytical Flash-HPCCC

An isocratic elution in both modes (RP and NP) was performed to determine the best suitable mode. Conditions are given in chapter 4.3.1.

In NP mode, a total of 94 fractions was collected. After thin layer chromatography (TLC) analysis, the fractions were combined to six fractions according to their fingerprint. These fractions were called MAM02v_01 – MAM02v_06.

Later these fractions were evaporated. They were analyzed by UPLC-ELSD detection with results shown in Figure 20.

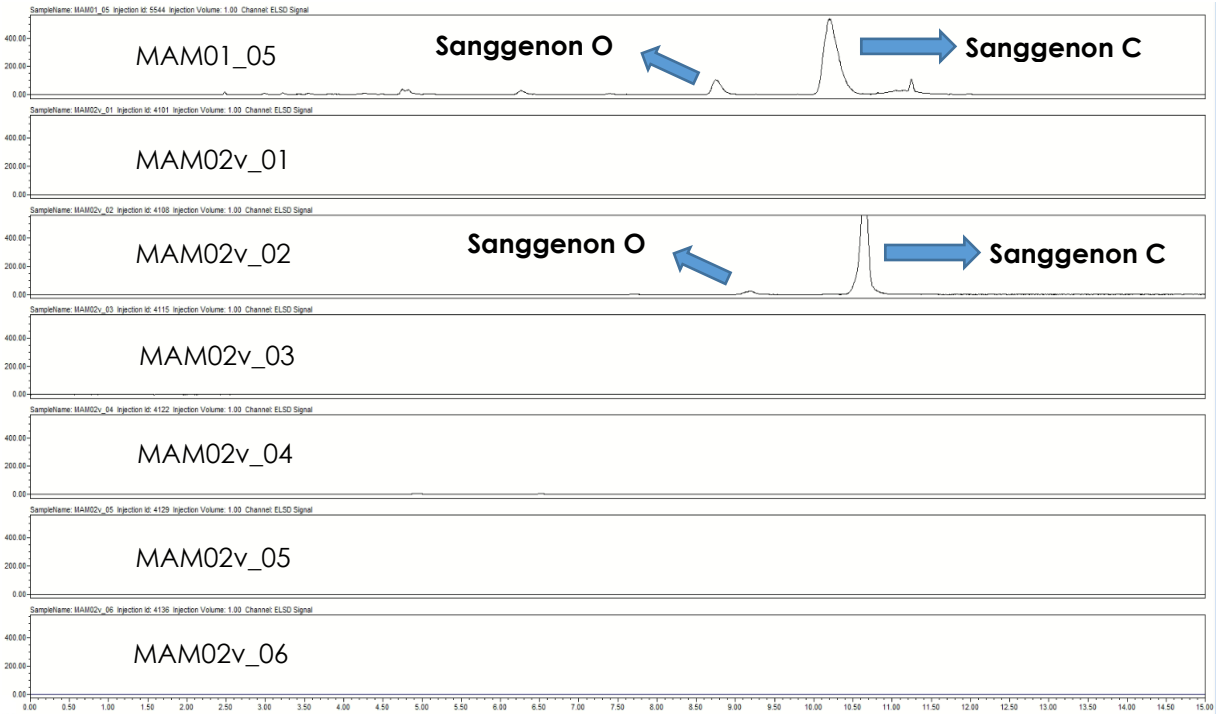

Figure 20. UPLC-ELSD analysis of Flash-HPCCC in NP with MAM01_05 (top) as reference and fractions MAM02v_01 – MAM02v_06. Method: MA_PDAELSD_col1_598_50iso_15m, see chapter 4.2.2.

In RP mode, a total of 101 fractions were collected, which were then combined to five fractions according to their TLC fingerprint. These fractions were called MAM02v_07 – MAM02v_11.

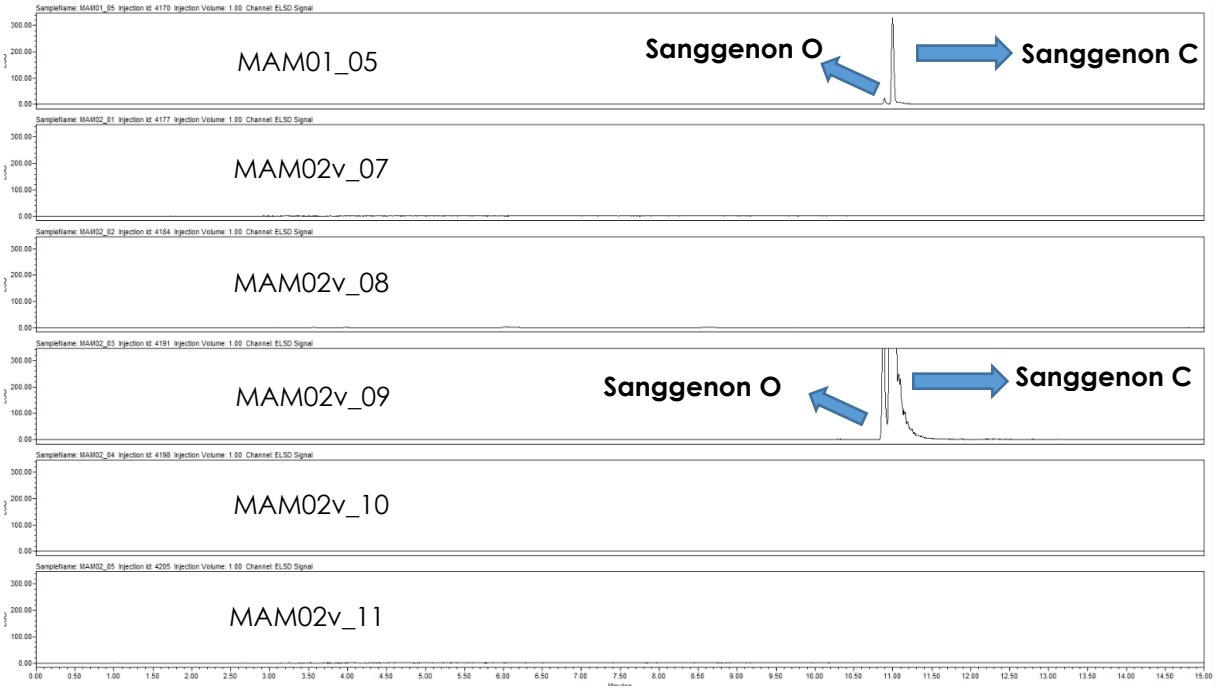

Figure 21. UPLC-ELSD analysis of Flash-HPCCC in RP with MAM01_05 (top) as reference and fractions MAM02v_07 - MAM02v_11. Method: MA_PDAELSD_col1_598_50iso_15m, see chapter 4.2.2.

After evaporation, the ELSD detection of the UPLC showed the following results (Figure 21):

No clear separation was achieved in either mode using HPCCC. In NP mode, both compounds are found in fraction MAM02v_02, while in RP mode they are found in fraction MAM02v_09. This led to the development of an alternative separation method using classical solid stationary phase material on the flash-chromatography (FC) (without hyphenation to HPCCC).

3.3 Separation of MAM01_05 by analytical FC

For the analytical preliminary experiments, the Interchim puriFlash® 4250 was equipped with a RP C_{18} column as stationary phase. The mobile phase consisted of a mixture of water and MeOH (preliminary experiment I) or a mixture of water and acetonitrile (ACN) (preliminary experiment II), respectively. The type of sample application was carried out using a dry load.

Therefore, a small amount of extract was dissolved in MeOH, the same amount of silica gel was added and the solvent was then evaporated using a rotary

evaporator. The resulting mixture was then transferred into a cartridge and filled with silica gel to the top. The fully filled cartridge was then connected to the instrument.

Detection was carried out, using the following integrated detectors of the FC:

- A PDA detection at a wavelength of 210 nm (orange line)
- A PDA detection with a wavelength scan from 200 to 600 nm (black line) and an
- Evaporative light scattering detection (ELSD) (red line)

The preliminary experiments were done with chromatographic parameters mentioned in chapter 4.3.2. Table 19 shows the conditions for preliminary experiment I, while Table 20 shows the conditions for preliminary experiment II.

Figure 22 and Figure 23 show the results of the respective experiments.

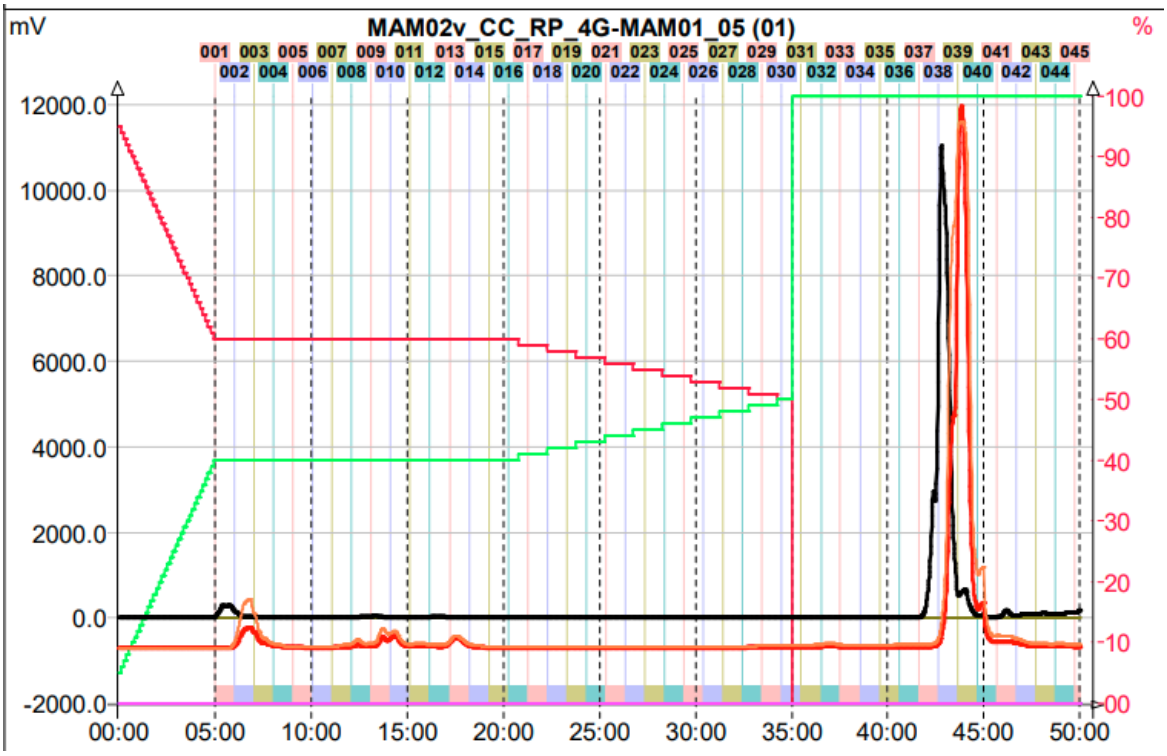

Figure 22. Preliminary experiment I: Analytical FC chromatogram of MAM01_05 in RP mode. Solvent A (red) = Water, Solvent B (green) = MeOH. Method: MAM02v_CC_RP_4G, see chapter 4.3.2.

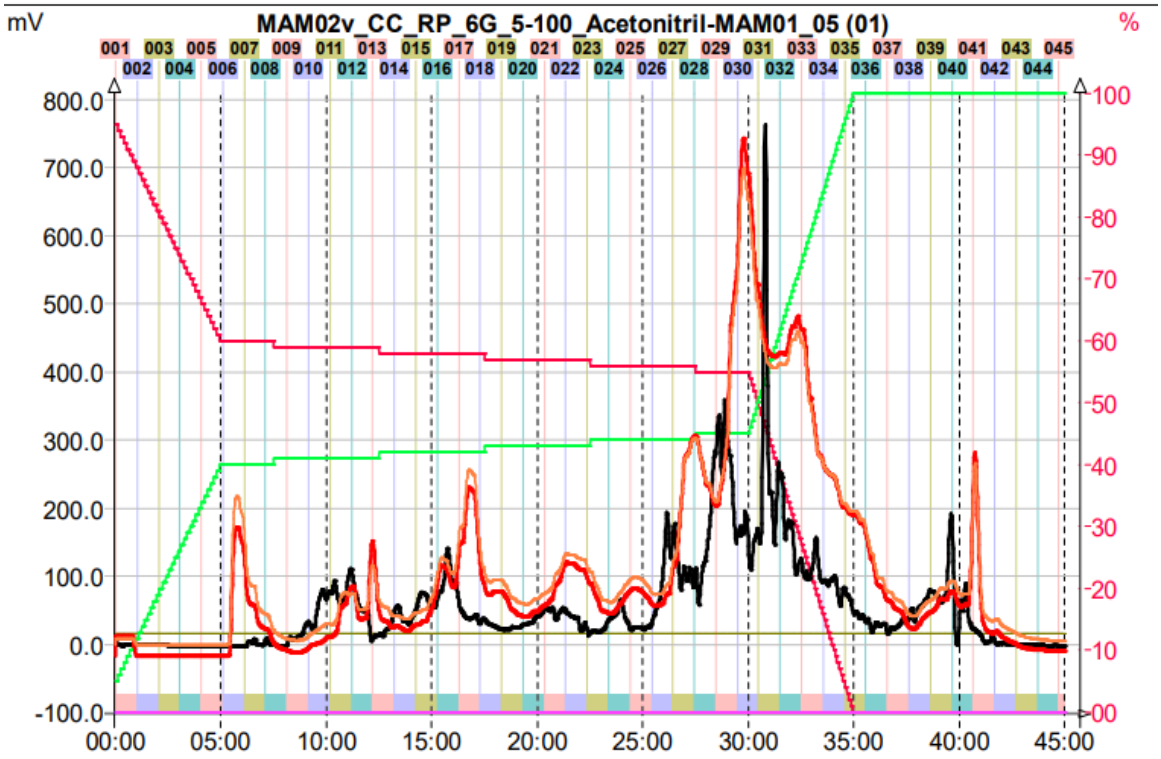

Figure 23. Preliminary experiment II: Analytical FC chromatogram of MAM01_05 in RP mode. Solvent A (red) = Water, Solvent B (green) = ACN. Method: MAM02v_CC_RP_6G_5-100_Acetonitrile, see chapter 4.3.2.

It turned out that the conditions of preliminary experiment II are more suitable for further separation. Therefore, it was performed on a preparative scale, subsequently.

3.4 Separation of MAM01_05 by preparative FC

For the preparative separation, some parameters were adapted (see chapter 4.3.3).

A preparative HPLC-column was connected to the instrument and the sample amount was upscaled to about 100 mg. Furthermore, the type of sample application was changed from using a dry load into direct injection as it was regularly leaking when using the dry load, which ultimately resulted in separation of lower quality. For using direct injection, the extract was simply dissolved in 2 mL methanol and, after equilibration, injected into a sample loop.

Figure 24 shows the chromatogram which resulted from this experiment (PDA detection, scan from 200 to 600 nm). The chromatogram shows several peaks, some of them could be assigned to compounds of high interest, for example sanggenon C.

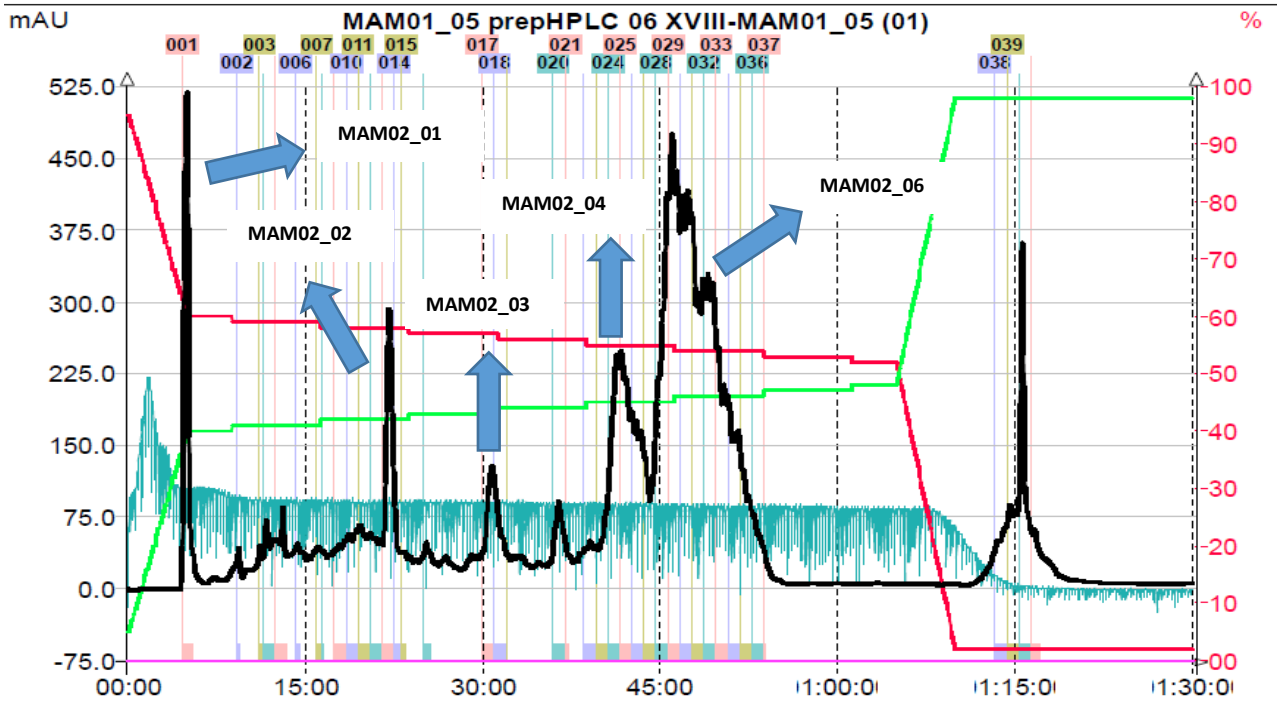

Figure 24. Preparative FC chromatogram of MAM01_05 in RP mode. Solvent A(red) = Water, Solvent B (green) = ACN. Blue line represents the pressure. Black line: PDA detection, scan from 200 to 600 nm. Method: MAM01_05prepHPLC, see chapter 4.3.3.

We then decided to collect the five peaks shown in Figure 24 in separate round bottom flasks. The area between sanggenon O and sanggenon C was collected in a sixth round bottom flask, which later turned out to be a mixture of the two compounds.

Table 6 shows the fractions obtained with the associated compound.

Table 6. MAM02_01 – MAM02_06 with associated compound

Fraction	Compound	Approximately collected fractions
MAM02_01	Unknown (polar compounds)	1-2
MAM02_02	Kuwanon L	14-16
MAM02_03	Sanggenon D	17-23
MAM02_04	Sanggenon O (not pure)	24-26
MAM02_05	Mixture of sanggenon O and C	27-29
MAM02_06	Sanggenon C	28-47

To check the purity of the compounds obtained, an aliquot of each fraction was transferred to an HPLC vial and subjected to UPLC-ELSD analysis, which resulted in chromatograms shown in Figure 25.

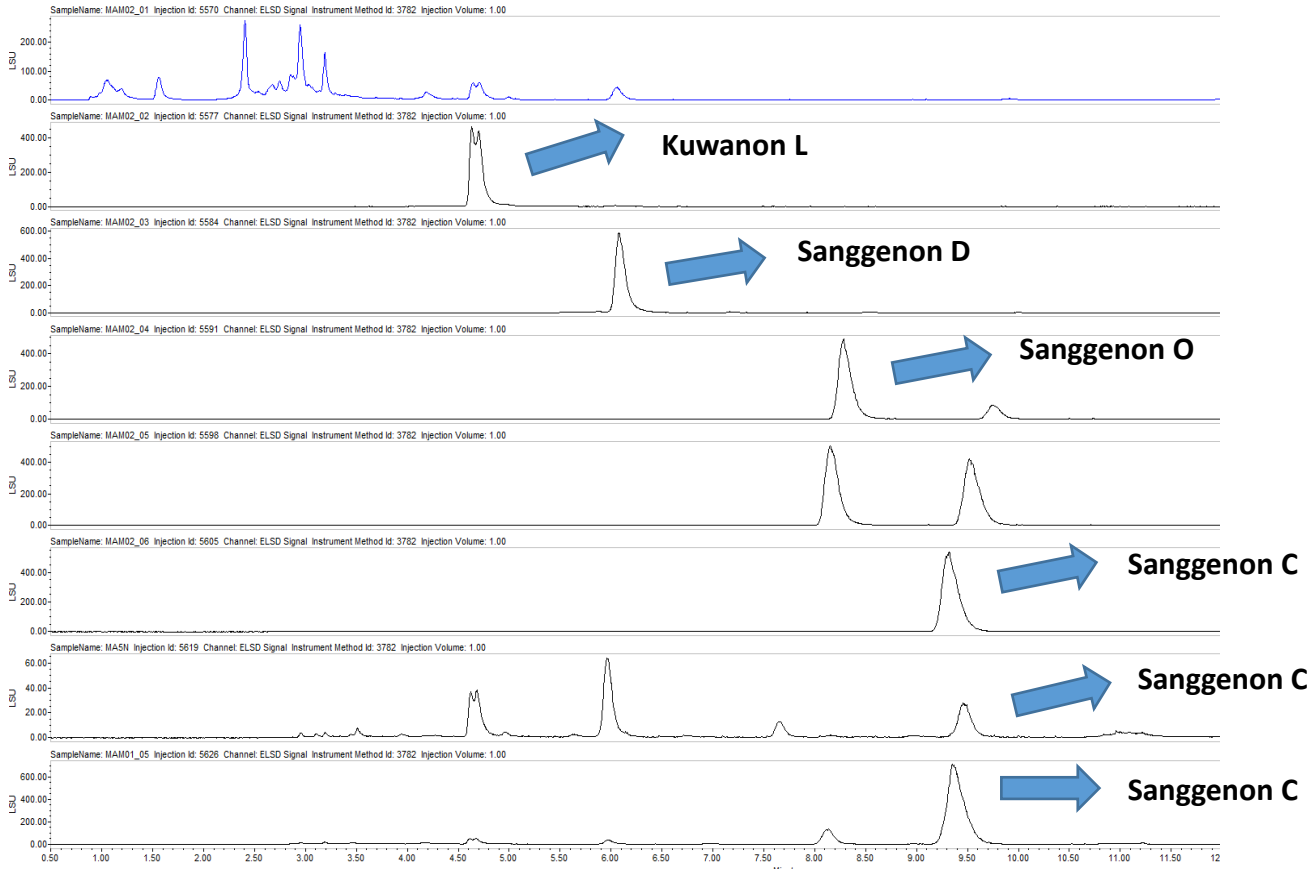

Figure 25. UPLC-ELSD analysis of MAM02_01 – MAM02_06 with MAM01_05 as reference. Method: MA_PDAELSD_col1_598_50iso_15m, see chapter 4.2.2.

The chromatograms show that all compounds could be obtained as more or less pure. The goal in the following flash runs was therefore to isolate as many pure compounds as possible. With the sanggenons O and C this turned out to be quite tricky since there was no baseline separation of the two peaks (Figure 24). In the end, the following purities of the collected compounds were achieved (Table 7).

Table 7. Purities of fractions MAM02_02 – MAM02_06

Fraction	Purity (%)
MAM02_02	97.14
MAM02_03	94.46
MAM02_04	84
MAM02_06	99.09

A total of 19 runs with approximately 100 mg of sample each were carried out in this way. Therefore, a total of about 2.5 g of fraction MAM01_05 was separated.

3.5 Combined fractions and yield of MAM01_05 fractions

As mentioned above, a total of six fractions was collected in respective round bottom flasks.

After the purity test using UPLC analysis, the solvents were evaporated using a rotary evaporator. In each case, a tared vial was prepared into which the isolated compounds were transferred. After a few days in the desiccator, the yield was determined.

Table 8 shows the yields of the individual constituents.

Table 8. Yields of the individual compounds

Fraction	yield (mg)
MAM02_01	1.9
MAM02_02	43.9
MAM02_03	40.9
MAM02_04	94.4
MAM02_05	25.0
MAM02_06	515.8

3.6 SEPARATION OF MAM01_06 BY PREPARATIVE FC

Fraction MAM01_06 was already quite pure which was determined using UPLC analysis with ELSD detection (Figure 26).

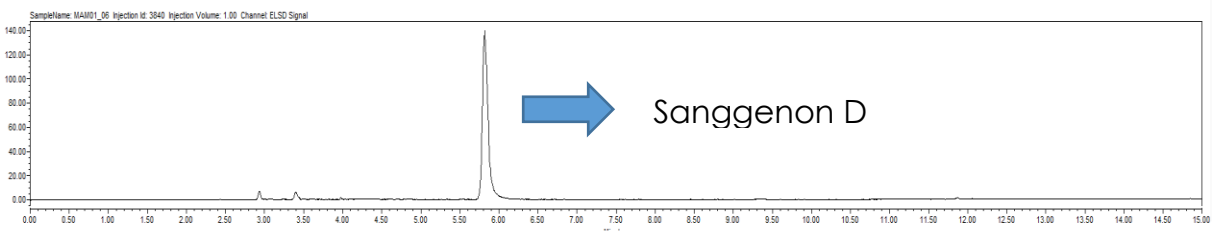

Figure 26. UPLC-ELSD analysis of MAM01_06. Method: MA_PDAELSD_col1_598_50iso_15m, see chapter 4.2.2.

The compound of interest in this fraction was assigned to be sanggenon D. For its isolation, preparative FC was used. In this case, however, the method originally generated for the separation of MAM01_05 was slightly adapted. The runtime was shortened significantly and a steeper gradient was applied. The reason for this is that sanggenon D elutes at an earlier retention time and there is no co-eluting compound from which it needed to be separated (see chapter 4.4).

Figure 27 shows the FC chromatogram of MAM01_06.

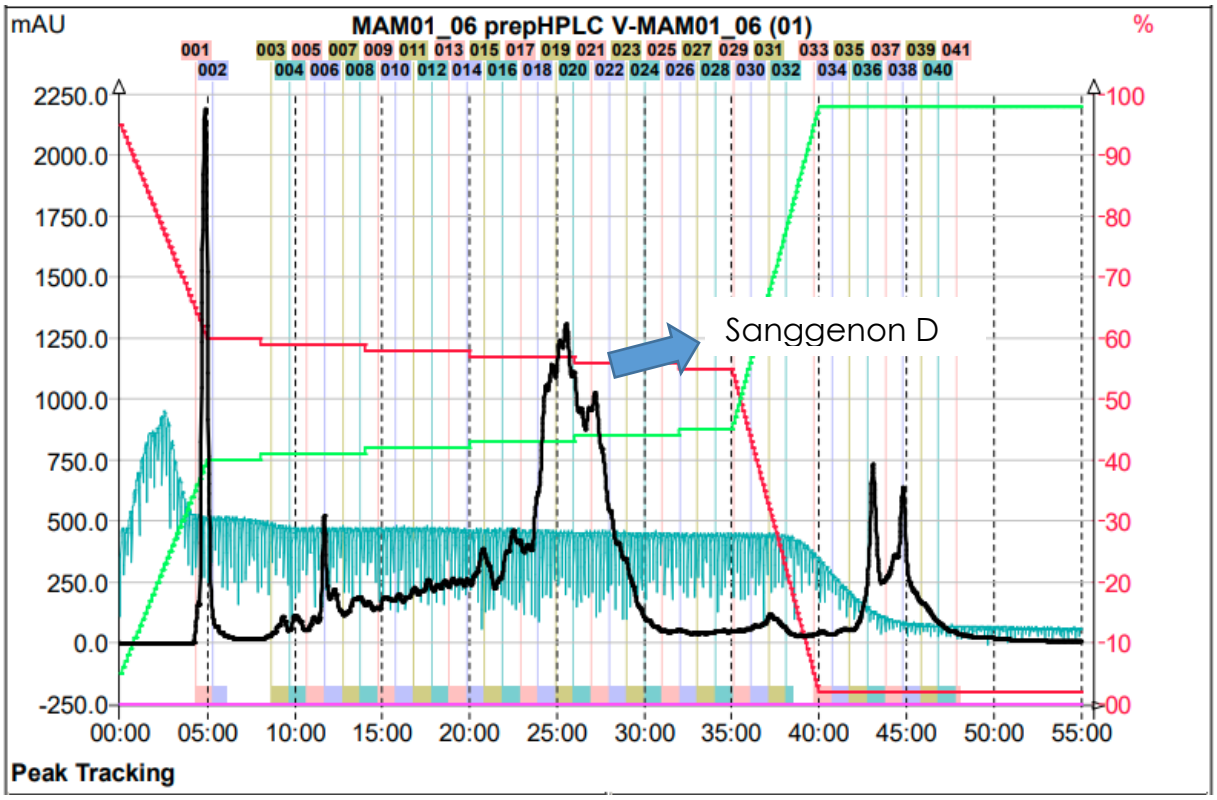

Figure 27. FC chromatogram of MAM01_06 in RP mode. Solvent A (red) = Water, Solvent B (green) = Acetonitrile. Blue line represents the pressure. Black line: PDA detection, scan from 200 to 600 nm. Method: MAM01_06prepHPLC, see chapter 4.4.

The fractions of the sanggenon D peak were again combined in a round bottom flask. Thus, the obtained fraction was called MAM03_01.

In this way, 29 separation runs were carried out and a total of approximately 3.5 g of fraction MAM01_06 were separated.

In the end, a purity check was performed again using UPLC analysis with fraction MA5N as reference (Figure 28).

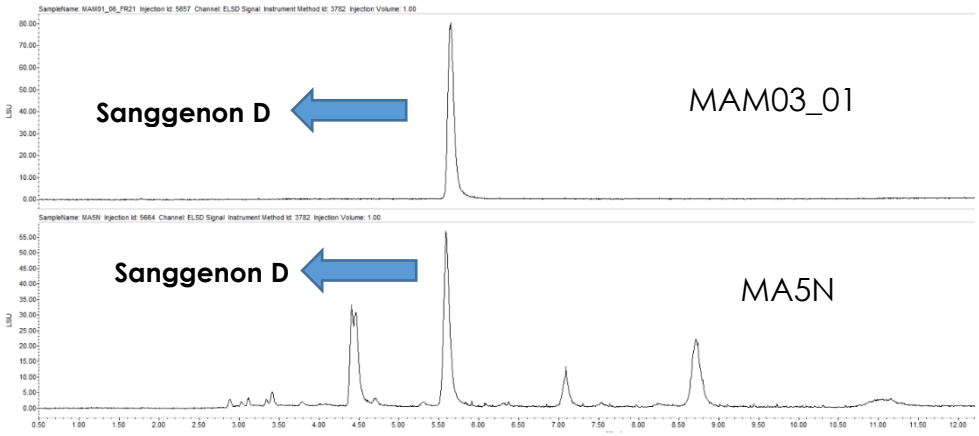

Figure 28. Purity check of MAM03_01 using UPLC-ELSD analysis. Method: MA_PDAELSD_col1_598_50iso_15m, see chapter 4.2.2.

A purity of 98.41% (UPLC-ELSD) was determined for MAM03_01.

3.7 COMBINED FRACTIONS AND YIELD OF MAM01_06

The yield was determined after the solvents were fully evaporated and the compound was transferred into a tared glass vial and dried in the desiccator (Table 9).

Table 9. Yield of MAM03_01

Fraction	Yield (mg)
MAM03_01	729.67

3.8 STRUCTURE ELUCIDATION OF ISOLATED COMPOUNDS

For final structure determination, approximately 5 mg of each isolated compound were dissolved in deuterated methanol (MeOD) and transferred into an NMR tube (Figure 29).

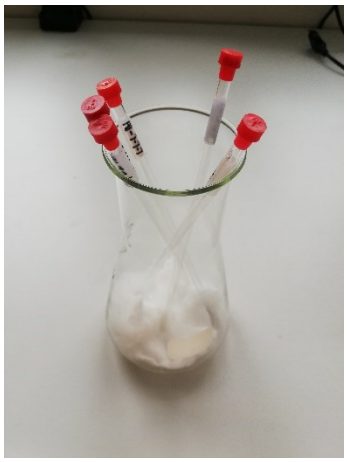

Figure 29. NMR tubes

One-dimensional (^{1}H NMR, ATP) as well as two-dimensional (HSQC, HMBC, COSY and NOESY) spectra were recorded. The instrument used for recording was a 500 MHz NMR spectrometer equipped with a cryo-probe head for enhanced sensitivity.

In this way, spectra of the already assigned compounds sanggenon D (MAM03_01), O (MAM02_04) and C (MAM02_06) were recorded.

The following chapters show the chemical structures (Figure 25, 27 and 28) and the chemical shifts of protons and carbons (Table 8, 10 and 11) of the individual compounds in comparison to literature.

3.8.1 ELUCIDATION OF MAM02_06 (SANGGENON C)

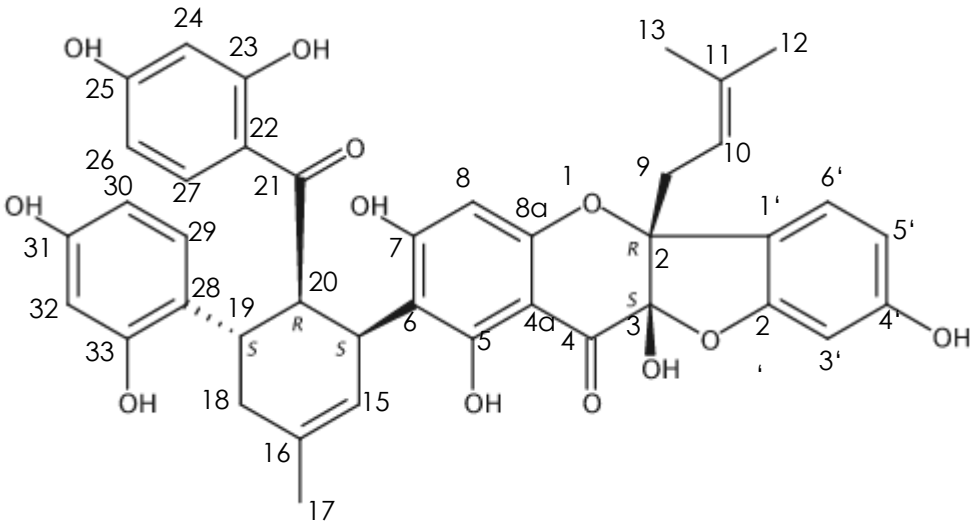

Chemical Formula: $C_{40}H_{36}O_{12}$

Molecular Weight: 708.71 g/mol

Figure 30. Sanggenon C, CAS Registry Number: 80651-76-9, edited by the author

Table 10. NMR spectroscopic data of MAM02_06 in MeOD in comparison to literature data

MAM02_06		Experimental	Experimental	Literature*	Literature**
Position		^{1}H	^{13}C	^{13}C	^{13}C
1'	C	-	121.5	122.2	122.2
2	C	-	92.1	92.0	92.0
2'	C	-	162.3	161.2	161.2
3	C	-	108.6	102.4	102.4
3'	CH	6.30	99.6	99.5	99.5
4	C	-	188.7	188.4	188.3
4'	C	-	162.2	161.2	161.2
4a	C	-	100.5	99.9	99.9
5	C	-	162.2	163.9	163.9
5'	CH	6.41	109.7	109.7	109.7
6	C	-	109.2	109.0	109.0
6'	CH	7.21	125.6	125.6	125.6
7	C	-	168.1	167.6	167.6
8	CH	5.63	95.9	96.5	96.5
8a	C	-	162.6	162.0	161.9
9	CH_2	2.68 / 3.01	32.3	32.0	32.0
10	CH	5.18	118.8	118.6	118.5
11	C	-	137.1	136.2	136.7
12	CH_3	1.58	18.1	18.1	18.1
13	CH_3	1.55	26.0	25.9	25.9
14	CH	4.16	34.1	35.8	35.9
15	CH	5.45	123.1	122.6	122.8
16	C	-	123.6	135.0	135.0
17	CH_3	1.82	23.7	23.7	23.7
18	CH_2	2.28 / 2.39	35.5	33.8	33.8
19	CH	3.87	36.0	32.8	32.8
20	CH	4.49	49.5	48.3	48.3

21	C	-	208.9	208.8	208.8
22	C	-	114.8	114.0	114.0
23	C	-	166.4	165.9	165.8
24	CH	6.17	103.7	103.8	103.8
25	C	-	164.3	166.8	166.8
26	CH	6.28	108.6	107.6	107.6
27	CH	8.07	134.6	129.0	129.0
28	C	-	109.2	121.3	121.3
29	C	-	156.9	156.5	156.5
30	CH	6.11	103.3	103.5	103.5
31	C	-	157.4	157.8	157.8
32	CH	6.25	107.3	108.7	108.7
33	CH	6.85	130.0	133.7	134.7

**: according to Nomura et al., 1981*

***: according to Rui-Chao and Mao, 2001*

The respective spectra are attached in the appendix (Figure A1 to Figure A6) alongside an excel-sheet which shows the HMBC and NOESY correlations (Figure A7). The following interpretations have been made on the basis of existing literature. The interpretational work started with the protons with a chemical shift of 1.55, 1.58 and 1.82. Due to their chemical shift and an integral of 3, it is likely that they are methyl groups and linked to their respective carbons that appear at 26.0, 18.1 and 23.7. The protons of 1.55 and 1.58 display a coupling to δ C 92.1, 118.8 and 137.1 as well as with the carbons of one another. This suggests that this is the prenyl group that is attached to position 2, although the carbon on position 9 shows no HMBC correlation to these protons. The protons with a chemical shift of 2.28/2.39 and 2.68/3.01 appear to be methylene groups linked to their carbons on position 9 and 18. Concerning position 9, the HMBC data indicate a connection to δ C 92.1, 118.8, 121.5 and 137.1, which once again completes the prenyl group, as well as its connection to the aromatic ring at position 1' (δ C 121.5). This ring shows three methine groups and three quaternary carbons, from which two (position 2' and 4') are

linked to an oxygen and have very similar surroundings. Hence, it is plausible that those two quaternary carbons show an identical chemical shift of δ C 162.2. The third quaternary carbon is the one already mentioned in position 1' (δ C 121.5). The three methine groups show typical proton shifts (δ 6.30, 6.41 and 7.21) for an aromatic ring and HMBC connections to one another as well as to all three quaternary carbons, except to the one of δ H 7.21 which does not display a coupling to δ C 121.5. When taking a look at ring A, there are similarities to the aromatic ring mentioned above, with the difference that five quaternary carbons (positions 4a, 5, 6, 7 and 8a) can be seen. Three of them, namely positions 5, 7 and 8a, have very similar surroundings and therefore show a chemical shift of δ C 162.2, 168.1 and 162.2 respectively. The remaining two quaternary carbons at positions 4a and 6 display chemical shifts of δ C 100.5 and 109.2 and show a HMBC connection to the one methine group on position 8 (δ H 5.63), which completes ring A.

Regarding the non-aromatic part with three stereochemical centers, only one quaternary carbon with a shift of δ C 123.6 is detectable (position 16). This hypothesis gets backed up by the HMBC data of the methylene group at position 18 as well as the methyl group at position 17, which both show a connection to position 16. The three stereochemical centers (position 14, 19 and 20), which all appear to be methine groups, not only show similar chemical shifts with δ H 4.16, 3.87 and 4.49, they also show similar HMBC data with the exception of position 14, which shows no HMBC connection at all. A reason for this might be due to stereochemical differences. Another point that stands out is that position 20 shows a slightly higher chemical shift of δ C 49.5, for which the reason could be the spatial proximity to the keto group at position 21. Which leads to the two carbons that are highly deshielded in this molecule. Position 21 with a chemical shift of δ C 208.9 and position 4 with δ C 188.7, that clearly stand out. Position 21 gets backed up by displaying a HMBC connection to position 19 and 20 as well as to the methine group on position 27.

The structure of the molecule is completed by two identical aromatic rings with two hydroxy groups, three methine and one quaternary carbon, which links the rings to the rest of the molecule. The methine groups of the rings show mostly very similar chemical shifts with δ H of around 6-7. One chemical shift though stands out with δ H 8.07 at position 27. The reason for this might be once again the spatial proximity to the keto group on position 21.

Most of the data gained in this thesis are clearly in line with the literature (Nomura et al., 1981) (Rui-Chao and Mao, 2001). A couple of positions (marked yellow in Table 10), namely 3, 16 and 28 stand out though with showing deviations in their chemical shift δ C compared to literature. A reason for this might be stereochemical differences, where position 3 is especially interesting and described in the following paragraph.

One point that clearly stands out though here is the stereochemistry. Nomura et al (1981) describe sanggenon C with the prenyl residue at position 3. SciFinder (American Chemical Society) and Rui-Chao and Mao (2001) show the prenyl residue at position 2 on the other hand. One reason why the prenyl group is more likely to be in position 2 is explained in Table 11 as well as Figure 31. Figure 31 shows the prenyl group with the surrounding area with the respective carbon (grey) and hydrogen (blue) atoms, while Table 11 shows the associated HMBC data.

Table 11. Recorded NMR spectroscopic HMBC data of MAM02_06

Position	Δ H	Δ C	Δ C HMBC
9	2.68	32.3	92.1 / 118.8 / 121.5 / 137.1
9	3.01	32.3	92.1 / 118.8 / 121.5 / 137.1
6'	7.21	125.6	92.1 / 99.6 / 162.2 / 121.5
3'	6.30	99.60	109.7 /121.5 / 162.2
5'	6.41	109.7	99.6 / 121.5 / 162.2

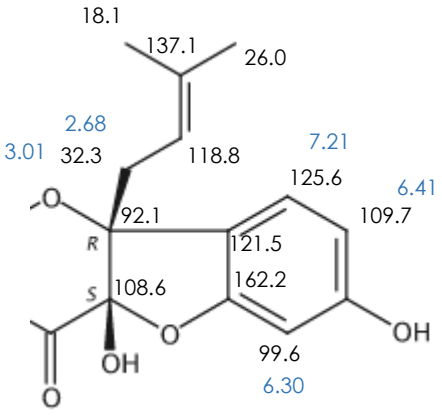

Figure 31. Section from sanggenon C with the corresponding prenyl group and associated NMR data gained in this thesis (American Chemical Society, 2020c, edited by the author).

The critical point in this case is position 1' with a chemical shift of δ C 121.59 ppm, which has an HMBC connection to the hydrogens on position 9, 6', 3' as well as 5'. If the prenyl group were to be in position 3 instead of position 2, such an HMBC connection to δ C 121.59 ppm would be less likely. There should also be an HMBC connection of the methylene-protons at position 9 to position 3 (δ C 108.63 ppm), which is not the case.

All this information suggests that the prenyl group is actually in position 2 and not in position 3 as described by Nomura et al. (1981).

3.8.2 ELUCIDATION OF MAM03_01 (SANGGENON D)

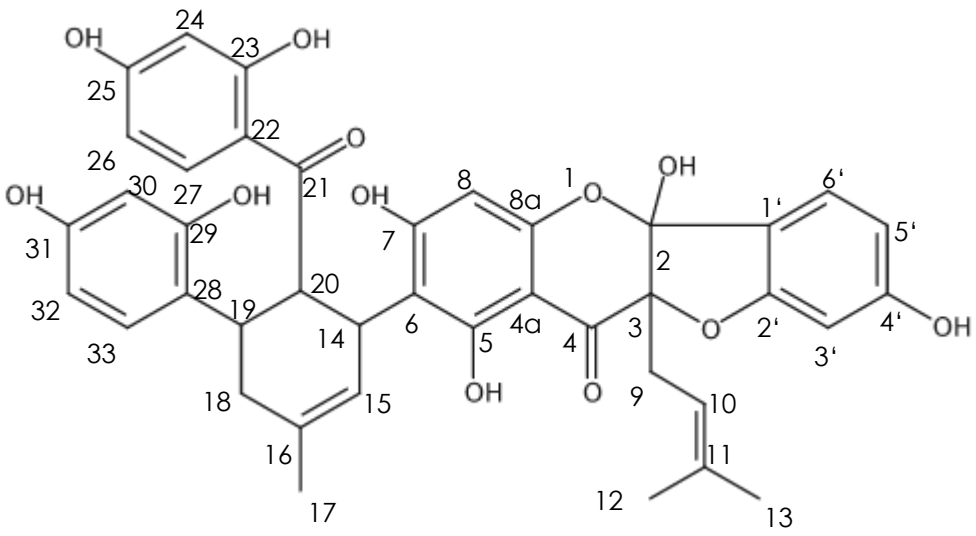

Chemical Formula: $C_{40}H_{36}O_{12}$

Molecular Weight: 708.71 g/mol

Figure 32 Sanggenon D, CAS Registry Number 81422-93-7. (American Chemical Society, 2020e) edited by the author

Table 12. NMR spectroscopic data of MAM03_01

MAM03_01		Experimental	Experimental	Literature*	Literature**
Position		^{1}H	^{13}C	^{13}C	^{13}C
1'	C	-	121.7	120.5	120.5
2	C	-	92.3	102.1	102.1
2'	C	-	162.3	159.7	159.7
3	C	-	165.8	90.7	90.7
3'	CH	6.35	99.8	98.7	98.7
4	C	-	188.8	187.0	187.0
4'	C	-	162.3	160.2	160.2
4a	C	-	101.0	99.0	99.0
5	C	-	161.6	164.3	164.3
5'	CH	6.42	109.7	109.1	109.1
6	C	-	110.2	109.1	109.1
6'	CH	7.20	125.5	124.9	124.9
7	C	-	167.0	167.0	167.0
8	CH	5.52	95.0	94.8	94.8
8a	C	-	162.3	160.2	160.2
9	CH_2	2.56 / 3.92	32.1	31.1	31.1
10	CH	4.97	118.4	117.5	117.5
11	C	-	137.4	135.5	135.5
12	CH_3	1.02	25.6	25.1	25.1
13	CH_3	1.37 / 1.51 / 1.58	18.0	17.6	17.6
14	CH	5.18	125.5	37.8	37.8
15	CH	5.15	119.2	124.3	124.3
16	C	-	137.0	131.9	131.9
17	CH_3	1.70 / 1.74	23.5	22.8	22.8
18	CH_2	2.67 / 3.02	32.3	37.8	37.8
19	CH	4.20	38.6	37.8	37.8
20	CH	4.40	37.6	45.2	45.2

21	C	-	n.d.[1]	208.6	208.6
22	C	-	116.1	114.3	114.3
23	C	-	166.0	164.3	164.3
24	CH	5.93	103.1	102.1	102.1
25	C	-	161.4	164.3	164.3
26	CH	5.97	108.3	107.3	107.3
27	CH	7.80	134.5	132.5	132.5
28	C	-	n.d.[1]	119.7	119.7
29	C	-	161.6	155.7	155.7
30	CH	6.10	103.7	103.1	103.1
31	C	-	161.6	156.1	156.1
32	CH	6.12	108.4	106.2	106.2
33	CH	7.56	134.1	129.0	129.0

[1] *not detected*

**: according to Nomura et al., 1982*

***: according to Nomura, 1988*

Considering the three described sanggenons (C, D and O) are stereoisomers, it could be assumed that the sum formula is identical. Also the data gained is highly in line with the literature with a few exceptions (marked yellow in Table 12), namely position 2, 3 and 14 from which positions 3 and 14 show massive differences to the literature. It appears as if position 2 and 3 are swapped in the literature data for sanggenon D (Nomura et al., 1982) compared to the literature data for sanggenon C (Nomura et al., 1981), which confirms the hypothesis that in this case the prenyl moiety is indeed at position 3 instead of position 2. Our experimental NMR data however show a chemical shift of δ C 165.8 in position 3 which represents a massive difference compared to the literature. A reason for that might be position 3 being a stereochemical center.

Position 14 also shows a huge difference between the experimental chemical shift of δ C 125.5 and the literature value 37.8. Once again, stereochemical proximity to the keto group on position 21 might be a reason.

3.8.3 ELUCIDATION OF MAM02_04 (SANGGENON O)

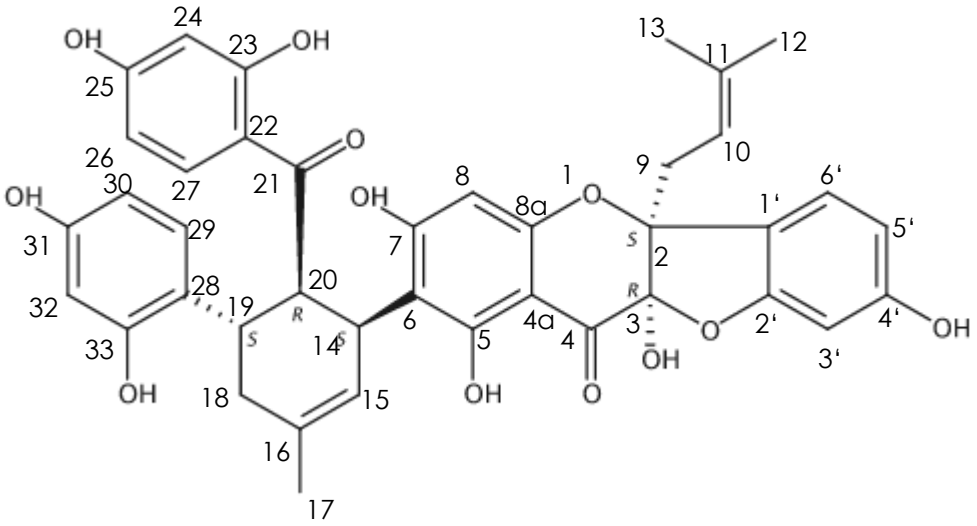

Chemical Formula: $C_{40}H_{36}O_{12}$

Molecular Weight: 708.71 ppm

Figure 33. Sanggenon O, CAS Registry Number 101664-32-8. (American Chemical Society, 2020f) edited by the author

Table 13. NMR spectroscopic data of MAM02_04

MAM02_04		Experimental	Experimental	Literature*
Position		^{1}H	^{13}C	^{13}C
1'	C	-	121.8	121.9
2	C	-	92.4	91.8
2'	C	-	161.6	161.1
3	C	-	109.2	102.2
3'	CH	6.31	99.6	99.3
4	C	-	189.0	188.2
4'	C	-	157.5	161.1
4a	C	-	100.6	99.8
5	C	-	162.3	163.4
5'	CH	6.43	109.7	109.5
6	C	-	109.3	96.4
6'	CH	7.22	125.5	125.5
7	C	-	168.2	167.5
8	CH	5.65	96.4	108.7

8a	C	-	162.3	161.8
9	CH_2	2.63 / 3.01	32.3	31.8
10	CH	5.01	118.9	118.4
11	C	-	137.2	136.8
12	CH_3	1.51	18.0	18.0
13	CH_3	1.17	25.6	25.4
14	CH	4.06	33.2	35.6
15	CH	5.50	123.3	122.6
16	C	-	135.2	135.1
17	CH_3	1.86	23.8	23.7
18	CH_2	2.23 / 2.42	34.2	33.6
19	CH	3.78	36.0	32.6
20	CH	4.50	48.3	47.9
21	C	-	209.6	208.5
22	C	-	114.5	113.8
23	C	-	167.0	165.8
24	CH	6.13	103.5	103.5
25	C	-	166.8	166.4
26	CH	6.29	103.7	107.3
27	CH	8.22	134.9	128.9
28	C	-	123.3	121.1
29	C	-	156.9	156.4
30	CH	6.31	103.7	103.2
31	C	-	157.8	157.6
32	CH	6.18	107.3	108.6
33	CH	6.87	129.3	134.6

**: according to (Rui-Chao and Mao, 2001)*

Considering the purity of sanggenon O of roughly 84%, the structure elucidation was easy to perform. The respective spectra and HMBC correlations are in the appendix (Figure A15 to Figure A 21).

As expected, the NMR data gained is well in line with the other sanggenons as well as with the literature (Rui-Chao and Mao, 2001). A few differences were recorded nevertheless (marked in yellow in Table 13). What stands out the most is position 8 with a chemical shift of δ C 96.4 compared to δ C 108.7 in literature.

Here it is remarkable that positions 6 and 8 have a very similar chemical shift of around δ C 109 and δ C 95 respectively in all sanggenons elucidated in this thesis. Even sanggenon C in literature (Rui-Chao and Mao, 2001) has such chemical shifts. The slight deviations in these positions might be due to impurity of the compound or the positions were swapped in literature.

3.9 NMR PREDICTION AND COMPARISON WITH AN NMR DATABASE

A ^{13}C NMR prediction as well as a comparison of carbon shifts with an NMR database was performed for every compound (sanggenon C, D and O) using "CSEARCH-NMR-Server" (N. Haider, W. Robien; https://nmrpredict.orc.univie.ac.at/c13robot/robot.php). Therefore, the structure was drawn into the program and the measured ^{13}C chemical shifts were entered. Finally, the program compares the entered data with the database concerning the respective compound and creates an NMR prediction as well.

The following figures (Figures 34-36) show the results of the respective predictions.

Table 14 shows the compounds with their associated "Overall similarity index (OSI)". The OSI provides information about the credibility of the data entered in comparison to the database. An OSI up to 3.0 stands for "reasonable", while an OSI above 5.0 stands for more or less "unbelievable" (N. Haider, W. Robien; https://nmrpredict.orc.univie.ac.at/c13robot/robot.php).

Table 14. Compounds with their associated OSI.

Compound	Overall similarity index (OSI)
MAM02_06 (sanggenon C)	3.3
MAM03_01 (sanggenon D)	4.8
MAM02_04 (sanggenon O)	2.4

MAM02_06 (sanggenon C)

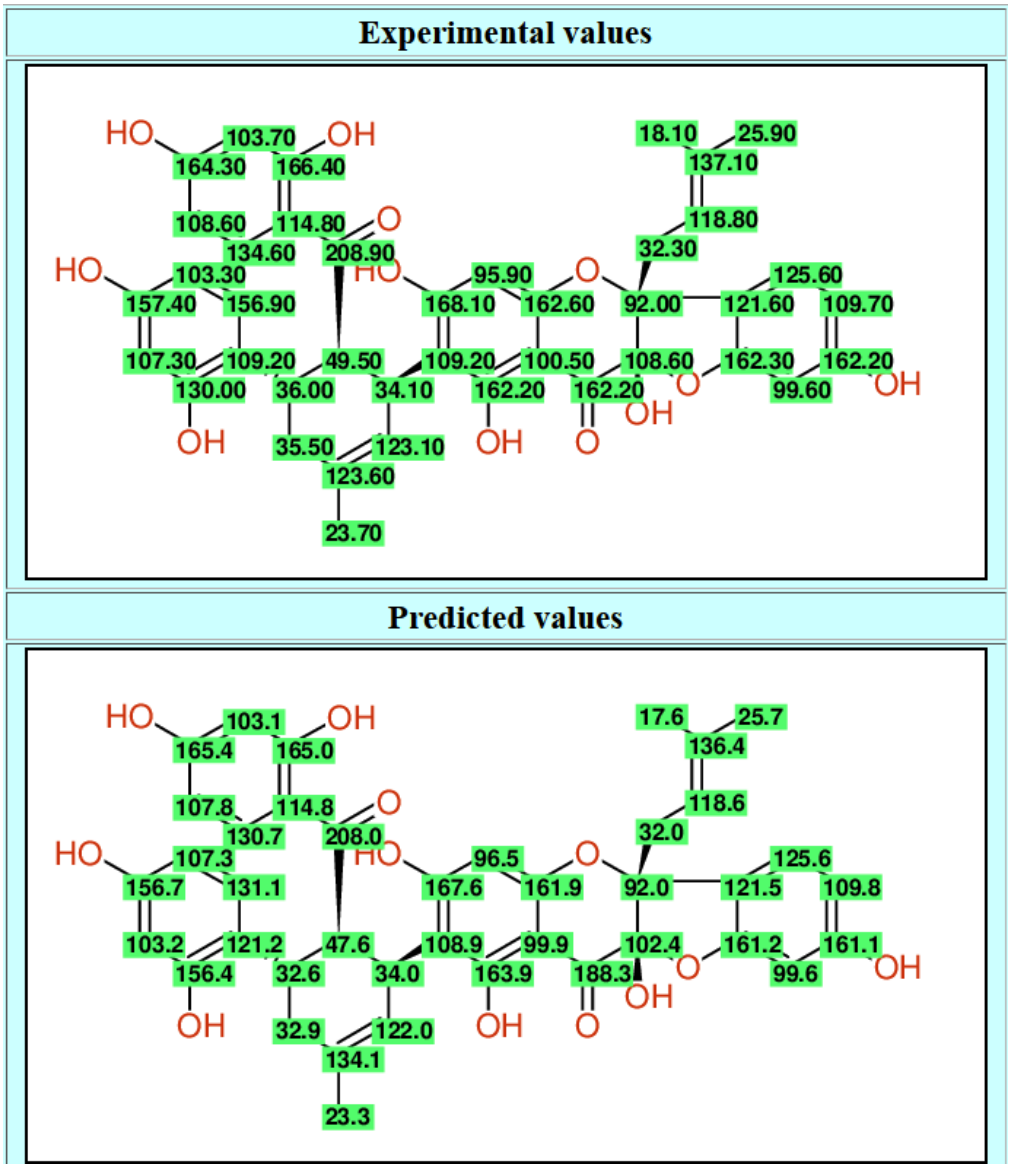

Figure 34. NMR data of MAM02_06 (sanggenon C) compared with predicted values.

MAM03_01 (sanggenon D)

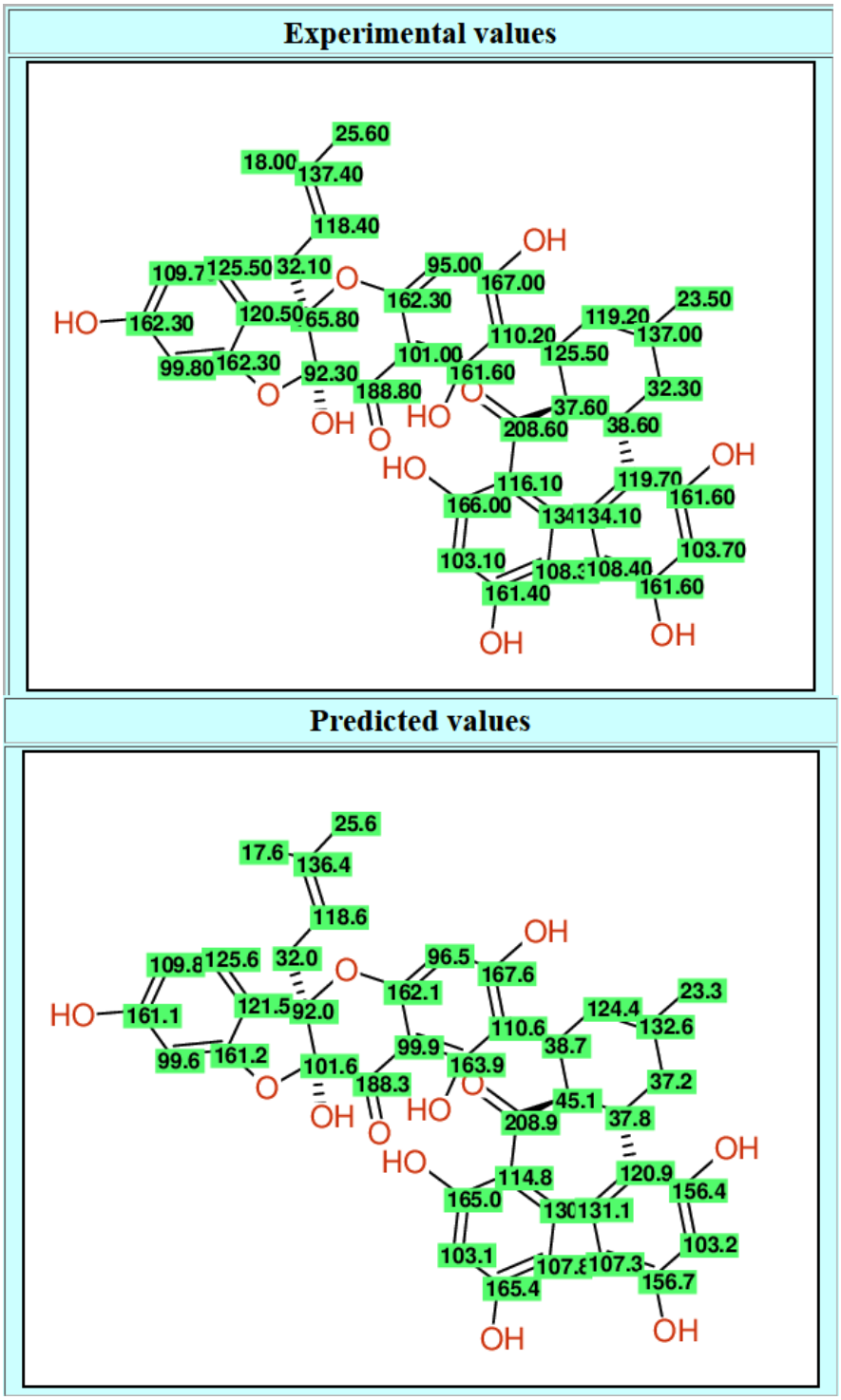

Figure 35. NMR data of MAM03_01 (sanggenon D) compared with predicted values.

MAM02_04 (sanggenon O)

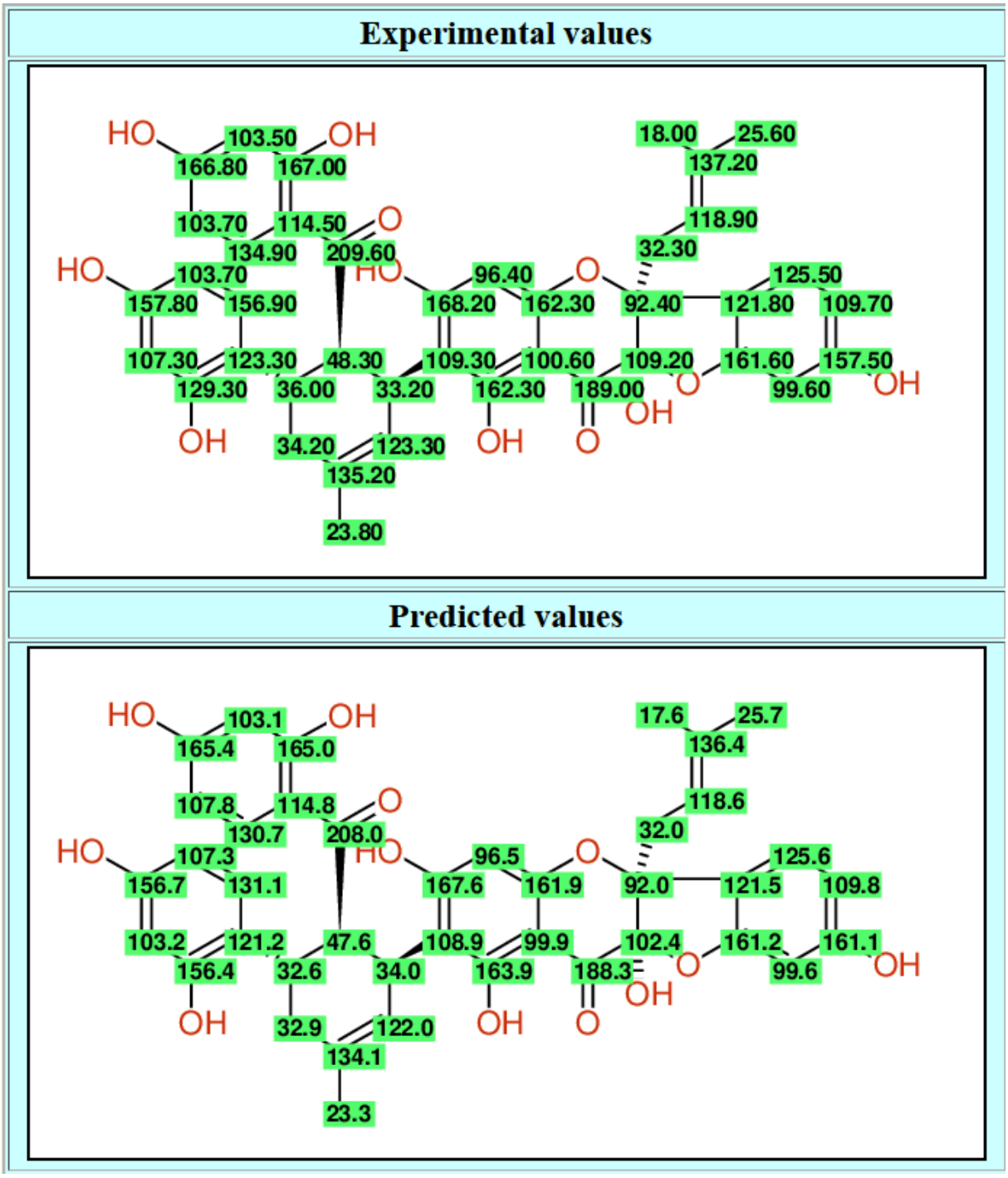

Figure 36. NMR data of MAM02_04 (sanggenon O) compared with predicted values.

3.10 Separation of MA5N by preparative FC

Another fraction from previous phytochemical investigations, called MA5N and obtained in 2009, contains sanggenon G, which showed the greatest inhibitory effect on the NA of IAV and *S. pneumoniae* of all prenylated flavonoids recently isolated from *M. alba* root bark (Figure 37)(Grienke et al., 2016).

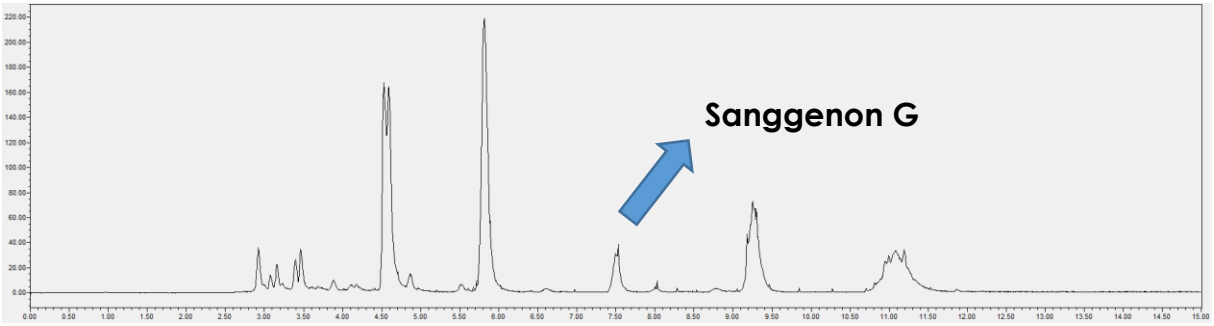

Figure 37. UPLC-ELSD analysis of MA5N. Method: MA_PDAELSD_col1_598_50iso_15m, see chapter 4.2.2.

Therefore, the aim was to re-isolate also sanggenon G in larger quantities.

A FC run was performed using the method described in chapter 4.5 with the results shown in Figure 38.

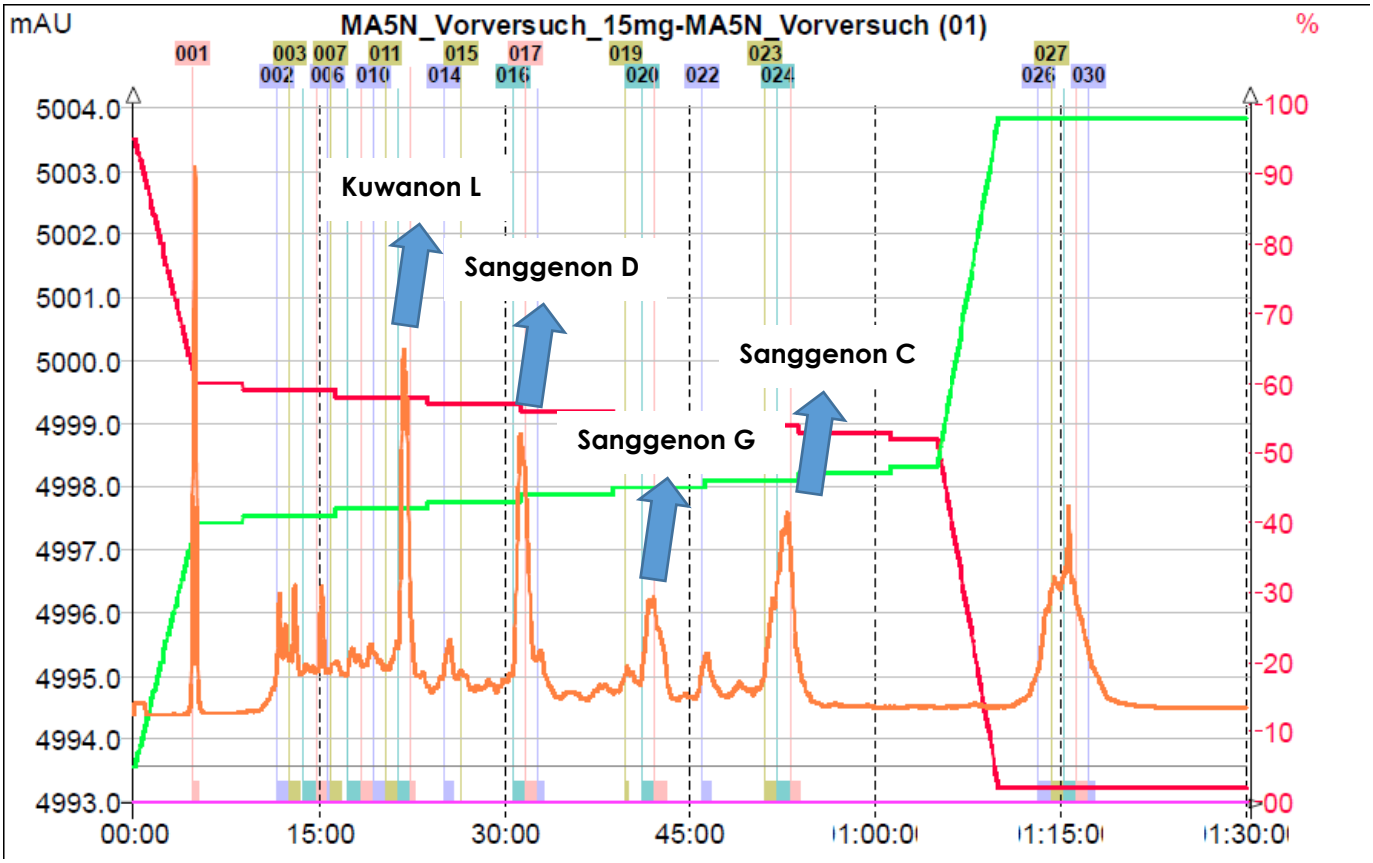

Figure 38. Preparative FC Chromatogram of MA5N in RP mode. Solvent A (red) = Water, Solvent B (green) = ACN. Detection: PDA at a wavelength of 210nm. Method: MA5N, see chapter 4.5.

Fingerprint and purity determination of fraction 22 were carried out using UPLC-PDA analysis (Figure 39).

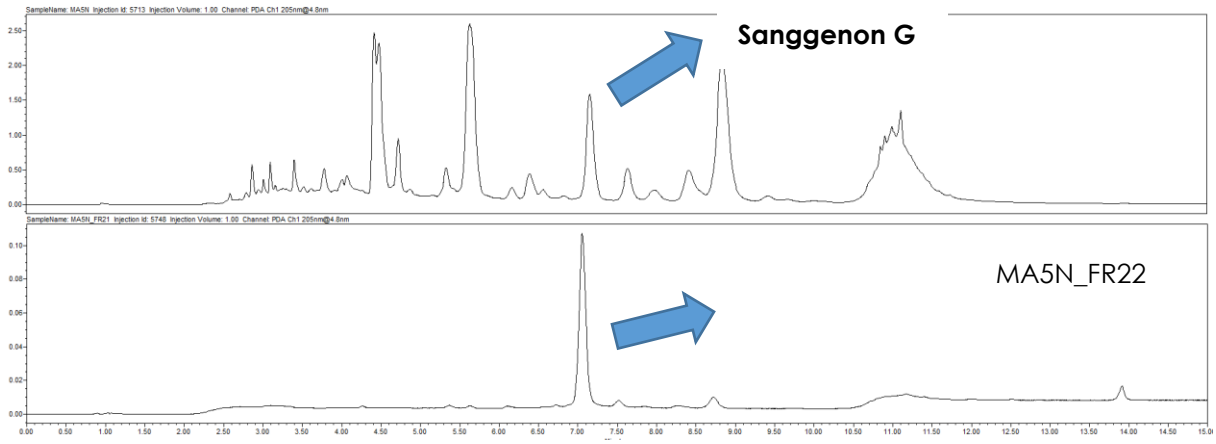

Figure 39. UPLC-PDA analysis of fraction 22 compared to MA5N. Method: MA_PDAELSD_col1_598_50iso_15m, see chapter 4.2.2

The method mentioned above (method name MA5N, see chapter 4.5) turned out to be suitable for isolating Sanggenon G. We then decided to collect the four distinct peaks shown in Figure 38 in separate round bottom flasks. The resulting fractions were called MA5N_01 – MA5N_04 (Table 15).

In this way, 27 separation runs were carried out and a total of approximately 3 g of fraction MA5N were separated.

3.11 Combined fractions and yield of MA5N fractions

The yield was determined after the solvents were fully evaporated and the compound was transferred into a tared glass vial.

Table 15. Yields of the individual compounds isolated from MA5N

Fraction	yield (mg)	Purity (%)
MA5N_01 (kuwanon L)	105.69	95.27
MA5N_02 (sanggenon D)	122.66	94.41
MA5N_03 (sanggenon G)	53.78	94.93
MA5N_04 (sanggenon C)	146.01	95.50

The purity check was performed again using UPLC analysis with fraction MA5N as reference (Figure 40).

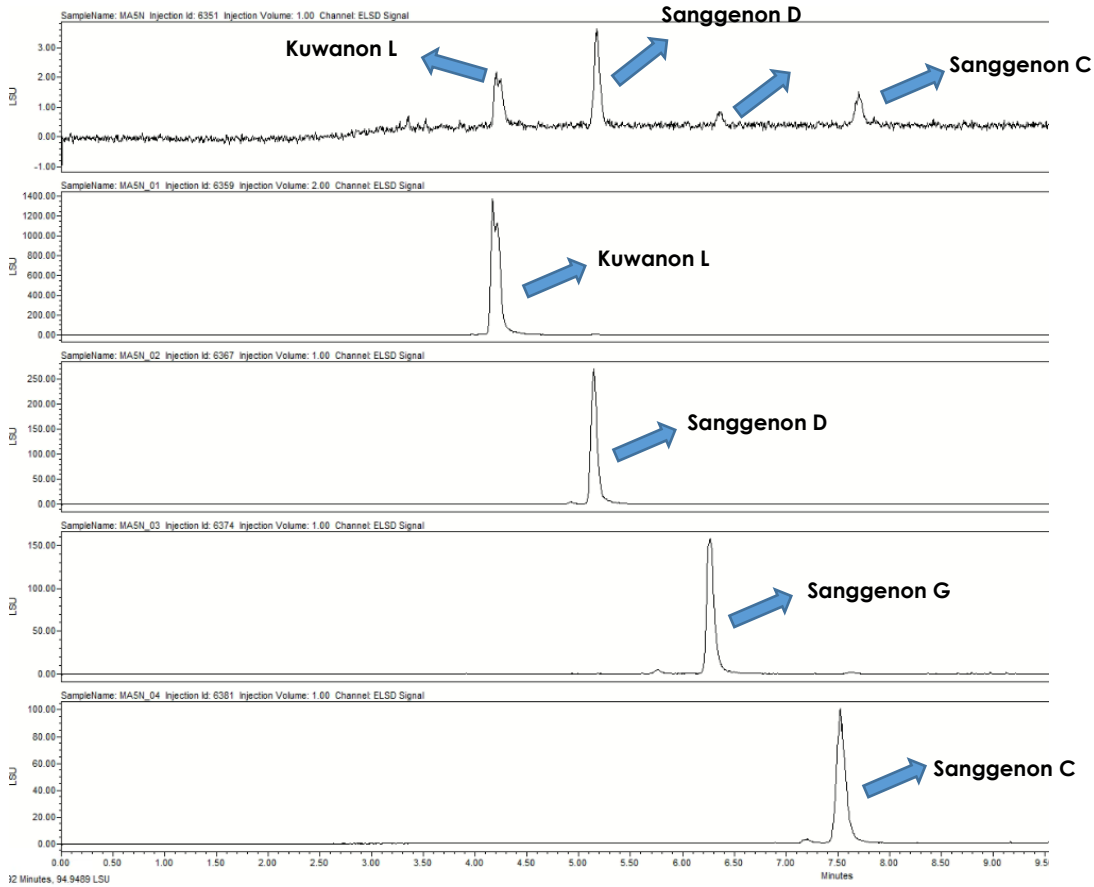

Figure 40. UPLC-ELSD analysis of fractions MA5N_01 – MA5N_04 compared to MA5N. Method: MA_PDAELSD_col1_598_50iso_15m, see chapter 4.2.2

4 MATERIAL AND METHODS

The following chapters show devices, solvents and instruments as well as methods used during this thesis.

4.1 DEVICES, SOLVENTS AND REAGENTS

Devices

Device	Technical Features / Brand
Balance	Sartorius BP210D
Centrifuge	Mini spin, Eppendorf
Centrifuge	Genevac, EZ-2 HCl Compatible
Sample concentrator	Sample concentrator FSC400D, Techne
HPCCC	Spectrum Dynamic extractions
Flash Chromatography	Interchim puriFlash 4250 Software: Interchim soft
Rotary Evaporator	R-210, Büchi Laboratorium Technologie AG
TLC Spray Cabinet	CAMAG TLC spray cabinet II
Ultrasonic Bath	Transsonic T 460, Elma
UPLC	Waters Acquity UPLC H-Class Modules: PDA and ELSD Software: Empower
UV Lamp	CAMAG
Vacuum Pump	V-710, Büchi
Vortex mixer	Genius 3
NMR structure elucidation	Software: MestReNova
NMR instrumentation	BRUKER 500 Ultrashield™ Prodigy CryoProbe (TCI) for enhanced sensitivity

Solvents and reagents

Solvent/reagent	Description
Acetonitrile	HiPerSolv CHROMANORM® ≥99.9%, gradient grade for HPLC
Ethanol 96%	ÖAB distilled
Ethyl acetate	ÖAB distilled
Methanol	ÖAB distilled
Methanol	HiPerSolv CHROMANORM® ≥99.8%, for HPLC
n-Hexane	ÖAB distilled
Petroleum ether	ÖAB distilled
Water	Double distilled

Column material

- Interchim prepacked column: PuriFlash Column 15C18HQ 6g
- Silica gel 60 (0.040-0.063 mm)

TLC-plates

TLC Silica gel 60 F_{254}

Spraying reagent: Sulfuric Acid - Vanillin

- Sulfuric Acid, 5% in Methanol
- Vanillin 1% in Methanol

4.2 ANALYTICAL METHODS

4.2.1 THIN LAYER CHROMATOGRAPHY

Thin layer chromatography (TLC) is a separation technique, in which the stationary phase is solid while the mobile phase is liquid. The stationary phase is on a thin plate (therefore "thin layer" chromatography) onto which the sample is applied alongside a reference substance. The mobile phase on the other hand is filled into a chamber, in which the TLC plate is transferred. The mobile phase migrates up the plate by means of capillary strength, while the substances are being separated due to different interactions between the two phases. After the separation process, the plate is dried and detected with a UV lamp. In most cases derivatization agents are needed to visualize analytes either under visible or under UV light.

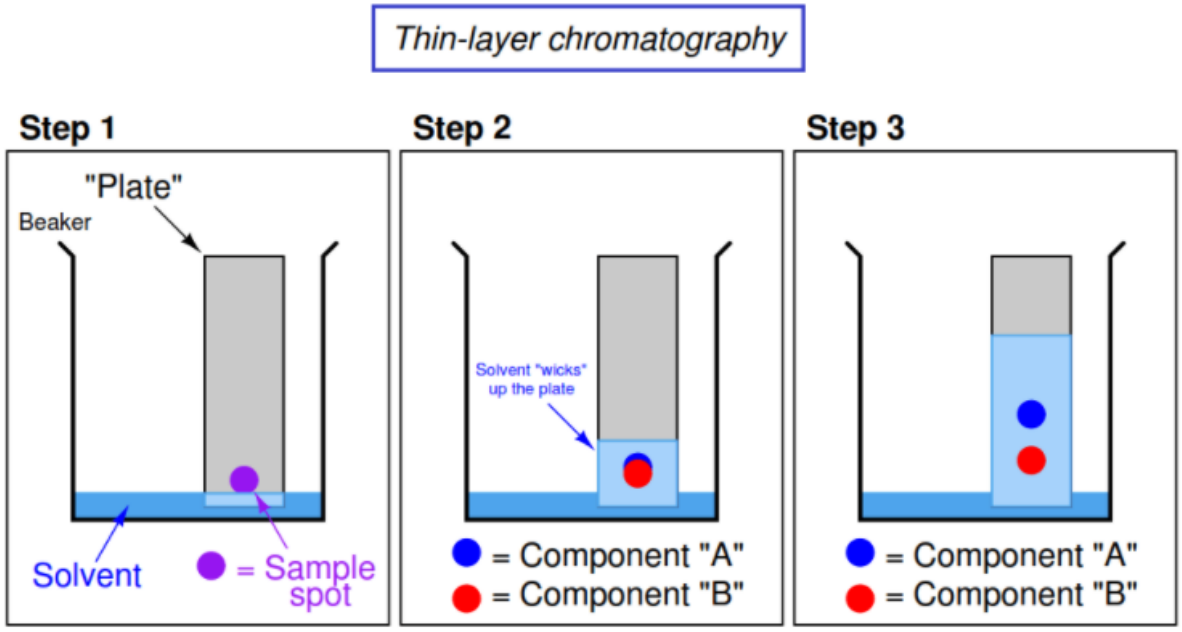

Figure 41. Steps of a TLC. https://instrumentationtools.com/thin-layer-chromatography-manual-method/, effective: November 2020

Throughout this diploma thesis the following parameters were applied in TLC analysis:

Stationary phase:	TLC Silica gel 60 F254 from Merck
Mobile phase:	DCM : MeOH (6 : 1)
Spraying agent:	sulfuric acid and vanillin
Detection:	UV_{254}, UV_{366} and VIS

4.2.2 UPLC – ANALYSIS

UPLC stands for ultra-performance liquid chromatography and is the more sophisticated high-performance liquid chromatography (HPLC) technique with higher sample throughput and lower sample volume. It uses columnar particles with a diameter of about 1.7 µm. The system used within this work is the "Acquity UPLC H-Class System" from the company "Waters Corporation" (Waters, 2020).

Figure 42. Acquity UPLC H-Class

UPLC conditions used for analysis of *M. alba* fractions and pure compounds were as follows (Table 16).

Table 16. UPLC conditions used for analysis of M. alba fractions.

Time (min)	A = H_2O (%)	B = ACN (%)
0	95	5
1	50	50
8.9	50	50
9	2	98
15	2	98

Flow rate: 0.3 mL/min

Column temperature: 40°C

PDA detection wavelength: 205 nm

Injection Volume: 1-5 µL

Equilibration time: 5 min

Column: ACQUITY UPLC BEH Phenyl, 130Å, 1.7 µm, 2.1mm X 150 mm

Method name: MA_PDAELSD_col1_598_50iso_15m

4.2.3 HIGH-PERFORMANCE COUNTER CURRENT CHROMATOGRAPHY

High Performance Countercurrent Chromatography (HPCCC) is a form of liquid-liquid chromatography. Therefore, not only the mobile phase is liquid but also the stationary phase. It is especially suited for natural products due to its high loading capacity and total sample recovery.

With the aim to enhance time effectiveness of the HPCCC separation, the Interchim puriFlash® 4250 was hyphenated to the Spectrum Dynamic extractions device. The Interchim instrument serves as the pump, whereas the HPCCC device serves as the column. This allows the use of detectors as well as the fraction collector that are integrated into the puriFlash®. The combination of these two instruments is later on referred to as 'Flash-HPCCC'.

Solvent selection

First, about 1 mg of MAM01_05 was dissolved in 5 ml solvent mixture. Two phases were formed, an aqueous and an organic phase, in which the compounds should distribute according to their physico-chemical features. Thereafter, 1 ml of each phase was removed and evaporated using a rotary evaporator. The resulting extracts were dissolved in an equal amount of MeOH and analyzed in the UPLC. Table 17 shows the various solvent systems which were tested for Flash-HPCCC separation.

Table 17. Solvent systems tested for Flash-HPCCC

No.:	Solvent system	Ratio
1	$CHCl_3$ + MeOH + H_2O	4:4:3
2	HEMWat	4:6:4:4
3	HEMWat	10:11:11:8
4	Pretroleum ether, ethyl acetate, ethanol, water	1:1,2:1,2:1
5	HEMWat 17	1:1:1:1
6	HEMWat 21	5:2:5:2
7	HEMWat 15	2:3:2:3

Establishing the HPCCC column

At first, the column was filled with stationary phase at a speed of 200 rpm. Once fully filled, the mobile phase was pumped into the system with a speed of 1,600 rpm (Figure 43). Once the equilibrium has been established, the sample was injected and the separation began.

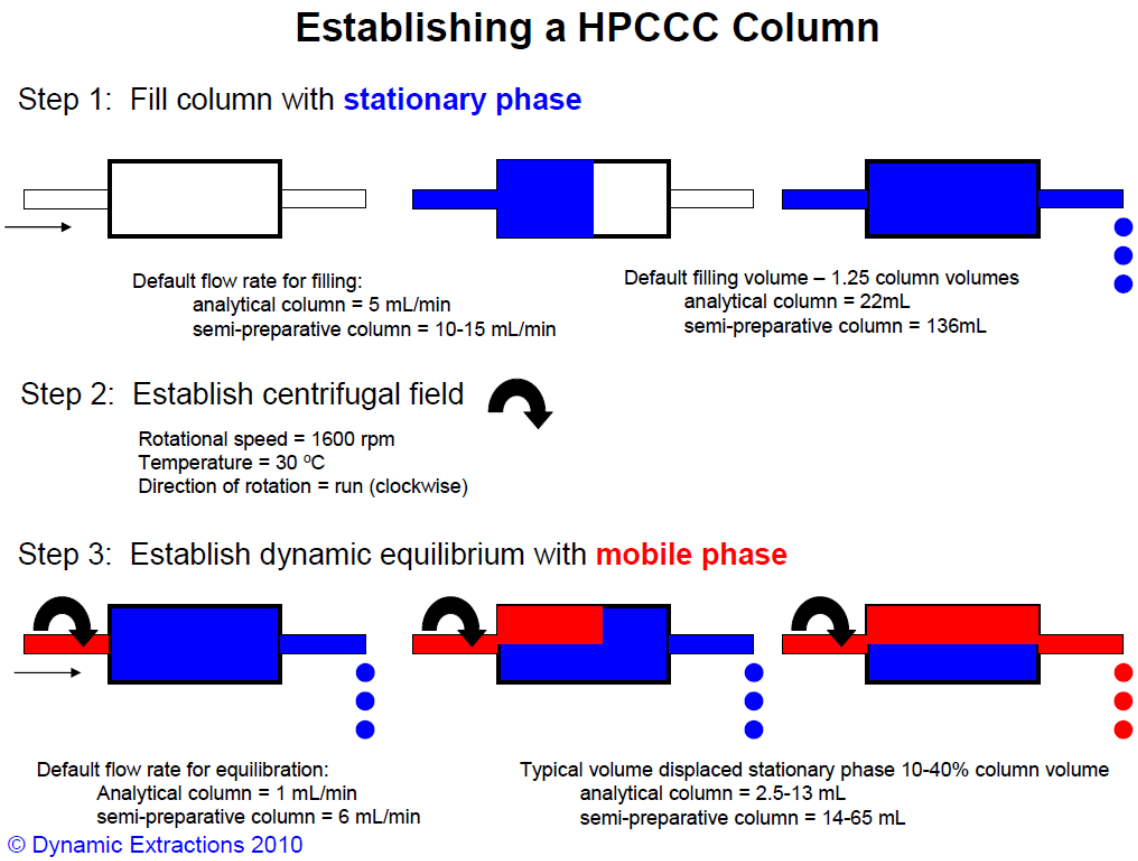

Figure 43. Process of establishing a HPCCC column. (Dynamic Extractions, 2010)

4.2.4 FLASH-CHROMATOGRAPHY

Flash-chromatography (FC) is a separation method applying medium pressure to push the mobile phase through the column. This results in the ability of using smaller silica particles as the stationary phase, higher resolution and shorter elution times (Swathi et al., 2015).

The instrument used for FC separations is the Interchim puriFlash® 4250.

Following chapters show the conditions used for analytical as well as preparative method development.

4.3 PHYTOCHEMICAL INVESTIGATION OF MAM01_05

4.3.1 SEPARATION BY ANALYTICAL FLASH-HPCCC

An analytical column with a volume of 22 ml and a sample loop of 1 ml was used. About 30 mg of fraction MAM01_05 were dissolved in 1 ml of a 1:1 mixture of mobile and stationary phases. An isocratic elution was performed. A volume of about 2.0 mL per fraction was collected in isocratic elution and extrusion.

The experiment was performed in reversed phase mode, which means that the stationary phase was the upper phase (nonpolar phase) of the solvents. Subsequently, the experiment was repeated in a normal phase mode, where the stationary phase was the lower phase (polar phase).

Flash-HPCCC was used for preliminary analytical experiments for which the parameters are shown below (Table 18).

Table 18. Gradient used in analytical Flash-HPCCC analysis. Solvents: Petrolether ; Ethylacetate ; Ethanol ; Water. A = Stationary phase, B = mobile phase

Time (min)	Flow Rate	% A	% B
00:00	2.0	100	0
40:00	2.0	100	0
42:00	1.0	100	0
04:57:05	1.0	0	100
05:02:05	1.0	0	100

4.3.2 SEPARATION BY ANALYTICAL PURIFLASH

Preliminary experiment I for MAM01_05:

Column: PuriFlash Column 15C18HQ 6g

Applied amount: 30 mg

Type of sample application: Dry load

Method name: MAM02v_CC_RP_4G

Table 19. Mobile phase solvents: A = Water, B = Methanol

Time (min)	Flow Rate	%A	%B
00:00	5 mL/min	95	05
05:00	5 mL/min	60	40
20:00	5 mL/min	60	40
35:00	5 mL/min	50	50
35:03	5 mL/min	0	100
45:00	5 mL/min	0	100
50:00	5 mL/min	0	100

Preliminary experiment II for MAM01_05:

Column: PuriFlash Column 15C18HQ 6g

Applied amount: 30 mg

Type of sample application: Dry load

Method name: MAM02v_CC_RP_6G_5-100_Acetonitrile

Table 20: Mobile phase solvents: A = Water, B = Acetonitrile

Time (min)	Flow Rate	%A	%B
00:00	5 mL/min	95	05
05:00	5 mL/min	60	40
30:00	5 mL/min	55	45
35:00	5 mL/min	0	100
45:00	5 mL/min	0	100

4.3.3 Separation by preparative PuriFlash

Flash chromatography of MAM01_05:

Column: GEMINI-NX 5µm C18 110Å (phenomenex®)

Applied amount: 100 mg

Type of sample application: Direct injection (sample dissolved in 2 mL MeOH)

Method name: MAM01_05prepHPLC

Table 21. Mobile phase solvents: A = Water, B = Acetonitrile

Time (min)	Flow Rate	%A	%B
00:00	5 mL/min	95	05
05:00	5 mL/min	60	40
01:05:00	5 mL/min	52	48
01:10:00	5 mL/min	02	98
01:15:00	5 mL/min	02	98
01:30:00	5 mL/min	02	98

Table 22. Overview of the collected fractions from the separation of MAM01_05 with the corresponding yields

Fraction	Approximately collected fractions	Yield (mg)
MAM02_01	1-2	1.9
MAM02_02	14-16	43.9
MAM02_03	17-23	40.9
MAM02_04	24-26	94.4
MAM02_05	27-29	25.0
MAM02_06	28-47	515.8

4.4 PHYTOCHEMICAL INVESTIGATION OF MAM01_06

Separation by preparative PuriFlash

Flash chromatography of MAM01_06

Column:	GEMINI-NX 55µm C18 110Å (phenomenex®)
Applied amount:	80 mg
Type of sample application:	Direct injection (sample dissolved in 2 mL MeOH)
Method name:	MAM01_06prepHPLC

Table 23. Mobile phase solvents: A = Water, B = Acetonitrile

Time (min)	Flow Rate	%A	%B
00:00	5 mL/min	95	05
05:00	5 mL/min	60	40
30:00	5 mL/min	55	45
35:00	5 mL/min	0	100
45:00	5 mL/min	0	100

Table 24. Overview of the collected fractions from the separation of MAM01_06 with the corresponding yield

Fraction	Approximately collected fractions	Yield (mg)
MAM03_01	18-22	729.67

4.5 PHYTOCHEMICAL INVESTIGATION OF MA5N

Separation by preparative PuriFlash

Flash chromatography of MA5N

Column: GEMINI-NX 55µm C18 110Å (phenomenex®)

Type of sample application: Direct injection (sample dissolved in 2 mL MeOH)

Applied amount: 100 mg

Method name: MA5N

Table 25. Mobile phase solvents: A = Water, B = Acetonitril

Time min	Flow Rate	%A	%B
00:00	5 mL/min	95	05
05:00	5 mL/min	60	40
01:05:00	5 mL/min	52	48
01:10:00	5 mL/min	02	98
01:15:00	5 mL/min	02	98
01:30:00	5 mL/min	02	98

5 DISCUSSION AND CONCLUSION

The aim of this diploma thesis was the re-isolation and identification of prenylated flavonoids in sufficient amounts for upcoming *in vivo* experiments. Starting point were different fractions prepared during a previously performed diploma thesis (Freisinger, 2020). Different chromatographic techniques, such as Flash-HPCCC, FC, UPLC and TLC were used for phytochemical investigation.

Flash-HPCCC turned out to be unsuitable for further separation of the fractions. Therefore, a different technique was used, whereupon FC resulted in the most suitable choice.

UPLC was applied for fingerprint analysis and purity determinations of the compounds isolated.

Four pure compounds, MAM02_02, MAM02_06, MAM03_01 and MA5N_03 (see 3.4 and 3.6) were isolated, and later confirmed to be kuwanon L, sanggenon C, sanggenon D and sanggenon G, respectively, using NMR spectroscopy. Although fraction MAM02_04 could only be enriched to a final purity of 84%, an elucidation via NMR spectroscopy was still possible.

Sanggenon C (MAM02_06) is a compound that is described intensively in the literature and is a subject of many studies. A study by Grienke et al (2016) has shown that it inhibits not only the viral NA of IAV but also pneumococcal planktonic growth and biofilm formation *in vitro*.

Sanggenon D has shown inhibition on the pneumococcal NA and on planktonic growth and biofilm formation, but not on the viral NA of IAV (Grienke et al., 2016).

Kuwanon L has also shown an inhibitory effect on pneumococcal NA as well as on planktonic growth and biofilm formation (Grienke et al., 2016).

However, it must be noted that these tests were carried out *in vitro*. In order to confirm efficacy and, above all, to obtain sufficient information on pharmacokinetics and safety issues, experiments have to be performed *in vivo*.

In future studies the pure compounds isolated in large amounts during this thesis will be tested in vivo for their anti-infective potential against influenza A virus and *S. pneumoniae*. This will then help to support the potential of *M. alba* root bark as a therapeutic remedy in low respiratory tract infections.

6 REFERENCES

Bundesministerium Soziales, Gesundheit, Pflege und Konsumentenschutz (BMSGPK) (ed.) (2020): Pneumokokken. online: https://www.sozialministerium.at/Themen/Gesundheit/Uebertragbare-Krankheiten/Infektionskrankheiten-A-Z/Pneumokokken.html, accessed on 10.11.2020.

Chan, Eric Wei-Chiang; LYE, Phui-Yan; Wong, Siu-Kuin (2016): Phytochemistry, pharmacology, and clinical trials of Morus alba. In: *Chinese Journal of Natural Medicines* 14 (1), p. 17–30. DOI: 10.3724/SP.J.1009.2016.00017.

Escribano-Ferrer, Elvira; Queralt Regué, Josep; Garcia-Sala, Xavier; Boix Montañés, Antoni; Lamuela-Raventos, Rosa M. (2019): In Vivo Anti-inflammatory and Antiallergic Activity of Pure Naringenin, Naringenin Chalcone, and Quercetin in Mice. In: *Journal of Natural Products* 82 (2), p. 177–182. DOI: 10.1021/acs.jnatprod.8b00366.

Freisinger, V. (2020): Analytics and fractionation of prenylated compounds. Diploma thesis. University of Vienna, Vienna. Department of Pharmacognosy.

Grienke, Ulrike; Richter, Martina; Walther, Elisabeth; Hoffmann, Anja; Kirchmair, Johannes; Makarov, Vadim et al. (2016): Discovery of prenylated flavonoids with dual activity against influenza virus and Streptococcus pneumoniae. In: *Sci. Rep.* 6 (1), p. 27156. DOI: 10.1038/srep27156.

Ito, Yoichiro (2005): Golden rules and pitfalls in selecting optimum conditions for high-speed counter-current chromatography. In: *Journal of Chromatography A* 1065 (2), p. 145–168. DOI: 10.1016/j.chroma.2004.12.044.

Kumar, Shashank; Pandey, Abhey K. (2013): Chemistry and biological activities of flavonoids. an overview. In: *Scientific World Journal* 2013 (Dec 29). DOI: 10.1155/2013/162750.

Nomura, T. (1988): Phenolic compounds of the mulberry tree and related plants. In: *Fortschr Chem Org Naturst.* 53, p. 87–201. DOI: 10.1007/978-3-7091-8987-0_2.

Nomura, T.; Fukai, T.; Hano, Y.; Uzawa, J. (1981): Structure of sanggenon C, a natural hyposensitive Diels-Alder adduct from Chinese crude drug "SANG-BAI-PI" (Morus root barks). In: *Heterocycles* 16, p. 2141–2148.

Nomura, Taro; Fukai, Toshio; Hano, Yoshio; Uzawa, Jun (1982): Structure of Sanggenon D, a natural hypotensive Diels-Alder adduct from chinese crude drug "Sang-Bai-Pi" (Morus root barks). In: *Heterocycles* 17, p. 381–389.

Rui-Chao, Shen; Mao, Lin (2001): Diels-Alder Type adducts from Morus cathayana. In: *Phytochemistry* 57, p. 1231–1235.

Sharma-Chawla, N.; Sender, V.; Kershaw, O.; Gruber, A. D.; Volckmar, J.; Henriques-Normark, B. et al. (2016): Influenza A Virus Infection Predisposes Hosts to Secondary Infection with Different Streptococcus pneumoniae Serotypes with Similar Outcome but Serotype-Specific Manifestation. In: *Infect Immun* 84 (12), p. 3445–3457. DOI: 10.1128/IAI.00422-16.

Swathi, G.; Srividya, A.; Ajitha, A.; Rao, V. (2015): Review on: flash chromatography. In: *World J. Pharm. Pharm. Sci.* 4 (8), p. 281–296.

Waters (ed.) (2020): ACQUITY UPLC System. online: https://www.waters.com/waters/de_AT/Original-UPLC-UHPLC-system-with-sub-2-micron-particle-technology-for-separations/nav.htm?locale=de_AT&cid=514207, accessed on 10.11.2020.

Wei, Hua; Zhu, Jing-Jing; Liu, Xiao-Qian; Feng, Wei-Hong; Wang, Zhi-Min; Yan, Li-Hua; Spencer, John (2016): Review of bioactive compounds from root barks of Morus plants (Sang-Bai-Pi) and their pharmacological effects. In: *Cogent Chemistry* 2 (1), p. 1212320. DOI: 10.1080/23312009.2016.1212320.

World Health Organization (WHO) (ed.) (2018): Influenza (Seasonal). online: https://www.who.int/en/news-room/fact-sheets/detail/influenza-(seasonal), accessed on 09.11.2020.

World Health Organization (WHO) (ed.) (2020a): Influenza. estimating burden of disease. online: https://www.euro.who.int/en/health-topics/communicable-

diseases/influenza/seasonal-influenza/burden-of-influenza, accessed on 10.11.2020.

World Health Organization (WHO) (ed.) (2020b): International travel and health. Pneumococcal disease. online: https://www.who.int/ith/diseases/pneumococcal/en/, accessed on 10.11.2020.

Yuan, Qingxia; Zhao, Longyan (2017): The Mulberry (Morus alba L.) Fruit. A Review of Characteristic Components and Health Benefits. In: *Journal of Agricultural and Food Chemistry* 65 (48), p. 10383–10394. DOI: 10.1021/acs.jafc.7b03614.

7 List of Abbreviations

ACN	Acetonitrile
BMSGPK	Bundesministerium für Arbeit, Soziales, Gesundheit und Konsumentenschutz (English: Federal Ministry for Labor, Social Affairs, Health and Consumer Protection)
$CHCl_3$	Chloroform
COSY	Correlated Spectroscopy
DCM	Dichloromethane
ELSD	Evaporative light scattering detector
HA	Hemagglutinin
HEMWat	Hexane – Ethylacetate – Methanol - Water
HMBC	Heteronuclear Multiple Bond Correlation
HPCCC	High Performance Countercurrent Chromatography
HPLC	High Performance Liquid Chromatography
HSQC	Heteronuclear Single Quantum Coherence
IAV	Influenza A Virus
MeOH	Methanol
NA	Neuraminidase
NMR	Nuclear Magnetic Resonance
NOESY	Nuclear Overhauser Enhancement Spectroscopy
NP	Normal Phase
OSI	Overall similarity index
PDA	Photo diode array
RP	Reversed Phase
SBP	Sang bai pi

TCM	Traditional Chinese Medicine
TLC	Thin Layer Chromatography
UPLC	Ultra Performance Liquid Chromatography
UV	Ultraviolet
WHO	World Health Organization

8 APPENDIX

Figure A1. ^{1}H-NMR-spectrum of MAM02_06 (sanggenon C)

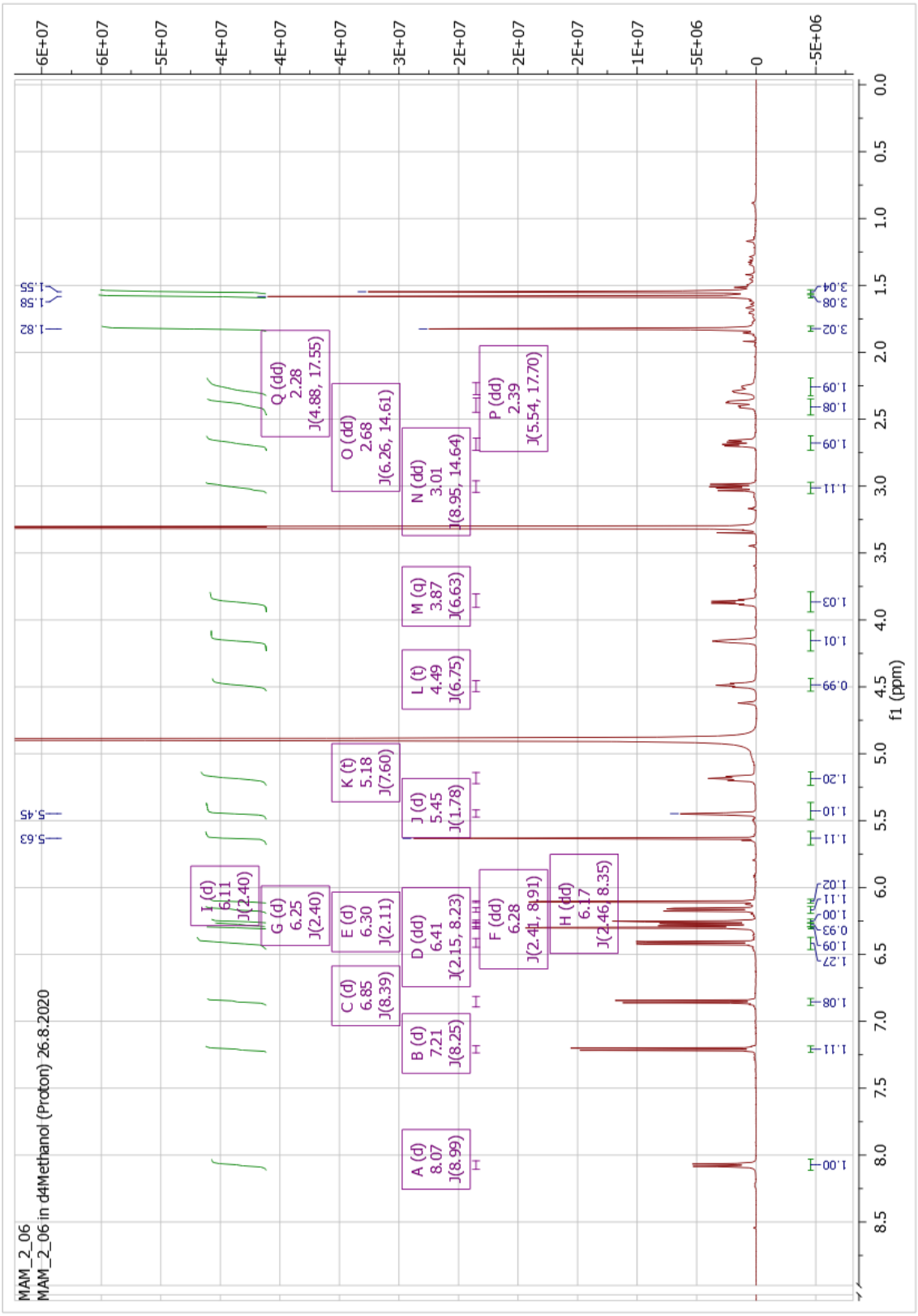

Figure A2. ^{13}C-NMR-spectrum (APT) of MAM02_06 (sanggenon C)

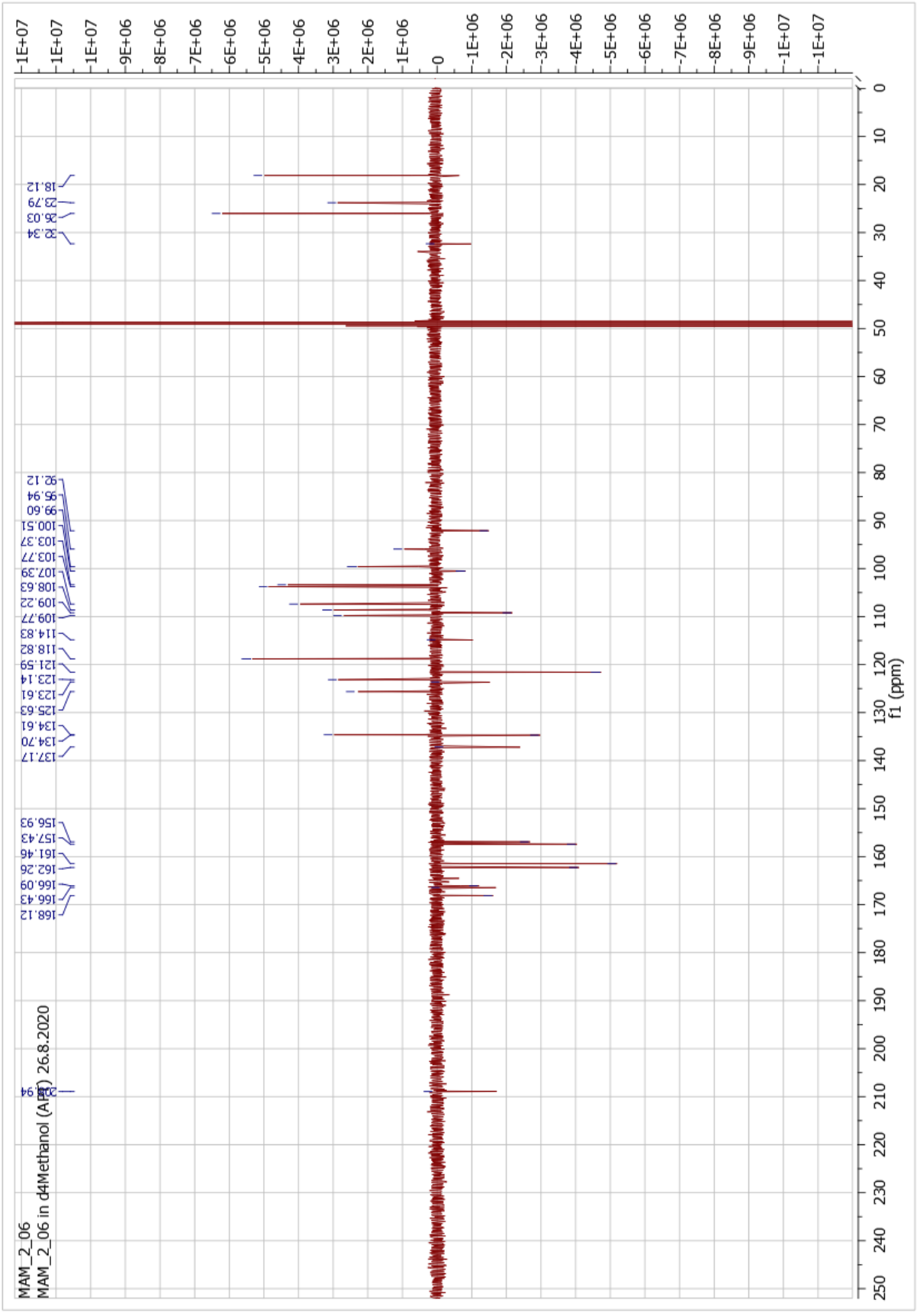

Figure A3. HSQC of MAM02_06 (sanggenon C)

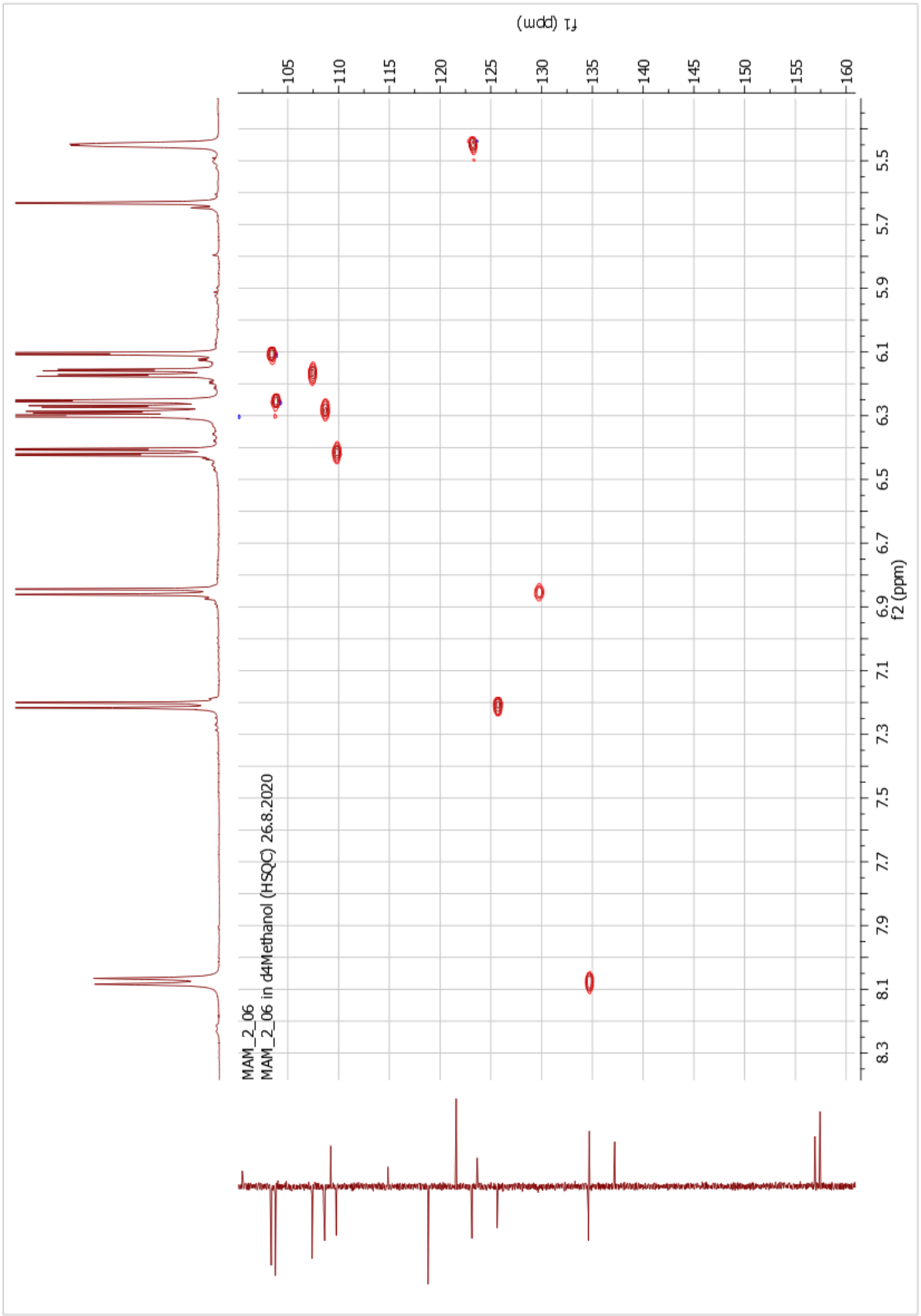

Figure A4. HMBC of MAM02_06 (sanggenon C)

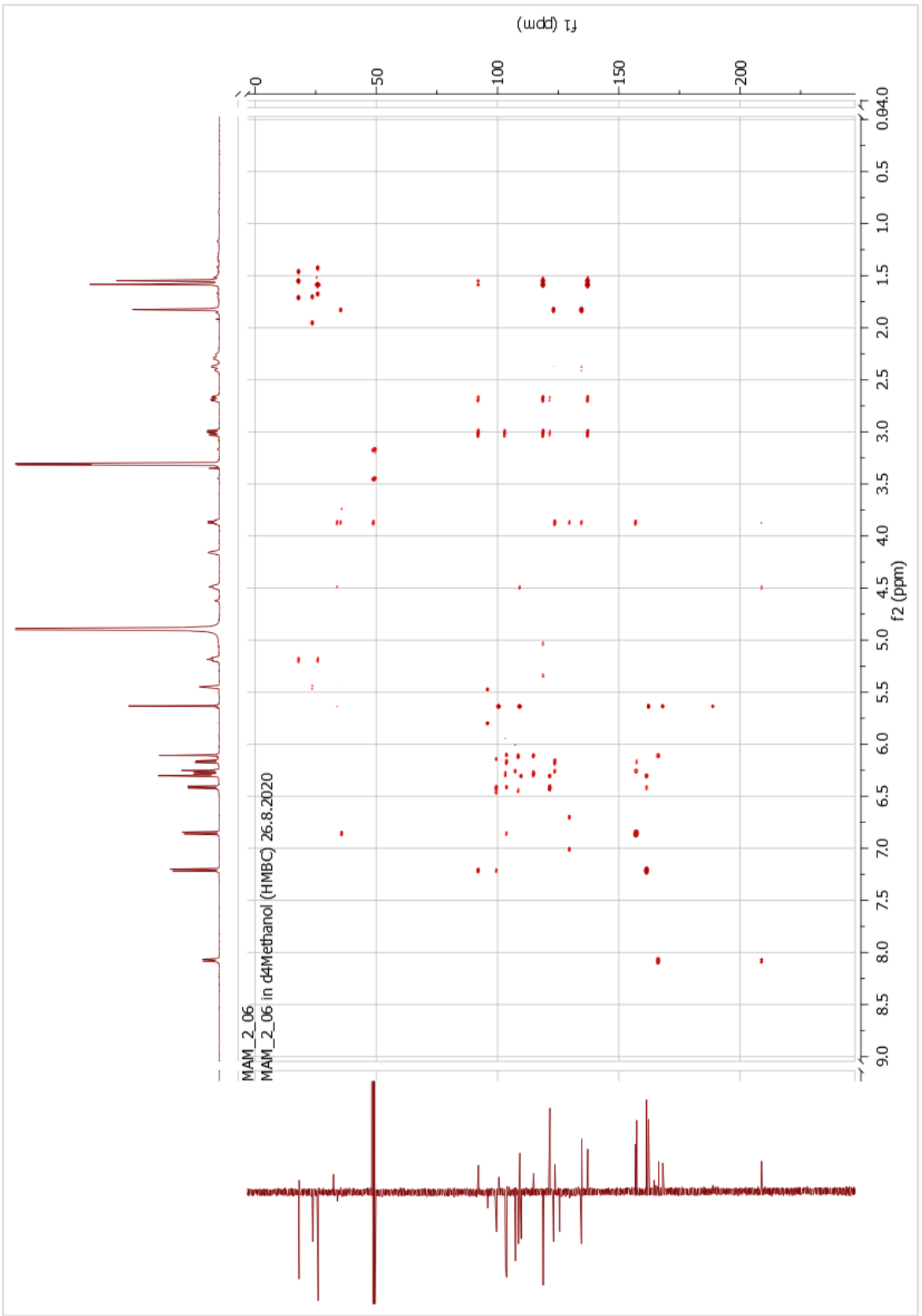

Figure A5. H, H-COSY of MAM02_06 (sanggenon C)

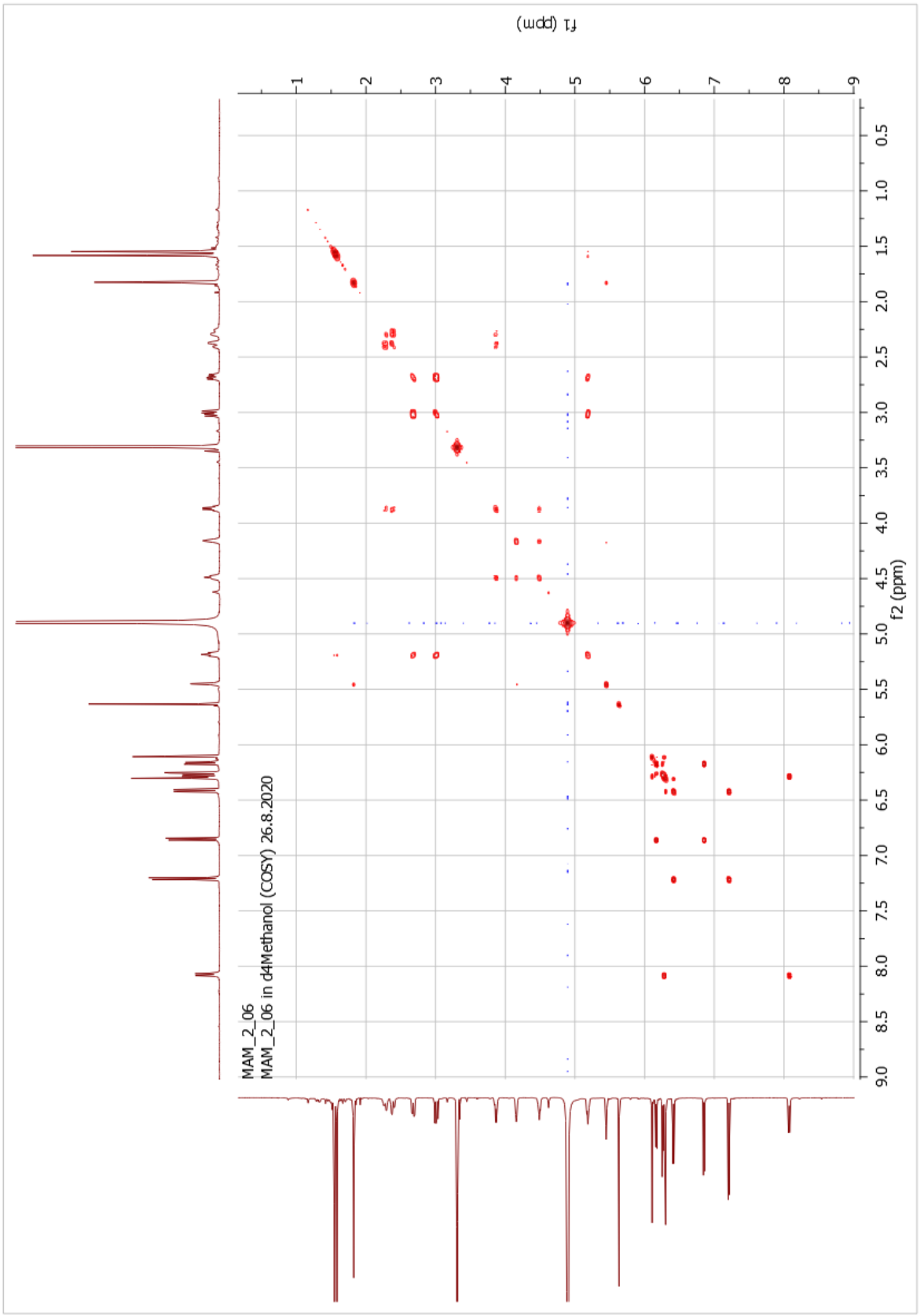

Figure A6. H-NOESY of MAM02_06 (sanggenon C)

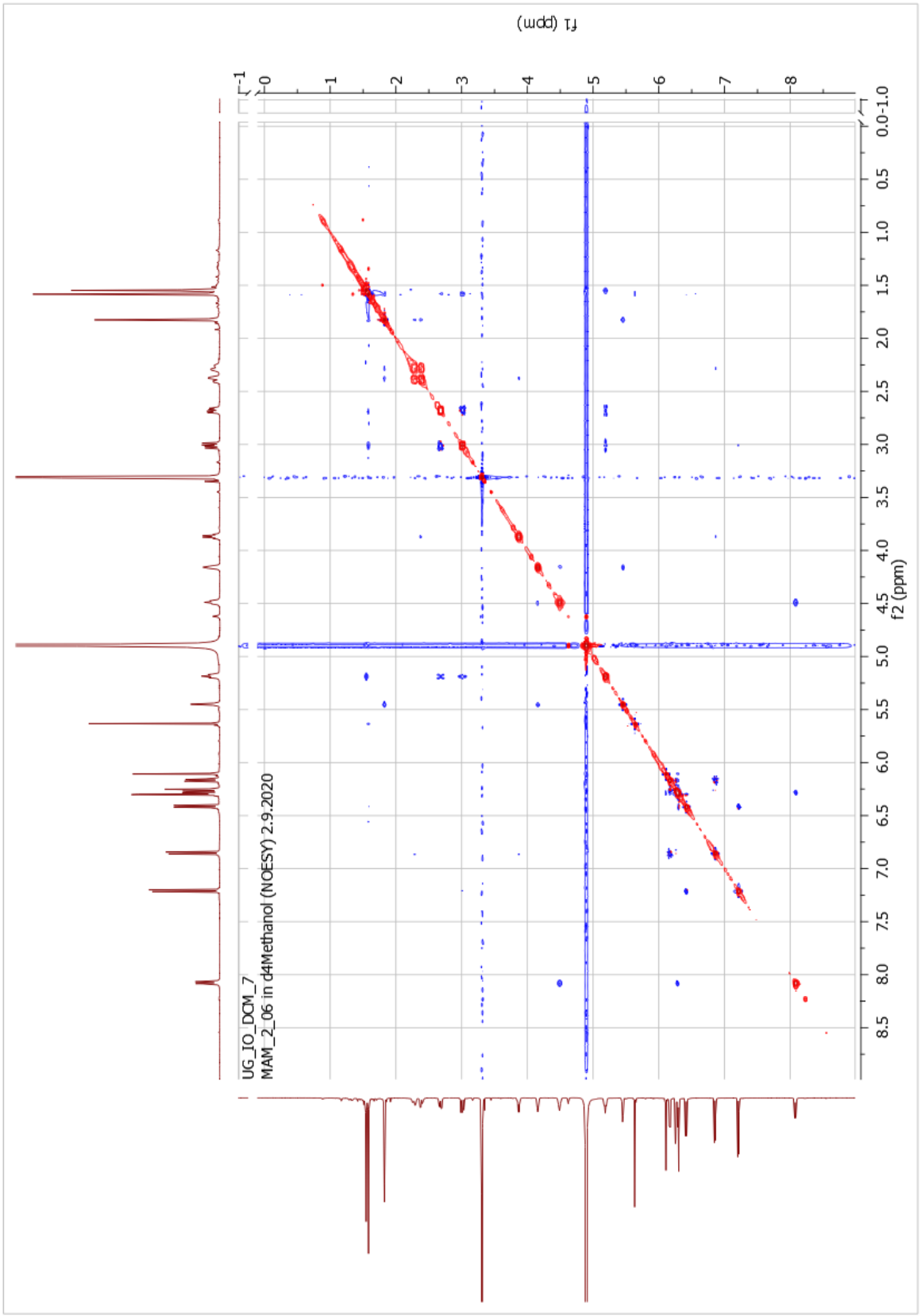

NMR spectral data of Sanggenon C

pos	∫ H	multipl (J)	δ H	δ C	C	δ C HMBC								δ H NOESY					
13	3	s	1,55	26,03	CH3	18,10	92,12	118,82	137,17					2,68	3,01	5,18			
12	3	s	1,58	18,12	CH3	26,03	92,12	118,82	137,17					2,68	3,01				
17	3	s	1,82	23,79	CH3	35,50	123,61							2,28	2,39	5,45			
18	2	dd (4.88, 17.55)	2,28	35,50	CH2	49,50	123,61							1,82	3,87	6,85			
18	2	dd (5.54, 17.70)	2,39	35,50		49,50	123,61							1,82	3,87				
9	1	dd (6.26, 14.61)	2,68	32,30	CH2	92,12	118,82	121,59	137,17					1,58	3,01	5,18			
9	1	dd (8.95, 14.64)	3,01	32,34		92,12	118,82	121,59	137,17					2,68	5,18	7,21			
19	1	q (6.63)	3,87	36,08	CH	34,05	35,50	49,50	123,60	130,00	208,94			2,28	2,39	4,49	6,85	8,07	
14	1	t	4,16	34,05	CH									4,49	5,45				
20	1	t (6.75)	4,49	49,50	CH	34,05	35,50	109,22	123,60	208,94				3,87	4,16	6,85	8,09		
10	1	t (7.60)	5,18	118,82	CH	18,12	26,03	32,34						1,58	2,68	3,01	7,21		
15	1	d (1.78)	5,45	123,14	CH	23,79	34,05	35,50	95.94?					1,82	4,16				
8	1	s	5,63	95,94	CH	34,05	100,51	109,22	162,26	168,12				2.68?					
30	1	d (2.40)	6,11	103,37	CH	103,77	114,83	109,22	166,43					6.28?					
24	1	dd (2.46, 8.35)	6,17	107,39	CH	103,77	123,61	157,43						6,85	6,28				
32	1	d (2.40)	6,25	103,77	CH	108,63	123,61	157,43						6,11	6,17	6,85			
26	1	dd (2.41, 8.91)	6,28	108,63	CH	103,37	114,83	157,43						6,11	6,17	6,85			
3'	1	d (2.11)	6,30	99,60	CH	109,77	114,83	121,59	162,26	166,43				6,41	7,21				
5'	1	dd (2.15, 8.23)	6,41	109,77	CH	99,60	103,77	121,59	162,26					6,30	7,21				
33	1	d (8.39)	6,85	130,00	CH	103,77	157,43							2,28	3,87	4,49	6,25	6,17	
6'	1	d (8.25)	7,21	125,63	CH	92,12	99,60	162,26						3,01	6,41	6,30			
27	1	d (8.99)	8,07	134,61	CH	103,77	166,43	208,94						4,49	6,28				
11				137,17	C														
2				92,12	C														
3				108,63	C														
2' / 4' / 5 / 8a				162,26	C														
1'				121,59	C														
4				188,79	C														
4a				100,51	C														
7				168,12	C														
6				109,22	C														
16				123,61	C														
21				208,94	C														
22				114,83	C														
29				156,93	C														
23				166,43	C														
31				157,43	C														
28				109,22	C														

Figure A7. Excel-sheet with HMBC and NOESY correlations of MAM02_06 (sanggenon C)

Figure A8. ^{1}H-NMR of MAM03_01 (sanggenon D)

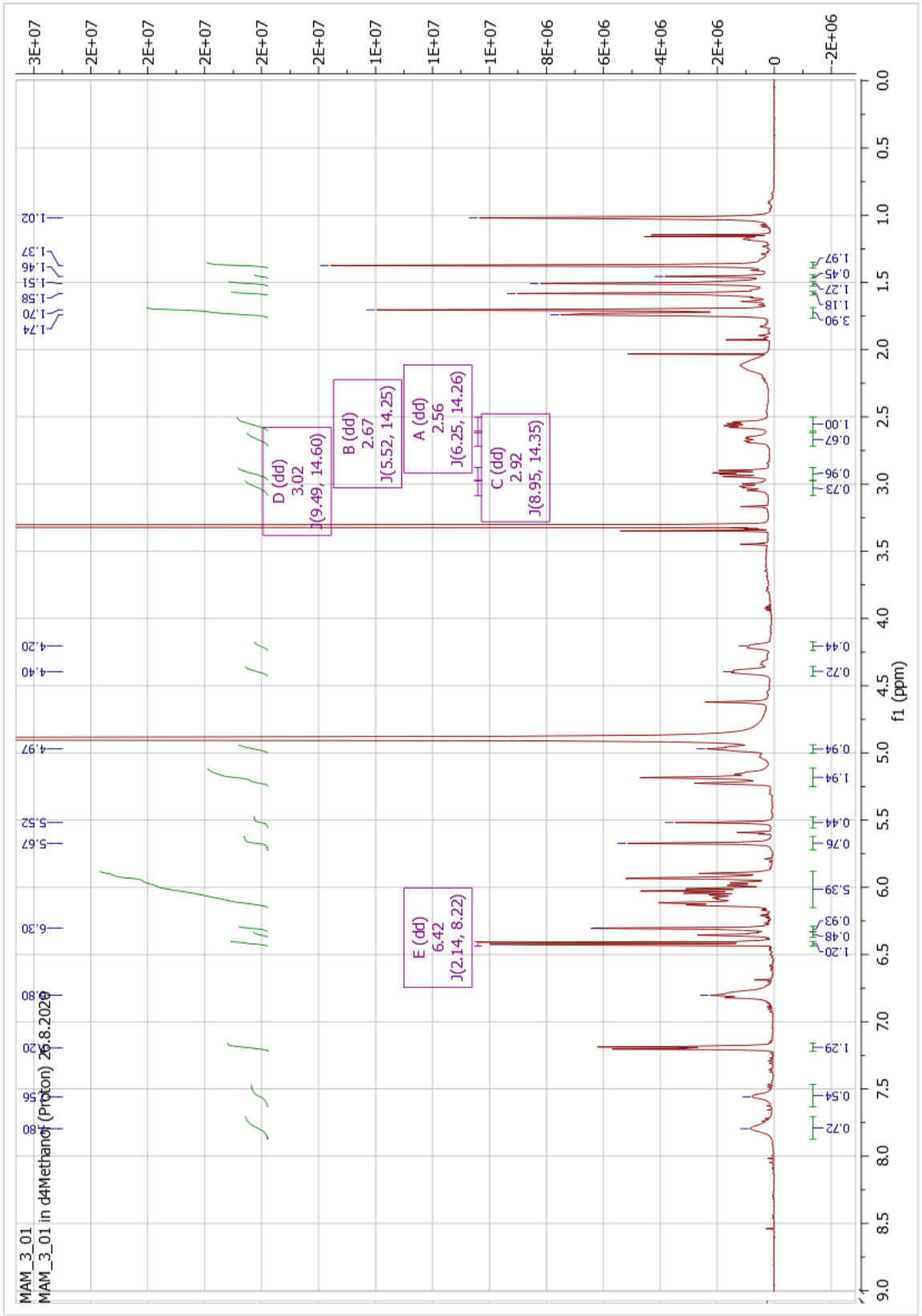

Figure A9. ^{13}C-NMR of MAM03_01 (sanggenon D)

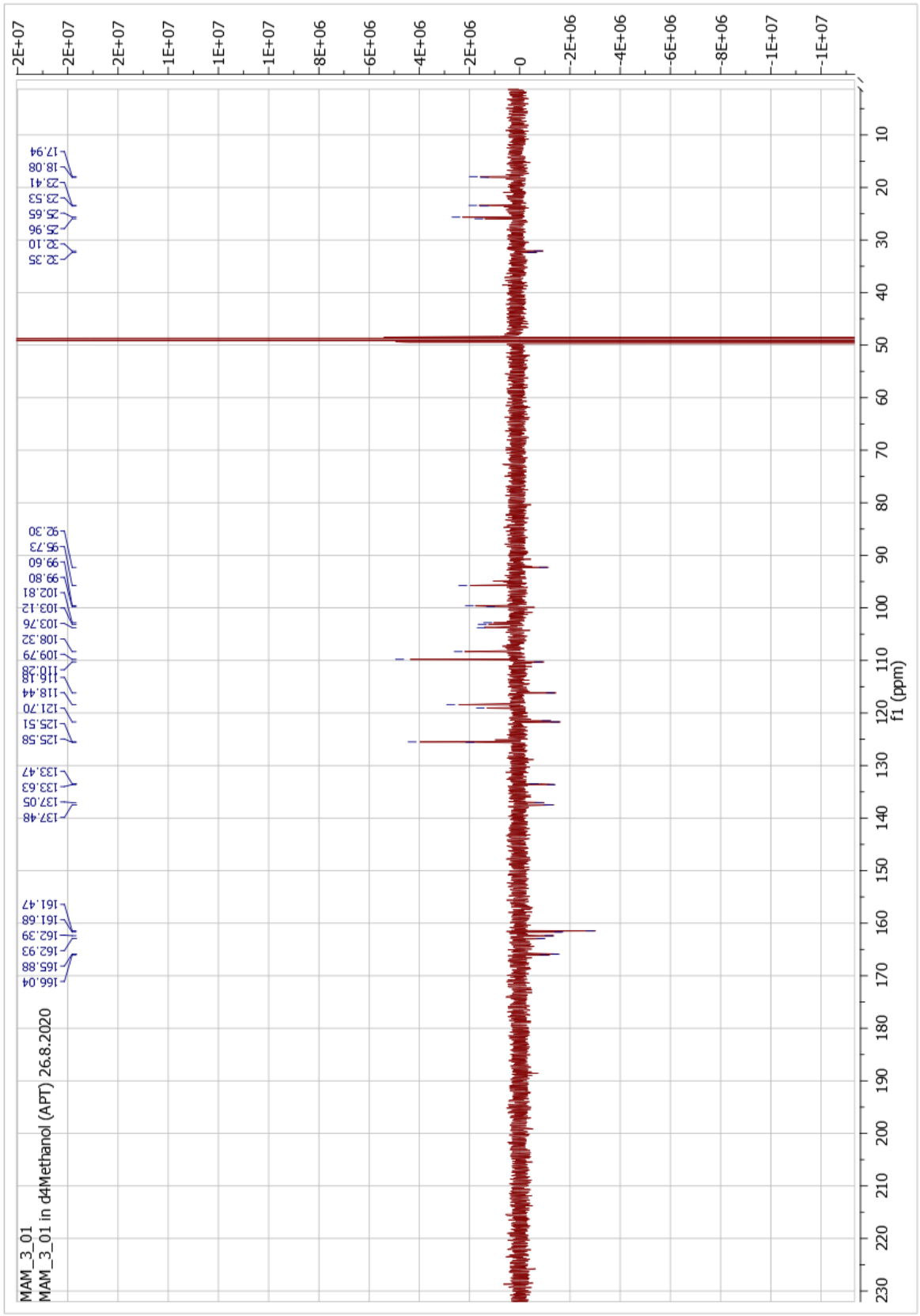

Figure A10. HSQC of MAM03_01 (sanggenon D)

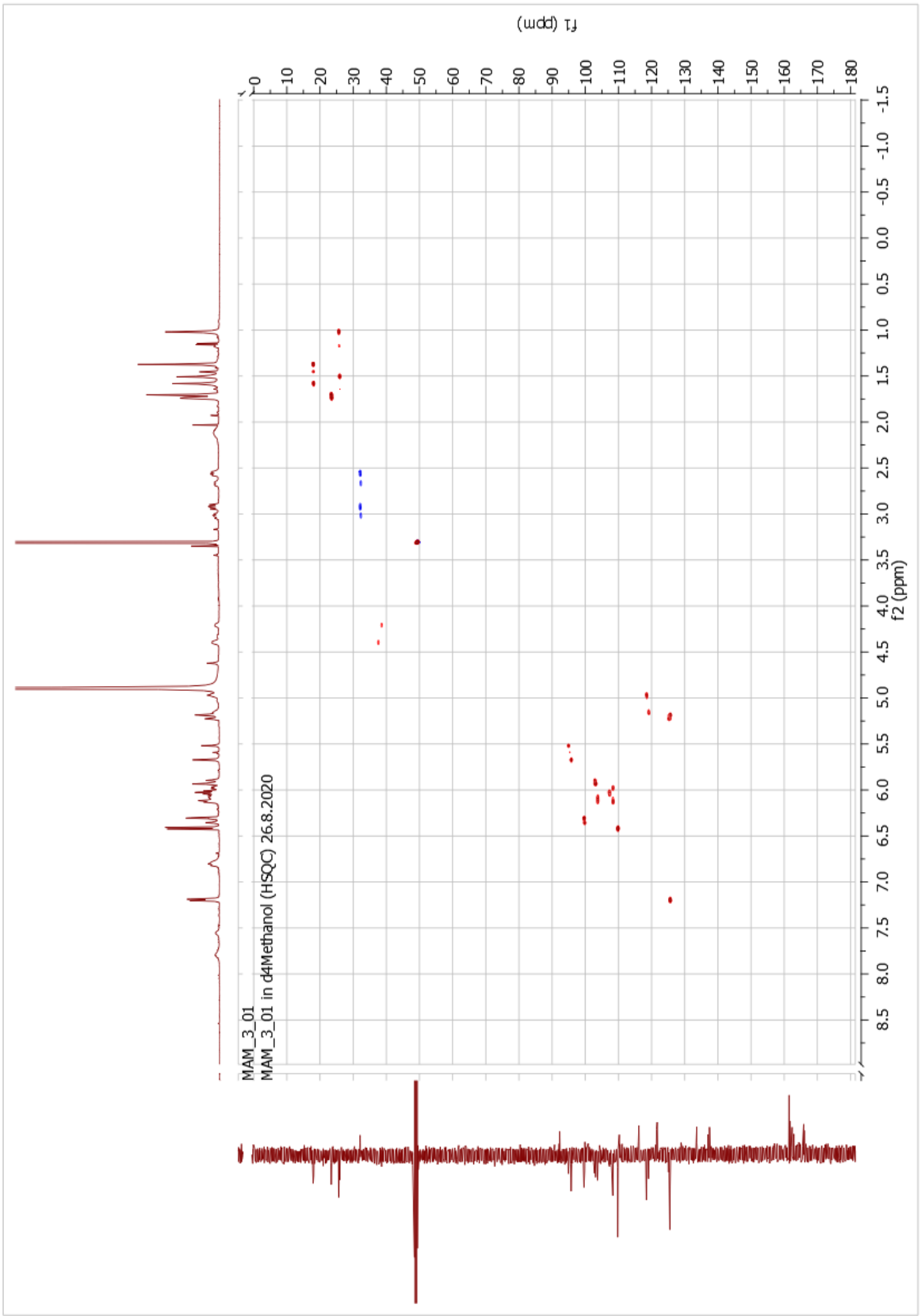

Figure A11. HMBC of MAM03_01 (sanggenon D)

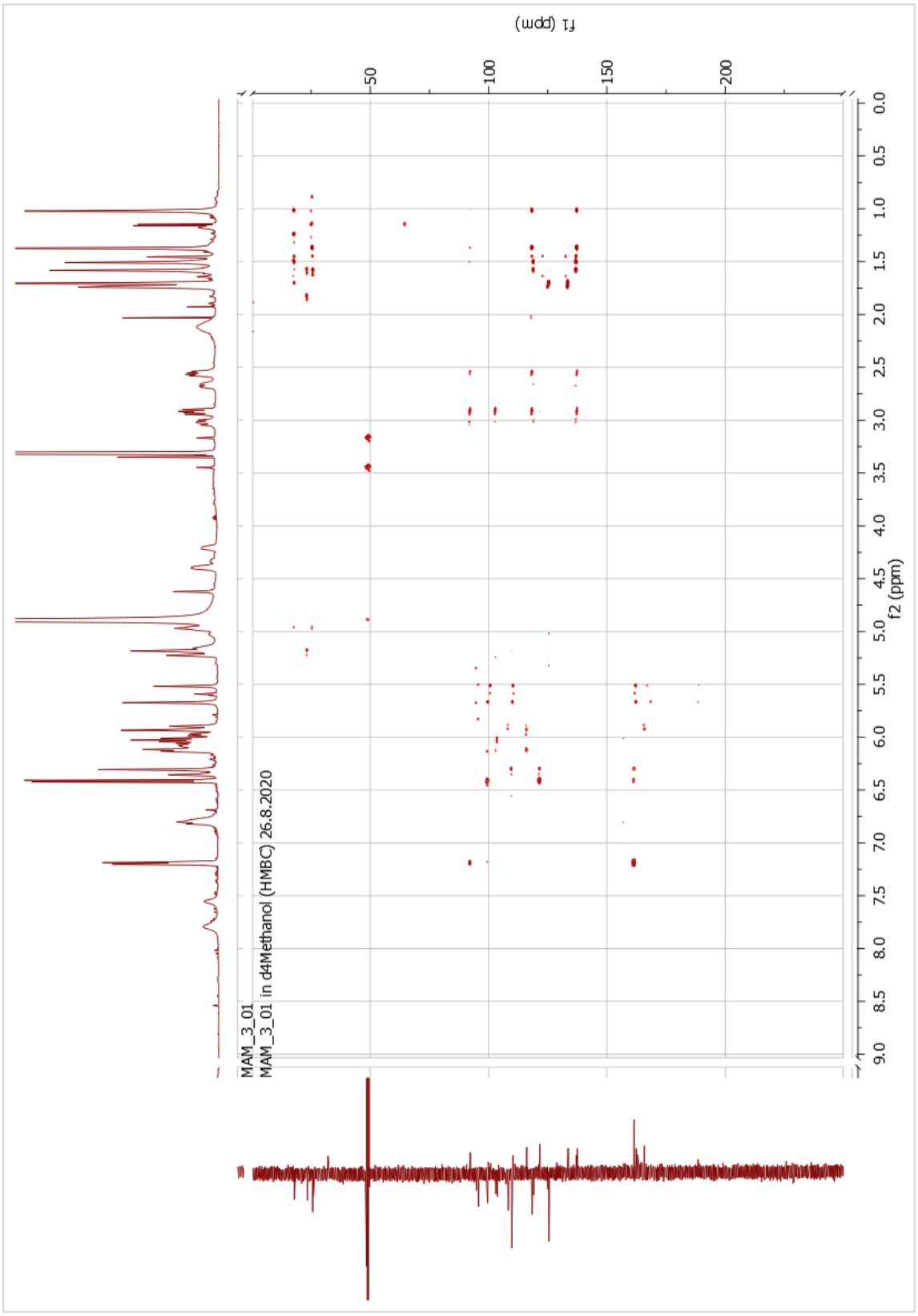

Figure A12. H, H-COSY of MAM03_01 (sanggenon D)

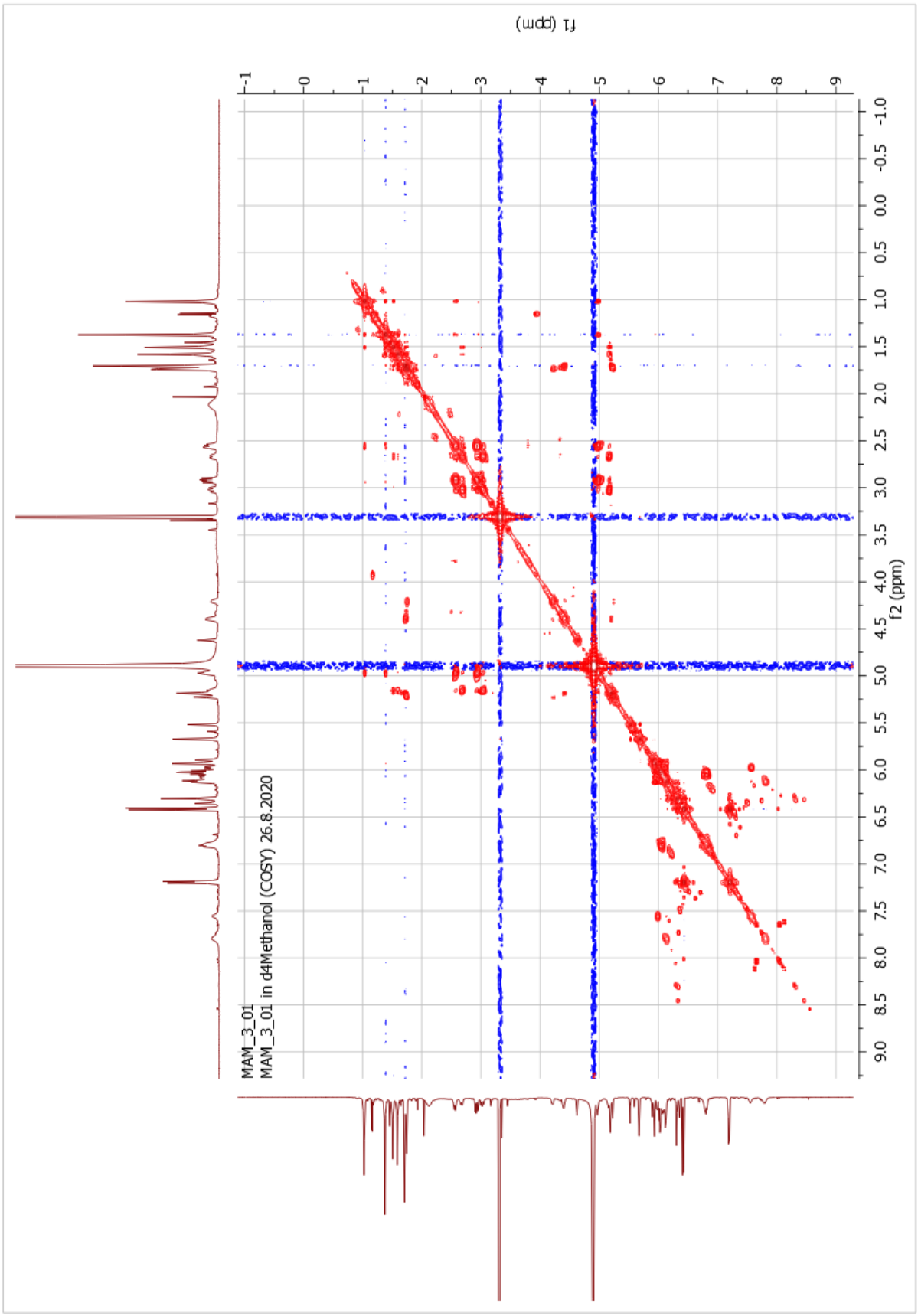

Figure A 13. H-NOESY of MAM03_01 (sanggenon D)

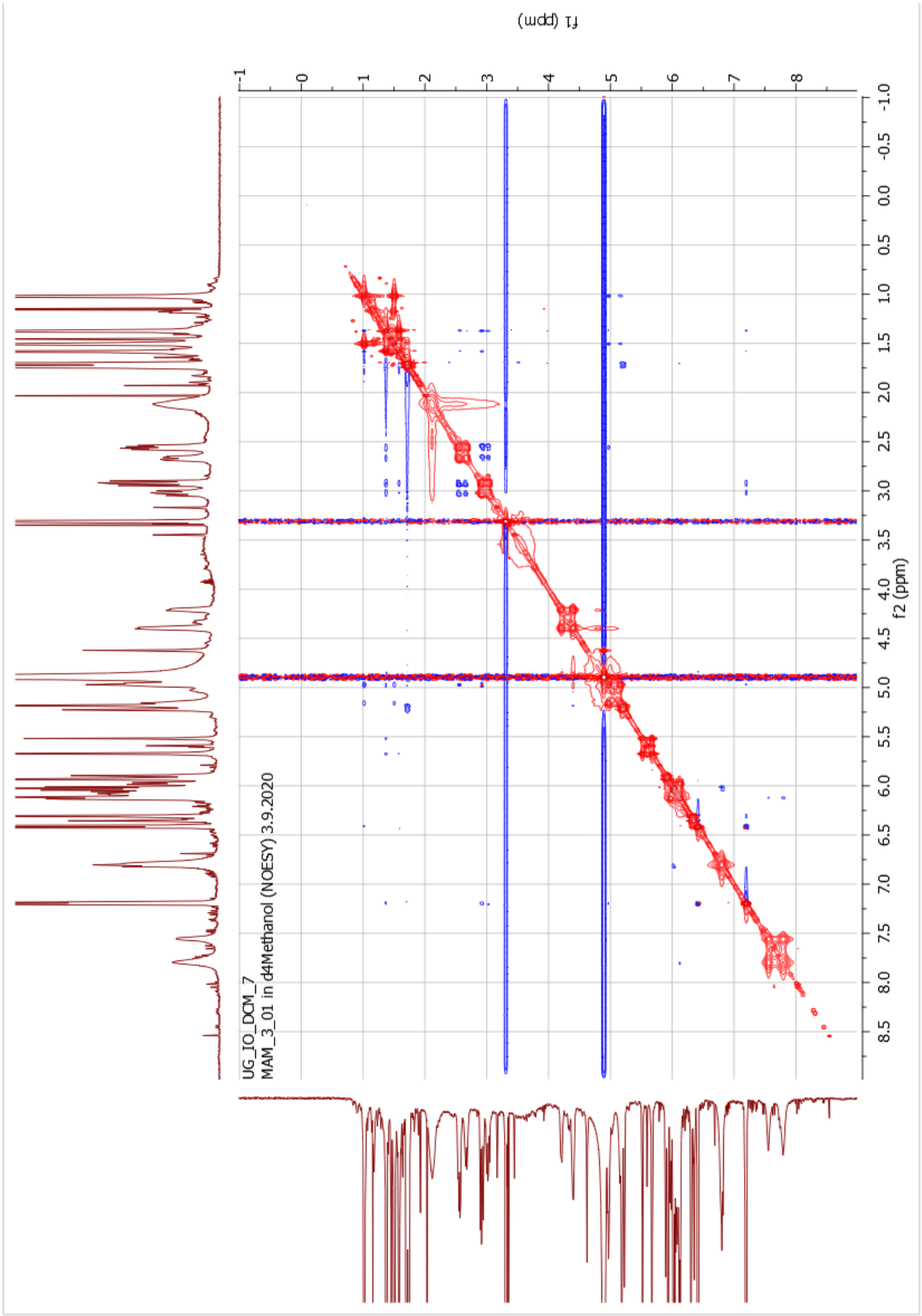

NMR spectral data of Sanggenon D

pos	∫ H	multipl (J)	δ H	δ C	C	δ C HMBC								δ H NOESY					
12	3	s	1,02	25,65	CH3	18,08	118,44	137,48						4,97	5.18?				
13	1	-	1,37	18,08		25,65	92,30	118,44	137,48					1,02	2,56	2,92			
13	1	-	1,51	18,08	CH3	92,30	119,22	137,48						4,97	5,18				
13	1	-	1,58	18,08		23,53	25,65	119,22	137,48					2,56	2,92				
17	1	-	1,70	23,53	CH3	125,58								5.15?					
17	2	-	1,74	23,53		125,58								5.15?					
9	1	dd (6.25, 14.26)	2,56	32,10	CH2	92,30	118,44	137,48											
9	1	dd (8.95, 14.35)	2,92	32,10		92,30	118,44	137,48						2,56	2,67	7.20?			
18	1	dd (5.52, 14.25)	2,67	32,35	CH2	119,22	137,05							2,93	3.03?				
18	1	dd (9.49, 14.60)	3,02	32,35		119,22	137,05							2,56	2,67	7.20?			
19	1	-	4,20	38,64	CH	nichts													
20	1	-	4,40	37,64	CH	nichts													
10	1	-	4,97	118,44	CH	18,08	25,65							1,02	1,37	1,51	2,56	2,92	
15	1	-	5,15	119,22	CH									1,02					
14	1	-	5,18	125,51	CH	110,28								1,74	4,40	4,20			
8	1	-	5,52	95,03	CH	101,06	110,28	162,39	167,05					1,38					
24	1	-	5,93	103,12	CH	108,32	116,18	166,04											
26	1	-	5,97	108,32	CH	116,18								7,56	7,80				
30	1	-	6,10	103,76	CH														
32	1	-	6,12	108,48	CH	103,76								7,56	7,80				
3'	1	-	6,35	99,80	CH	109,79	121,70												
5'	1	dd (2.14, 8.22)	6,42	109,79	CH	121,70	99,80	162,39						7,20					
6'	1	-	7,20	125,58	CH	92,30	99,80	162,39						1,37	2.56?	2,92	3,02	4,97	
33	1	-	7,56	134,17	CH									6,12					
27	1	-	7,80	134,55	CH									6,12					
11				137,48	C														
2				92,30	C														
1'				121,70	C														
3				165,88	C														
2' / 4' / 8a				162,39	C														
4				188,80	C														
4a				101,06	C														
5 \ 29 \ 31				161,68	C														
6				110,28	C														
7				167,05	C														
16				137,05	C														
22				116,18	C														
23				166,04	C														
25				161,47	C														
28				120???	C														
21				208???	C														

Figure A 14. Excel-sheet with HMBC and NOESY correlations of MAM03_01 (sanggenon D)

Figure A15. ^{1}H-NMR of MAM02_04 (sanggenon O)

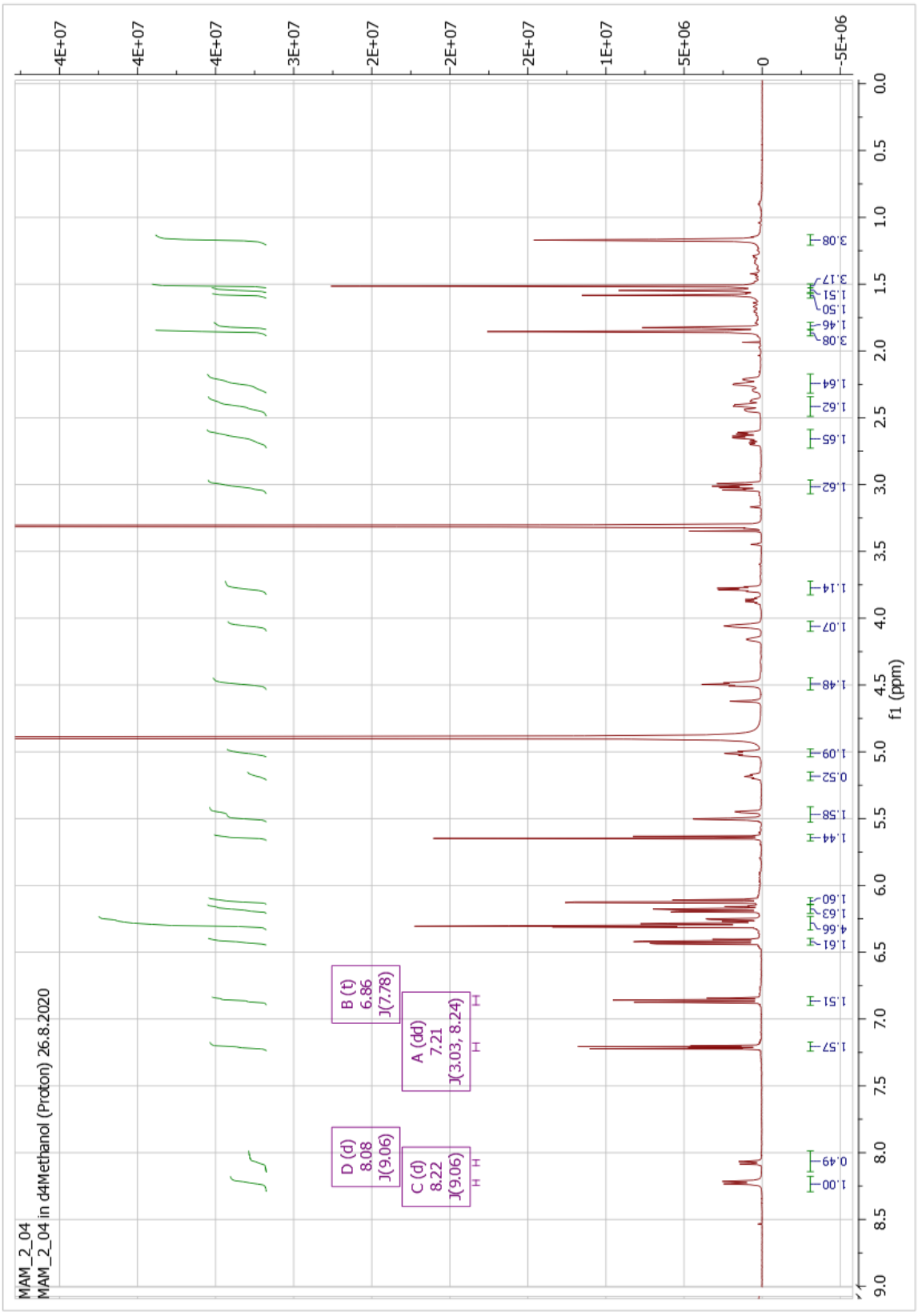

Figure A16. ^{13}C-NMR of MAM02_04 (sanggenon O)

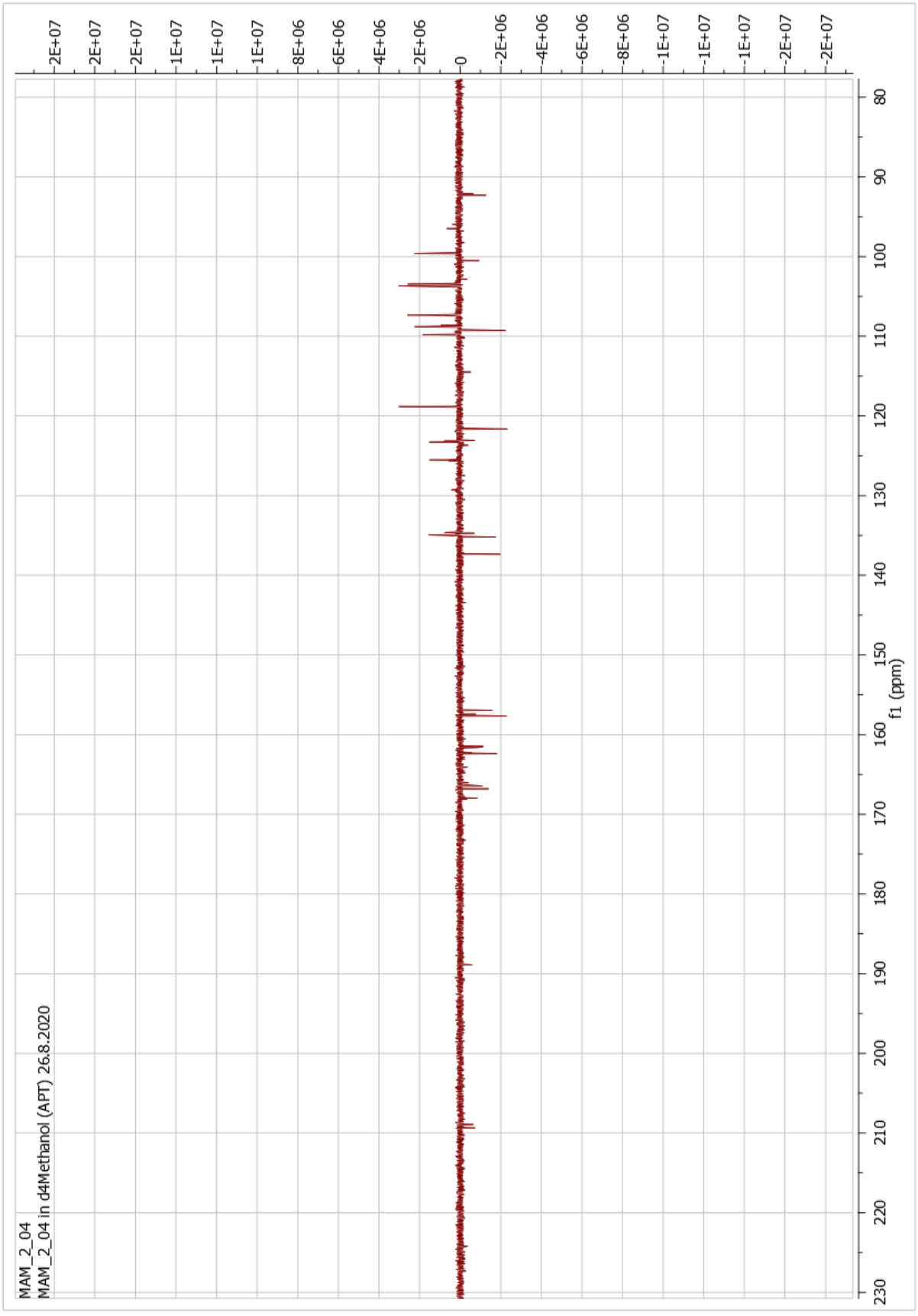

Figure A17. HSQC of MAM02_04 (sanggenon O)

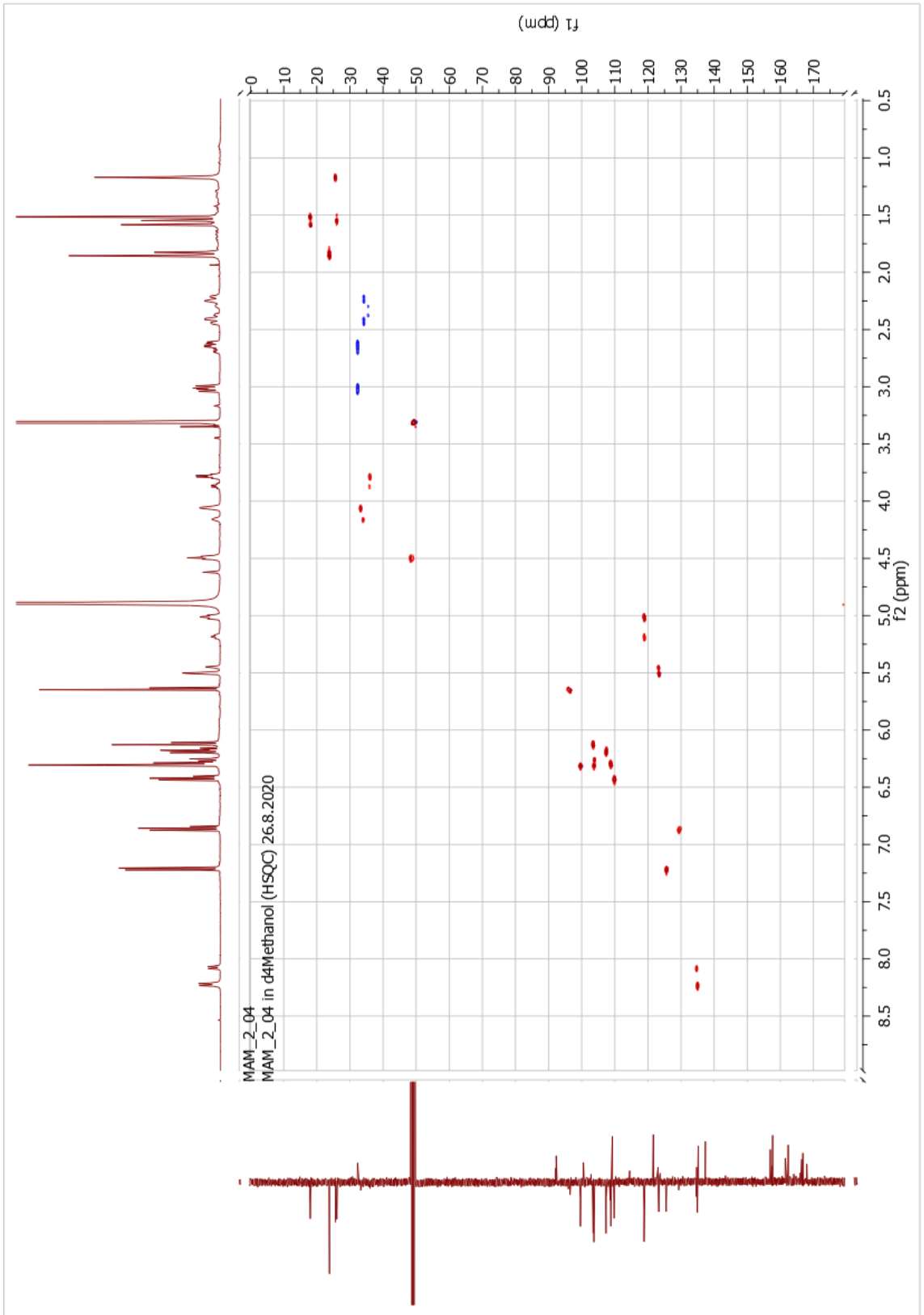

Figure A18. HMBC of MAM02_04 (sanggenon O)

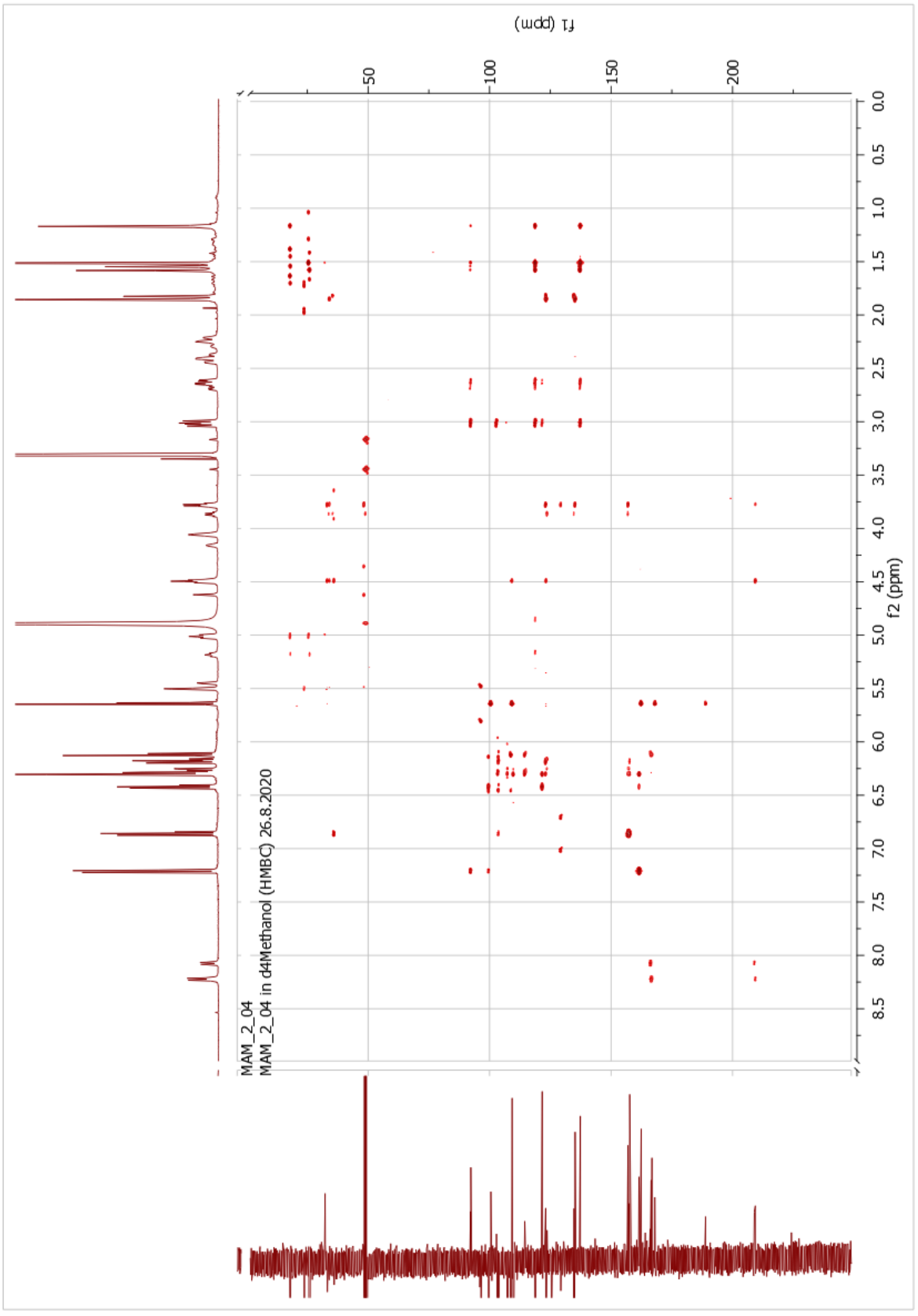

Figure A19. H, H-COSY of MAM02_04 (sanggenon O)

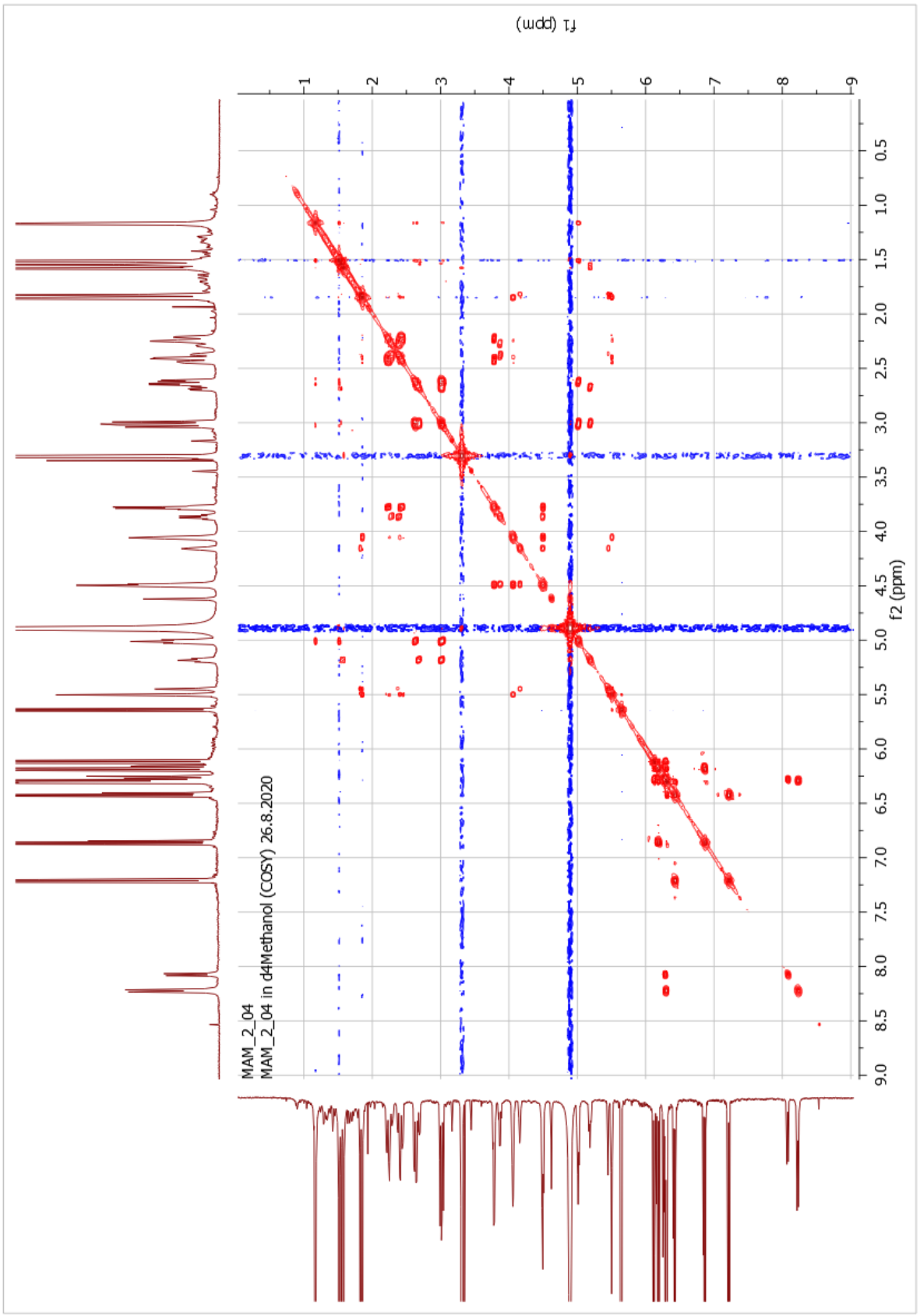

Figure A20. H-NOESY of MAM02_04 (sanggenon O)

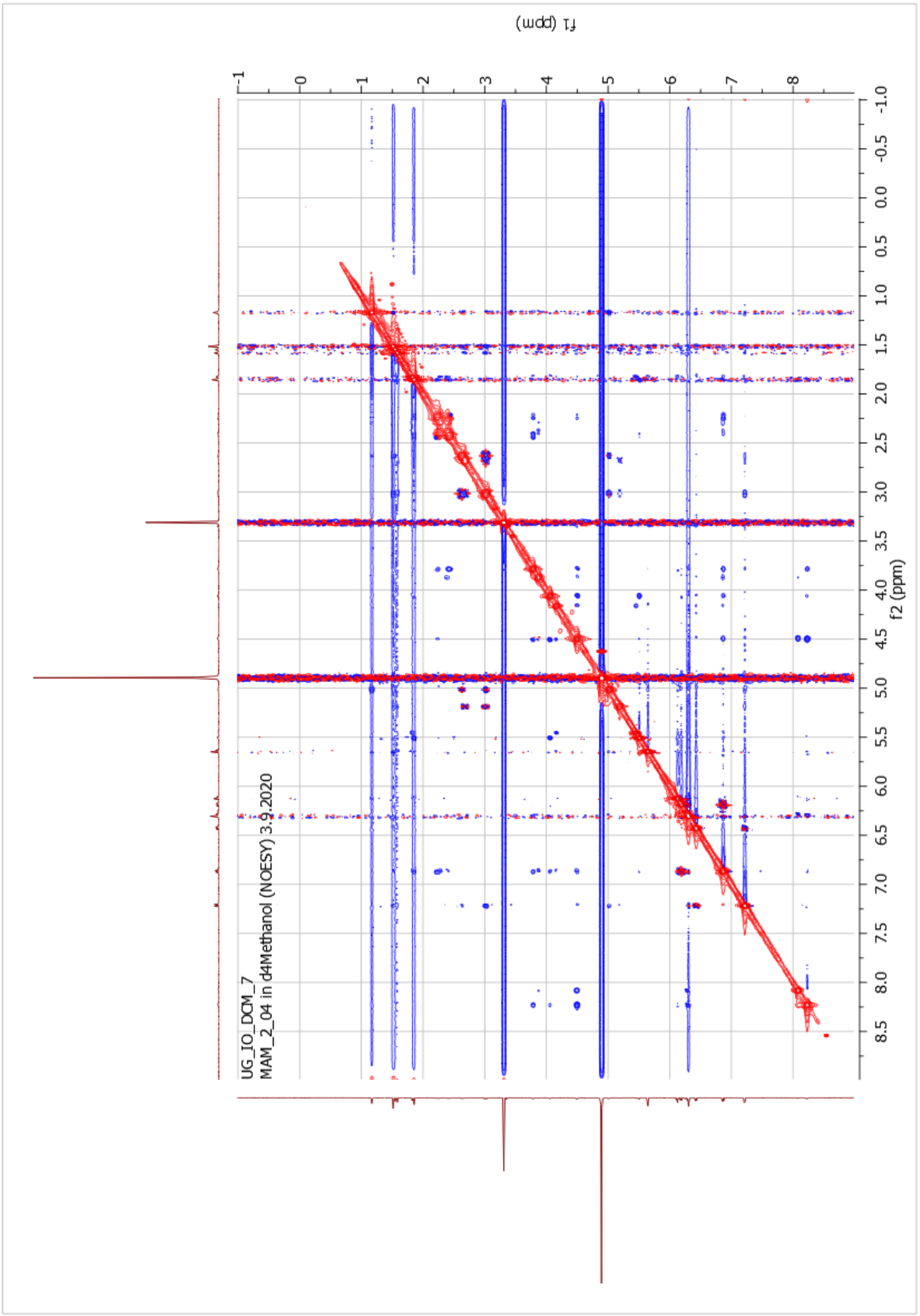

NMR spectral data of Sanggenon O

pos	∫ H	multipl (J)	δ H	δ C	C	δ C HMBC								δ H NOESY					
13	3	s	1,17	25,67	CH3	18,01	92,43	118,90	137,28					5,01	1,51				
12	3	s	1,51	18,01	CH3	25,67	32,33	92,43	118,90	137,28				1,17	3,01	5,65			
17	3	s	1,86	23,85	CH3	34,24	123,30	135,21						5,50	2,23	2,42			
18	1	-	2,23	34,24	CH2									6,87	3,78	2,42			
18	1	-	2,42	34,24										2,23	3,78				
9	1	-	2,63	32,33	CH2	92,43	118,90	121,81	137,28					1,51	3,01	5,01	7,22		
9	1	-	3,01	32,33		92,43	118,90	121,81	137,28					1,51	2,63	5,01	7,22		
19	1	-	3,78	36,07	CH	123,30	135,21							2,23	2,42	4,50	6,87	8,22	
14	1	-	4,06	33,27	CH									4,50	5,50	6,87			
20	1	-	4,50	48,39	CH	33,27	34,24	36,07	109,34	123,30				3,78	4,06	6,87	8,22		
10	1	-	5,01	118,90	CH	18,01	25,67							1,17	2,63	3,01	7,22		
15	1	-	5,50	123,30	CH	23,85								1,86	4,06				
8	1	-	5,65	96,49	CH	100,69	109,34	162,32	168,20	189,02				1,51					
24	1	-	6,13	103,53	CH	114,56	166,84												
32	1	-	6,18	107,37	CH	103,70	123,36	157,85						6,87					
26	1	-	6,29	103,70	CH	103,53	114,56							6,87	8,22				
30	1	-	6,31	103,70	CH	103,70	107,37	157,85											
3'	1	-	6,31	99,65	CH	121,81	157,85	161,64											
5'	1	-	6,43	109,77	CH	99,65	121,81	161,64						7,22					
33	1	d	6,87	129,32	CH	103,70	157,85							2,23	3,78	4,06	4,50	6,18	
6'	1	dd (3.03, 8.24)	7,22	125,54	CH	92,43	99,65	161,64						3,01	6,43				
27	1	d	8,22	134,93	CH	167,02	209,62							3,78	4,50	6,29			
11				137,28	C														
2				92,43	C														
1'				121,81	C														
4'				157,58	C														
2'				161,64	C														
3				109,21	C														
4				189,02	C														
4a				100,69	C														
8a				162,32	C														
7				168,20	C														
5				162,37	C														
6				109,34	C														
16				135,21	C														
28				123,36	C														
29				156,94	C														
31				157,85	C														
21				209,62	C														
22				114,56	C														
23				167,02	C														
25				166,84	C														

Figure A 21. Excel-sheet with HMBC and NOESY correlations of MAM02_04 (sanggenon O)